The Dawn of Civilization
Metal Trade and the Urban Revolution*

Matthias Flückiger, Mario Larch, Markus Ludwig, and Luigi Pascali†

February 16, 2023

THIS IS A VERY PRELIMINARY AND INCOMPLETE VERSION.
PLEASE DO NOT CIRCULATE.

Abstract

Approximately around 3300 BCE, our ancestors experienced the Urban Revolution, a very rapid transition from agricultural villages to state-level, urban societies. In less than five centuries and in regions as far as the Nile Valley, Mesopotamia, Central Asia, and the Indus Valley, cities appeared for the first time in human history, together with writing, large states, and unprecedented levels of socio-economic inequalities. What caused this transition? Why did it emerge in some regions but not in others? We propose that the turning point is the invention of bronze, in the second half of the 4th millennium. For the first time in human history, elaborate trade arrangements had to be made: bronze is an alloy made with copper and tin and these two metals can be found only in remote regions that are very distant from each other. The trade routes connecting large populations with far-away mining regions were constrained to pass by some regional bottlenecks: it is precisely in these bottlenecks that a new elite, relying on taxing transit trade, could rise, leading eventually to the rise of cities and states. We test this theory by combining global data on the distribution of metal resources, ancient mining activity, ancient trade relations, and the spread of the urban revolution.

Keywords: Urban Revolution, Cities, Trade, Bronze Age
JEL Codes: D02, F10, H10, N40, O43

*We thank seminar audiences at University of Michigan, York, Maastricht, Stanford, New York University, Princeton, Drexel and Harvard. Luigi Pascali acknowledges financial support from the Spanish Ministry of Economy and Competitiveness, through the Severo Ochoa Programme for Centres of Excellence in R&D (CEX2019-000915-S).

†Flückiger: University of York (matthias.flueckiger@york.ac.uk); Larch: CEPII, CESifo, ifo, GEP, and University of Bayreuth (mario.larch@uni-bayreuth.de); Ludwig: CESifo and Technical University of Braunschweig (markus.ludwig@tu-braunschweig.de); Pascali: Universitat Pompeu Fabra, Barcelona GSE, Barcelona IPEG, CAGE, and CEPR (luigi.pascali@upf.edu).

1 Introduction

Approximately around 3300 BCE, our ancestors transitioned from agricultural villages to state-level, urban societies. What is striking is the speed of this transition. While we do not see any city in the first five thousand years since the spread of farming, in less than half millennium and in regions as far as the Nile Valley, Mesopotamia and the Indus Valley, cities appeared for the first time in human history, together with writing, large states, and unprecedented levels of socio-economic inequalities. Few centuries later, a similar transition occurred in Anatolia, China, Greece and in large parts of the Mediterranean coast. Gordon Childe coined the expression "Urban Revolution" to describe this process to emphasise that it was a fundamental step in the evolution of societies in-between the Neolithic Revolution and the Industrial Revolution. The rise of the Urban Revolution raises intriguing, fundamental questions. What caused this transition? Why has it emerged in some regions but not in others? These are fundamental questions in comparative development as an early start in the civilization process has been argued to be an important determinant to explain the comparative economic success of nations[1].

The fact that the era of the early civilizations coincides with the technological classification of the Bronze Age is a clue to the technological basis of these societies. The discovery of bronze enabled people to create metal tools, which made farming and hunting more efficient, and metal weapons. Bronze became the most important material of the early civilizations, and elaborate arrangements had to be made to ensure a continuous supply of it for essentially two reasons. First, metals were generally scarce in those regions, where agriculture was most productive and the population was denser. Second, bronze is an alloy made primarily with copper and tin. Tin is a relatively rare element in the Earth's crust and tin deposits are located in areas far away from copper deposits. The result was an explosion of long-distance trade.

A series of prominent theories in anthropology, archaeology, and political sciences, which we illustrate in Section 2, have related the urban revolution with the rise of long-distance trade in metals generated by the invention of bronze. Trade routes connecting large populations with far-away mining regions were constrained to pass by some clear bottlenecks. It is precisely in these bottlenecks that the rise of a new elite was sustained by the capability to tax the transit trade and the need to provide the peace and order necessary to exploit the welfare

[1]Recent research in the field of comparative development has highlighted an exceptional persistence in the levels of economic, technological, and political development around the world until 1500 AD (Comin, Easterly and Gong, 2010; Ashraf and Galor, 2011; Maloney and Valencia Caicedo, 2016; Davis and Weinstein, 2002; Olsson and Paik, 2020). Although the European colonisation seems to have created a "reversal of fortune" among European colonies (Acemoglu, Johnson and Robinson, 2002), once accounting for migration between countries, ancient economic disparities are still explaining a large portion of current economic disparities (Putterman and Weil, 2010; Chanda, Cook and Putterman, 2014). See Matranga and Pascali (2021) for a literature review.

gains from the metal trade.

Despite a large narrative historical literature, to the best of our knowledge, there are no previous studies that have attempted to study, in a systematic econometric framework, the causal impact of trade in metals on the rise of early civilizations. This study is a first attempt to close this gap: it combines global data on the distribution of metal resources with Bronze Age data on land productivity, farming and metal mining, trade relations, and the spread of the urban revolution to identify the impact of metal trade on the rise of the first cities and large socioeconomic inequalities across the ancient world.

In Section 4, we identify the transit regions in the Bronze-Age metal trade network. We use a definition that goes back to Ramsay (1890), who proposed the concepts of "road-knots": the passages in which a series of routes, dictated by natural topography, intersect. To locate these areas, we start by constructing the Bronze-Age natural transportation network. Specifically, we combine data on natural topography and bilateral trade relationships (inferred from archaeological artefacts) to infer the least-cost paths between any two grid cells (1×1 degree) in the Old World. Long-distance trade during the Bronze Age is essentially an exchange of metals, mainly copper and tin, for cereal grains. We identify the "road-knots" in the resulting trade network by counting the number of least-cost paths that transit each grid cell, while connecting the cells with tin and copper mines with all the other reachable cells, weighted by their respective cropland areas.

In Section 5, we test the causal impact of transit metal trade on the rise of the Urban Revolution. Our research question doesn't allow for one perfect randomised controlled trial that could prove and disprove our thesis. Plus, to our knowledge, there does not exist a perfect global database that coherently measures the different defining aspects of the Urban Revolution. We therefore perform multiple imperfect tests based on different datasets. We present our empirical analysis in four subsections, each using different data, that capture different aspects of the Urban Revolution, and different identification strategy, as dictated by the nature of the underlined data.

The first subsection focuses on the rise of the first cities. We use two readily available datasets to capture the evolution of urban settlements over time: Reba, Reitsma and Seto (2016) and HYDE 3.1 provide respectively data on the location of cities and urbanisation rates from the fourth millennium BCE. Figure 1 illustrates the grid cells that we have identified as road-knots in the metal trade network and the cities dating before the collapse of the Bronze Age (1300 BCE). Almost all cities in the sample arose in potential transit areas in the metal trade routes, a result confirmed by our cross-sectional OLS estimates. Still, several factors prevent a causal interpretation of this correlation. In particular, our measure of transit trade potential is likely to be affected by the rise of cities and the urban revolution itself as it depends on the distribution of mines and cropland areas around the globe, which are clearly endogenous to the location of cities and complex hierarchies. To get closer to a causal link

between metal transit trade and the rise of cities, we use a 2SLS panel estimation framework. The instrumental variable is an alternative measure of transit trade potential, which does not rely on the endogenous distribution of metal mines and cropland, is not affected by human intervention, and is purely driven by geography and climate. It is constructed by counting the number of least-cost paths that transit a certain cell, while connecting the cells with tin and copper natural deposits (not the Bronze-Age mines) to the other cells in the Old World, weighted by their approximate net primary production (NPP), a measure of the potential maximum biomass that can be produced in a certain region, given the local geo-climatic conditions[2], [3]. The 2SLS panel regressions confirm the results of the OLS panel regressions. An additional trade path passing by a grid cell is associated with an increased probability of a city rising in that grid cell in the order of 25%.

The results based on ancient cities are not conclusive. First, due to the cross-sectional nature of the data we cannot exclude potential omitted geographic factors that might be driving the 2SLS results (though we do control for a large set of potential confounders). Moreover, an analysis of pre-trends is not possible as, with a couple of exceptions, there are no cities pre-dating bronze usage. Second, the rise of cities is just one of the aspects of the Urban Revolution and it does not capture other crucial features like the increase in socioeconomic inequalities and hierarchical complexity.

To overcome these limitations, in the second subsection, we employ two additional data sources, which report radio-carbon data on the location of archaeological sites in the Old World, which presumably indicate social and political hierarchy (e.g., pyramids, ancient temples, and palaces). The first one is an historical atlas of the most relevant archaeological sites (Whitehouse and Whitehouse, 1975) and the second is a gazetteer for ancient history (the Pleiades Project, Bagnall, 2022). Using a difference-in-difference design, we show that road-knots are associated with a relative increase in settlements archaeological sites during the Bronze Age (as compared to the Stone Age). This result is confirmed in both OLS and 2SLS estimates and is not explained by pre-trends. Our estimates suggest that metal trade accounts for approximately a third of the increase in sites indicative of complex social hierarchies. Admittedly, these back-of-the-envelope calculations are very crude estimates and should be taken with a grain of salt as they assume that the rollout of the metallurgical techniques was uniform across the globe. Still, overall, our estimates suggest that the invention of bronze was definitely not just a by-product of the Urban Revolution but an important driver.

The two sources to capture the rise of social and political hierarchies in this subsection have

[2]To estimate the NPP, we used a paleoclimate simulator, which reconstructs past climate conditions in a high-resolution manner (Karger et al., 2021) in conjunction with a well-established model of habitat development in response to climate (Miami model, see Lieth, 1975)

[3]Using the NPP to measure land productivity comes with important advantages: it is unaffected by human intervention and it captures land productivity for both hunter-gatherers and farmers, independently from the mixed of crops and animals (domesticated or not) used for subsistence.

some caveats: one is dated and the second one is skewed towards Eurasia and Mediterranean Africa. For this reason, in the following two empirical subsections, we move to high-quality regional data (at the cost of losing a global perspective).

In the third subsection, we use the Atlas of Chinese Relics, a 47-volume atlas published by the Chinese National Heritage Administration with detailed information on 500,000+ archaeological sites dating from the Neolithic onwards. We digitise the atlas and we use a Naïve Bayesian text algorithm to identify those sites that are indicative of the rise of the Urban Revolution. Specifically, the algorithm recognize those sites that are indicative of some of the criteria that Gordon Childe use to define the Urban Revolution: large settlements, labour specialisation outside of subsistence, monumental public works, specialised ruling class exempt from manual tasks, a system of recording used in the production process, written documents, and artistic expression. Once again, using both an OLS and 2SLS difference-in-difference design, we find that metal trade led to a statistically significant relative increase in all these seven elements defining the Urban Revolution.

In the fourth subsection, we look at Bronze-Age Europe. We digitise the Prähistorische Bronzefunde, a series of monographs on metal artefacts dating from 3000 to 500 BCE. Specifically, we focus on swords and axes found in graves, which have been argued to be a relevant indicator of relative social status. One of the advantages of focusing on Europe is that we can date the majority of copper and tin mines serving the continent depending on whether they were operating during the middle or late Bronze Age. We can thus study how changes in the road-knots, induced by new mineral discoveries, affected social hierarchy during the Bronze Age. We find that doubling the optimal paths transiting by a grid cell is associated with a three-fold increase in the probability of observing metal weapons in the Bronze-Age graves located in that cell.

The results so far document that metal trade was an important driver of the Urban Revolution: cities and unprecedented inequality were much more likely to emerge in the trade road-knots compared to other regions. But, why is it that road-knots were so crucial to the rise of cities and complex hierarchies? We propose a simple theory that emphasises the appropriability of transit trade. When long-distance trade exploded following the invention of bronze, a new elite relying on taxing transit trade could emerge, leading eventually the rise of cities and more complex hierarchies. We note that transit trade is appropriable not just by a would-be elite, but also by bandits – therefore it also generated a demand for protection and at the same time facilitated taxation to finance the supply of such protection by an elite.

In Section 6, we test for this appropriability mechanism. Guided by theory, we construct a grid-cell measure of the potential revenues from taxing the local transit trade. For each grid cell in the Old World, we compute the increase in global transportation costs in the metal trade network if that cell is removed from the network. The intuition is that fiscal revenues from taxing transit trade in a certain location cannot exceed the transportation

costs that traders would have to incur to avoid passing by that location. Essentially, this variable identifies the bottlenecks in the metal trade network. We then study whether the Urban Revolution is predicted by our measure of potential transit trade (i.e., the road knots) or our measure of potential fiscal revenues (i.e., the bottlenecks). It turns out that, when both variables are included as regressors, only the latter one consistently seems to predict the rise of cities, settlements and archaeological sites produced during the Bronze Age. This result points towards our appropriability theory as the main candidate to explain the impact of transit trade on the rise of the Urban Revolution.

To provide further evidence in support of the appropriability theory, in Section 6, we present six case studies, that illustrate the role of trade in spurring the rise of cities, socio-economic inequalities and states in Mesopotamia, Anatolia, the Indus Valley, the Aegean Sea and China.

The city-state of Assur, the capital of what would become the Assyrian Empire, provides an example of how trade in metals fostered the rise of cities and states in the Bronze Age. Originally, Assur was a small settlement lying on the least productive edge of Mesopotamia at equal distance from Anatolia and Iran. Its fate changed when the bronze metallurgy diffused in the Near East. Anatolia had a dense population supported by productive agriculture but was lacking an indigenous source of tin. The most feasible method for the Anatolians to import tin was engagement with Assyrians, who in turn probably obtained it from the mountains of southwest Iran. Assur became a nodal point on this route. The chiefs of Assur promoted this transit trade by guaranteeing a series of privileges and protection to the traders passing by the city (see Section 7.3 for further details). By the dawn of the second millennia, Assur became the capital of a trade civilization. Assyrian chiefs established a series of trading colonies along the trade routes connecting Assur with the small Anatolian city-states. These trade posts reproduced the legal and financial institutions of Assur and played a crucial role in fostering the economic, institutional, and demographic development of Anatolian city-states. In particular, they were instrumental to the rise of a local elite of Anatolian kings, which were both guaranteeing protection for passing merchant caravans and maintaining roads and bridges in exchange for tolls and taxes on transit trade.

Let us emphasise here, that complex hierarchies and trade pre-date the invention of Bronze. The circulation of prestige goods in the Neolithic indicates both the presence of chiefs, who were able to control the surplus produced in areas with storable crops, and the existence of a system of exchange within a limited territory, with occasional short-lived long-distance connections. What is fundamentally different in the Bronze Age is the scale in both hierarchical complexity and long-distance exchanges. During the Neolithic, there were no states and no long-distance trade networks of the kind that provided all Bronze Age communities, on a regular basis, with metals coming from mines thousands of kilometres away. The shift from local exchange to high-end international trade created, especially through rivers, seacoast and valleys, some clear bottlenecks. Controlling these bottlenecks allowed the rise of a new elite,

which was based on the control (or ownership) of passage routes, rather than agricultural land for storable crops. An example of such a shift from the Neolithic to the Bronze Age is provided by the distribution of tells in Hungary. In the Neolithic, tells were concentrated in the highly fertile lowlands lands along the Tsiza. Archaeological findings of the prestige goods, dating from the period, are found with a typical fall-off curve from the tell indicating a regional economy with very rare long-distance exchanges. During the Bronze Age, new tells formed in vacant areas, lined up along the Danube. These locations made little sense for agriculture: villages located on the bank of a large river have access to only half of the circular catchment area of villages located in the middle of their agricultural land. They made sense, however, in the eyes of a new elite that could easily tax the resulting transit trade. This link between the elite and metal trade is confirmed by the presence of metal hoards in the palaces and bronze objects in the elite burials. These objects also testify the development of regular interregional economic interactions and division of labour (see Kristiansen and Suchowska-Ducke, 2015).

The paper is organised as follows. Section 2 describes the previous literature. Section 3 provides a detailed description of the data used for the empirical analysis. Section 4 lays out the empirical strategy to identify the passage routes in the metal trade network. Section 5 identifies the impact of metal trade on the rise and diffusion of cities and inequality in the Old World. Section 6 describes and tests the appropriability mechanism. Section 7 presents six case studies that are consistent with a metal trade theory of the Urban Revolution. Some concluding remarks close the paper.

2 Previous Literature

Our work speaks essentially to two separate bodies of literature in the social sciences.

First, it contributes to a large empirical literature in economics that studies the role of international connections and market access for comparative development. To our knowledge, our work is a first attempt, within this literature, to go back to the very beginning of the civilization process, has a global scope and provide some empirical validation to the view that trade might have actually been the *raison d'être* of the Urban Revolution. The closest work is Barjamovic et al. (2019), which shows that natural transportation networks are critical in explaining the hierarchy of ancient city sizes in Central Turkey during the Middle Bronze Age (2000-1650 BCE)[4].

Second, our findings contribute to the body of literature that emphasise the role of geography in explaining the emergence of cities and complex hierarchies. Within this literature, three

[4]A recent literature has documented the role of trade in ancient development during the Iron Age. See Bakker et al. (2021) on Phoenician cities, Adamson (2021) on Greek city-states and Flückiger et al. (2022) on Roman cities.

sets of theories have emerged. The first set of theories relates the emergence of the Urban Revolution to the increased productivity of labour that came with agriculture. An example of such a "productivity" theory is provided by Diamond (1998), who famously argued that the early comparative development of Eurasia lies in a series of environmental advantages, which resulted in a larger variety of domesticated crops and animals, and ultimately in both an earlier transition to farming and more productive agriculture[5]. The second set of theories suggests that the Urban Revolution is linked to an increased appropriability in the product of labour by an emerging elite: complex hierarchies and cities are more likely to emerge in regions in which the output of farmers could be easily taxed (or expropriated). An influential "appropriability" theory goes back to Carneiro (1970)'s circumscription theory, which contends that supranational polities emerge in areas with high agricultural productivity surrounded by geographic barriers that prevented farmers from escaping from an expropriating elite[6],[7]. The third set of theories relate the emergence of complex hierarchies with a series of functions that a powerful elite can provide. Prominent "functionalist" theories focus on the demand for the construction and maintenance of hydraulic infrastructures[8] or storage facilities[9] and the demand for stability and security[10] as means to increase the productivity of workers. These three sets of theories provide different mechanisms through which the alluvial lowlands of the Tigris and the Euphrates in Mesopotamia, the Nile in Egypt, the Indus and the Ghaggar-Hakra in India, and the Yellow River in China became the cradles of civilization. The productivity theories highlight the agricultural productivity of alluvial lands, the appropriability theories emphasise the circumscription of these areas or the relatively high productivity of cereal grains, and the functionalist theories point towards the higher scope for a series of infrastructure, like dams or irrigation systems. We propose a different mechanism, which speaks to both the appropriability and the functionalist approaches. Rivers were the highways of the Bronze Age: long-distance trade in metals and grains was forced to transit these rivers, thus creating local demand for a state, able to guarantee the welfare gains from

[5]The productivity theories on the rise of early complex hierarchies have a long pedigree in social sciences. Adam Smith argued that the Neolithic transition produced in some regions large farming surpluses. These surpluses made it possible to have a class of bureaucrats, as a result of labour specialisation, and increased the demand for an extended role of government (Smith, 1978, p. 65). Friedrich Engels (1942) argued similarly that the surplus generated by the adoption of agriculture was a prerequisite for the transition to a class society. More recently, a growing empirical literature in comparative development has shown that a richer prehistoric availability of domesticates is an important predictor of the timing of the Neolithic transition (Ashraf and Galor, 2011), the early emergence of macro-level polities (Borcan, Olsson and Putterman, 2018; Petersen and Skaaning, 2010), independence from colonial powers post 1500 CE (Ertan, Fiszbein and Putterman, 2016) and higher per-capita GDP today (Bleaney and Dimico, 2011; Hibbs and Olsson, 2004).

[6]Mayoral and Olsson (2020) and Schönholzer (2020) provide systematic evidence in support for the circumscription theory of state formation. See also Allen, Bertazzini and Heldring (2022).

[7]More recently, Mayshar, Moav and Pascali (2022) show that the first urban civilizations emerged in regions in which farmers were constrained by geography to grow cereal grains, which are storable and easy to transport, making it relatively easy for an elite to confiscate them and transport them to distant centres of power.

[8]See Wittfogel (1957) and Bentzen, Kaarsen and Wingender (2017).

[9]See Testart et al. (1982).

[10]See Dal Bó, Hernández-Lagos and Mazzuca (2022).

trade, and making it possible to have a state, as transit trade could be easily taxed. Cities in the Bronze Age, with few exceptions, were located on either alluvial valleys or, after 2000 BCE, in coastal regions. One clear advantage of our proposed mechanism is that it can explain not only cities along the rivers but also cities along the coast, as coastal navigation provides an alternative to river navigation to move bulky materials. None of these first coastal cities was located in areas in which agriculture was exceptionally productive, while all of them were located in strategic trade nodes. For instance, in the Mediterranean, the Aegean cities related with the Minoan (from 1900 BCE) and the Mycenean (from 1600 BCE) civilization emerged on a crucial passing point between Europe and the Near East, while the city of Troy (from 1400 BCE), on the Bosporus Strait, could control all trade in and out of the Black Sea. Notice that the long-distance trade explanation of the origin of the Urban Revolution also provides some rationality for a fascinating hypothesis that relates the invention of ironworking with the collapse of the Bronze Age civilizations[11].

The idea that long-distance trade in metals was a fundamental driver of the civilization process is of course not new. Metal trade has been cited repeatedly as a factor in primary state development (Childe, 1930; Sanders, 1968; Polanyi, Pearson and Ahrensburg, 1957). Our theory is particularly close to recent works of Timothy Earle and Kristian Kristiansen[12]. These authors have emphasized the role of long-distance metal trade in fostering a regional economic division of labor. Specifically, they argue that bottlenecks in commodity flows created potential for social segments to control the production and flows of critical metal goods and this eventually led to more complex and ranked societies and the rise of networks of integrated polities[13].

Other authors have emphasised the role of long-distance trade in metals in fostering the development of specific civilizations. Famously, Gordon Childe suggested that the origins of the Egyptian states could be found in the copper long-distance trade between the Nile region

[11] In the 13th century BCE, ironworking starts spreading from present-day Bulgaria and Romania, while all major civilizations in Europe, West Asia and Africa collapsed. Within five decades, almost all cities were destroyed, trade relations were severed, writing systems vanished and populations living along the coast moved to the interior. Palmer (1962) suggested that spread of ironworking might be the reason behind the Bronze Age collapse. Iron is superior to bronze for weapons and agricultural tools and can be found almost anywhere in the Old World. The diffusion of the ironworking technology might have been detrimental for the Bronze Age main civilizations for two reasons. First, it undermined the role of Bronze-Age cities as it nullified their locational advantage on the trade routes towards copper and tin mines and it made obsolete a series of city-institutions constructed to protect interregional trade. Second, it undermined an elite based on the control of metal trade and it allowed newly formed peripheral armies with iron weapons to quickly destabilise entire states.

[12] See Earle (2013); Earle and Spriggs (2015); Earle et al. (2015); Kristiansen and Suchowska-Ducke (2015); Kristiansen and Earle (2015)

[13] According to Kristiansen and Earle (2015): "Participation in the metal trade and in other new forms of long-distance trade in wool/textiles and salt would have demanded the creation of political alliances linking polities together – sometimes in confederations – in order to protect traders and their products. Participation in such institutionalized networks (providing wealth finance) and the formation of institutionalized warrior groups enabled local chiefs and centrally located tells to mobilize local resources (stable finance) by controlling the distribution of metal for both subsistence and prestige goods."

and the Red Sea[14]. In a series of works, Guillermo Algaze (Algaze, 1993, 2001, 2009) argued that the emergence of early cities and complex states in the southern Mesopotamian alluvium was a result of regional imbalances in the availability of various resources and a geographical framework of the area, which allowed for the efficient movement of commodities via water transport. These two factors led to the emergence of long-distance trade, mainly in metals. Local elites would appropriate the gain from this trade either directly, through state control of trade, or indirectly, utilising state control of both the commodities that were exchanged and the means of production. This inception of exchange systems would then be a powerful mechanism for the emergence of more complex sociopolitical structures. Kuhrt (1995) argued that the Assyrian elites were deriving their wealth mainly from taxing transit trade and that the main Assyrian cities emerged in areas that were not particularly productive but that were crucial trade nodes in the tin and copper trade. A long tradition, dating back to Herodotus, attributed the flourishing of the Minoan and Mycenaean civilizations with trade in metals in the Aegean first and the wider Mediterranean Sea later[15]. With respect to this literature on metal trade and the Urban Revolution, our approach has two advantages. First, we do not focus on a particular region or society: we test a general theory on the role of Bronze and trade in metals on the rise of the first urban civilizations using data covering the entirety of the Old World. Second, we use a natural experiment of history to infer causality.

3 Data

3.1 Urban settlements

Data on urban settlements are drawn from the spatially explicit dataset of urban settlements developed in Reba, Reitsma and Seto (2016). This dataset spans the time period 3700 BCE–2000 CE.[16] We focus on the period up to 1300 BCE and construct a simple cross-sectional dummy, indicating whether a city had emerged in a grid cell by the end of the Bronze Age (i.e., by 1300 BCE).[17] As an alternative outcome, we compute the number of cities located within a given grid cell. There are a total of 63 cities which fall into 45 separate grids. The location of these cities are represented by the grey-shaded dots in Figure 1.

[14] In the words of Childe (1930): "Some favourably situated villages grew into real towns, and the chief of one of them, Abydos, that commanded one main caravan route to the Red Sea and the East, was eventually able to master the whole land to the Mediterranean coasts, founding what is termed the First Dynasty (about 3100 BCE).

[15] In a different context, Bates (1983) argues that "the origins of the state lie in the welfare gains that can be reaped through the promotion of markets". He supports this view by showing that, on a set of 34 African agrarian societies the proportion of societies with central monarchs was higher around ecologically diverse environments. Fenske (2014) provides further supportive evidence for this theory on a larger sample of pre-colonial African societies.

[16] The dataset is based on urban population estimates reported in Chandler (1987) and Modelski (2003).

[17] Results are not sensitive to the exact choice of the cutoff date. We obtain extremely similar results when we use any date between 1500 BCE and 500 BCE as a cutoff.

In a robustness test, we use urban population data from the HYDE 3.1 database (Klein Goldewijk, Beusen and Janssen, 2010). This data source offers spatially explicit urban population estimates for every 1000 years. For our analysis, we use estimates for the year 2000 BCE.[18]

3.2 Archaeological sites

We draw on two separate data sources on the location of archaeological sites. The first source is Whitehouse and Whitehouse (1975)'s Archaeological Atlas of the World. The atlas contains information on the most relevant global prehistoric archaeological sites known at that time and includes a total of 4,215 sites that are all radiocarbon dated. We geocode these sites and use information in the map titles and accompanying texts to identify which sites were established in the Stone and Bronze Age, respectively. Of all sites, 1,487 are assigned to the former and 1,373 to the latter period.[19] For the empirical analysis, we create a 1×1 degree grid cell level panel data set with two time periods: Stone Age and Bronze Age. Our primary outcome is an indicator that takes the value of one if any site is present in a given grid and period.

The second source we exploit to construct time-varying outcomes is the Pleiades Project (Bagnall, 2022).[20] For the purposes of our analysis, we draw on the pleiades-places dataset which lists the location of historic places along with a categorisation of each place. Following Bakker et al. (2021), we use only places for which the location is precisely known and create two classes of places: archaeological sites and settlements.[21] The first class includes all places characterised by the presence of any man-made structures. The second class of places—settlements—is restricted to places that Pleiades labels as 'settlement' or 'urban'.

To assign the Pleiades places to time periods we use two alternative approaches. First, we use the (textual) description given in the Pleiades database to identify the time period in which a place was created.[22] For our analysis, we keep all places that were established during the Stone or the Bronze Age. This leaves us with a total of 930 places. Of these, 251 exist during the Stone Age and 679 during the Bronze Age.[23] We then count how many settlements and sites, respectively, fall into a given 1×1 degree grid cell and period. The result is thus a two-period grid-cell level panel dataset.

As a second way of assigning places to time periods, we exploit the (numeric) estimates of start and end date of a place which are reported in the Pleiades database. On the basis of these dates we construct a panel dataset that covers the years 6000–1300 BCE at a 1,000 year

[18] Using estimates for the year 1000 BCE leaves our results unchanged.

[19] Figure A.1 shows the spatial distribution of these sites.

[20] See `pleiades.stoa.org/docs` for detailed documentation.

[21] Bakker et al. (2021) refer to these two classes as 'wide' and 'narrow'. See Bakker et al. (2021, p.658) for more details.

[22] The time period information is listed for each place. Examples of descriptions for different time periods are: 'Middle Bronze Age Anatolia', 'Mesolithic Levant', 'Iron Age Britain', or 'Roman'.

[23] The spatial distribution of the sites used in our analysis is depicted in Figure A.2.

interval.[24] For each millennium we then determine how many settlements and archaeological sites lie within a grid cell in a given millennium. This gives us a five-period grid-cell level panel dataset.

3.3 China

Data on the rise and spread of the Urban Revolution in China are drawn from the Chinese Cultural Heritage Atlas, the most comprehensive catalogue of Chinese archaeological sites. This source is based on joint efforts between the Chinese central and provincial cultural heritage bureaus to compile a mapping of all excavated monuments and remains in China. The catalogue is completed for 28 out of 34 provinces (data for the provinces of Taiwan, Macau, Hong Kong, Jiangxi, Guizhou and Hainan are still under construction). Each archaeological site is geocoded, dated and described in detail. We OCR the 31 volumes that compose the Atlas and focus on the 85,000+ sites dating Before the Common Era. The spatial distribution of these sites is illustrated in Appendix Figure E.1. Each site contains a long description (on average 58 words). For a tenth of the sample, we manually coded whether this description makes any reference to one of the following features: 1) urban settlements, 2) full-time specialists in non-subsistence activities, 3) ruling class exempt from manual tasks, 4) monumental building, 5) a standardised system of measures and recordings used in exchange and production, 6) writing, 7) highly developed art forms. After developing this training sample, we use a naïve Bayesian classifier to classify all sites in the Atlas according to these seven criteria. Appendix Figure E.2 reports a correspondence plot which details the words that are overused to describe the sites classified according to each criteria. For instance, in the top right, we can see that words like "city", "township", "wall", "village" are associated with the criteria "Urban Settlements", while words like "Han", "Dynasty" , "State", are associated with the criteria "Ruling Class". Once each site has been classified, we then count how many sites associated with criteria indicative of the Urban Revolution in each 1×1 grid cell in the Paleolithic, Neolithic and Bronze Age.

3.4 Europe

Europe is the most studied region in world archaeology. In this context, we attempt to measure the evolution of socio-economic stratification during Bronze Age, by studying the findings of high-value grave goods—particularly bronze weapons—which are indicative of the existence of local chiefdoms (Renfrew and Bahn, 2016, pp. 175, Earle et al., 2015).

We extract information on location and type of bronze weapons from the *Prähistorische Bronzefunde* (PBF). This research project systematically gathers information on archaeological *metal* artefacts (predominantly bronze artefacts) excavated in Europe. Since 1966, the project has published 186 volumes which record details on individual metal finds dating from

[24] The time intervals are: [6000, 5000), [5000, 4000), [4000, 3000), [3000, 2000), [2000, 1300]

3000 to 500 BCE. PBF organises these volumes into series of books—referred to as *Abteilungen* (divisions)—according to the type of artefact. For example, *Abteilung IX* covers axes and hatchets and includes 29 volumes. Each of these volumes, in turn, covers axes and hatchets excavated in one specific region. The PFB typically commissions an archaeologist specialising in this region to collate information on excavated artefacts from a variety of sources (e.g., museums).[25]

Throughout, we focus on Bronze Age weapons. Specifically, we draw artefacts classified as 'axes and hatchets' and 'swords' (*Abteilung IX* and *Abteilung IV*). The former contains 29 volumes, the latter 10 volumes. We supplement these data with artefacts from the 'Bronze- und urnenfelderzeitliche Schwerter' database (Hahnekamp, 2011).[26] We provide further details on the sources and data construction processes in Appendix F.

For each individual artefact in our database,we observe following three key pieces of information: (i) the geographical location of the excavation site, (ii) the nature of the excavation site (e.g., burial site), and (iii) the archaeological type or archaeological family of the artefact (e.g., Pădureni axe type). Based on (ii) we can identify if a bronze weapon was a grave good or not. The detailed description of the artefact itself, (iii), allows us to assign the individual artefact to specific cultures which, in turn, enables us to map them to time periods (Early-, Middle- and Late Bronze Age).

For our empirical analysis we create a 1×1 degree grid cell panel data set comprising two time periods: Early/Middle Bronze Age [3000 BCE, 1300 BCE) and Late Bronze Age [1300 BCE, 500 BCE]. Using aspects (i)–(iii) we define our measure of hierarchy as a dummy that takes the value one if a bronze weapon is discovered at a Bronze Age burial site in a given cell and period, and zero otherwise. Table A.3 reports summary statistics of the dataset.

3.5 Bilateral trade flows

We reconstruct trade flows for prehistoric periods using archaeological artefacts. For artefacts to be included in our analysis, two requirements have to be fulfilled. A first prerequisite is that an artefact's find site as well as its provenance can be identified. This allows us to reconstruct trade flows by defining the archaeological excavation site as the destination and the production site as the origin.[27] The second prerequisite is that the period of production is known. In the main analysis, we will focus on goods produced and traded during the Bronze Age. For robustness checks, we will alternatively use goods produced during the Stone Age.

Combining existing databases we were able to identify approximately 7,500 artefacts that fulfil the two inclusion requirements. These artefacts vary in type and range from weapons, to jewellery and utensils. For the Bronze Age, we estimate trade costs based on 3,744 metal-

[25] For example, the volumes on bronze axes and hatchets excavated in Romania (*Abteilung IX: Äxte, Beile—Die Äxte und Beile in Rumänien I–II*) were written by Alexandru Vulpe a Romanian archaeologist.

[26] http://chc.sbg.ac.at/schwerter/map.php

[27] See Flückiger et al. (2022) for a similar use of archaeological data.

based artefacts. These data are taken from Flückiger et al. (2022). For the Stone Age we can draw on around 3,700 artefacts. Data are taken from two existing databases (Pétrequin et al., 2012; Schauer et al., 2020). A more detailed description, including figures depicting the spatial extent of the trade data, is presented in Appendix B.

Based on the geocoded information on provenance and excavation site, we assign the artefacts to their respective 1×1 degree grid cell of origin and destination. We then aggregate this information to the grid-cell-pair level giving us the number of artefacts excavated in grid cell j and produced in grid cell i for the Stone Age and Bronze Age, respectively.

3.6 Mines

We compile our dataset on location of metal mining sites in an extensive review of the archaeological literature. The requirement for inclusion of mines in our analysis is that the location of the mine as well as activity during the Bronze Age is identifiable. Our final dataset encompasses 44 tin mines (that fall into 30 distinct 1×1 degree grid cells) and 121 copper mines (located in 79 separate grid cells). Figure A.3 in Appendix A shows the spatial distribution of these mines. The appendix also provides a detailed description of the data gathering process and a list of mines. For a subset of mines, we do—in addition to knowing that they were active during the Bronze Age—have estimates on the years during which they were active. However, these estimates are often associated with a substantial degree of uncertainty and therefore to be interpreted with caution. In our main analysis, we therefore assume that the mines are active during the whole Bronze Age period. For Europe—the worldwide best-researched area—more reliable estimates on start and end dates of mining are available. We exploit this in our case study of Europe (Section 5.4).

3.7 Other data

We construct a range of additional grid-cell level geographical characteristics for our empirical analysis. Time-invariant aspects include the distance to the coastline, the latitude of the grid cell centres, and a dummy indicating whether a grid cell touches the coast. To account for the importance of rivers, we use the Strahler order of streams. This is an index that ranges from one to six, representing the size of the largest river (Vörösmarty et al., 2000). Furthermore, we extract elevation data from WorldClim (v. 2.1) on the basis of which we also calculate terrain ruggedness using the index devised in Riley, Degloria and Elliot (1999).[28] We account for the Caloric Suitability Index (CSI) developed in Galor and Özak (2016). This index captures the average potential yields within each cell attainable given the set of crops that are suitable for cultivation in the pre-Columbian period. Finally, we also construct a measure for the proximity to mines. We define this as the metal-weighted sum of transport costs to the cost-minimising copper and tin mine. We take the inverse of these costs in order to interpret

[28] This index is, for example, also used in Nunn and Puga (2012).

it directly as a measure of proximity.[29]

Time-varying factors constructed for analysis include average temperature and precipitation (Karger et al., 2021) and the grid cells' proximity to (all) other croplands, i.e, its market potential. The latter represents a measure of centrality with respect to (potential) consumer markets. Following the literature, we define the market potential as the inverse transport cost-weighted distance to cropland area (Harris, 1954).[30]

Summary statistics for all datasets are presented in Table A.3. For our empirical analysis, we transform the trade transit index and the instrumental variable using the inverse hyperbolic sine transformation (IHS).[31] Continuous variables that do not contain zeroes are transformed using the natural logarithm function. To facilitate comparison of effect sizes across different variables, we standardise all variables to a mean of zero and a standard deviation of one.

4 Bronze Age transit trade

4.1 Period-specific transport costs

Of central importance to our analysis are transport costs. These allow us to determine how costly transport is to and from metal mining sites. Transport costs are also a key input in the prediction of transit trade intensity.

To the best of our knowledge, widely accepted estimates of per-unit distance transport costs are not available for the Bronze Age. Existing estimates of pre-historic transport costs produced by archaeologists and historians are based on spatially confined case studies (see Jones and Madsen, 1989; Brannan, 1992, and references therein). Additionally, some scholars have used (minimum) travel times for humans as proxy for transport costs (e.g., Barjamovic et al., 2019; Özak, 2010). The latter approach is not suited for the purposes of our analysis, as time-minimising transport routes can differ substantially from routes that minimise the cost of transporting goods (see, e.g., Flückiger et al., 2022).

To overcome existing limitations, we take a spatially explicit approach to estimating relative per-unit-distance transport costs for different shipping modes. More specifically, we infer sea, river and overland transport costs on the basis of prehistoric trade flows reconstructed from archaeological artefacts (see Section 3 for details). Using this bilateral trade data we use the following procedure to estimate Bronze Age-specific trade costs: We start by dividing the

[29] Formally proximity to mines M_g is defined as: $M_g = \sum_{m \in \text{copper, tin}} \frac{1}{C_g^m} \times w_m$, where C_g^m is the cost associated with shipping metal from the cost-minimising mine producing metal m to grid g, and w_m reflects the input weights (i.e., 0.9 for copper and 0.1 for tin).

[30] Formally, the proximity to cropland (PC) is given by $PC_{g,p} = \sum_{c \notin g} \frac{1}{C_d^g} \times crop_{c,p}$, where C_d^g are the transport cost from grid cell c to cell g and $crop_{c,p}$ is the croplands area of cell c in period p.

[31] The IHS is defined as $IHS(x) = \left(x + \sqrt{x^2 + 1}\right)$. It approximates the natural logarithm function but is well-defined at zero.

world into transport surface grids of 0.25×0.25 degrees and assign each grid cell to one of the following shipping modes: sea, river, or land.[32] Each of these modes is associated with a per-unit distance transport cost: $\left(\alpha_{BA}^{sea}, \alpha_{BA}^{river}, \alpha_{BA}^{land}\right) = \boldsymbol{\alpha_{BA}}$. As only relative transport costs can be identified, we normalise transport over sea to one throughout, i.e., $\alpha_{BA}^{sea} = 1$. The vector $\boldsymbol{\alpha_{BA}}$ thus captures how expensive a given shipping mode is relative to maritime transport during the Bronze Age.

Because $\boldsymbol{\alpha_{BA}}$ is unknown, we infer relative per-unit shipping costs by searching over values of $\boldsymbol{\alpha_{BA}}$ that minimise the log-likelihood of a standard gravity regression, where trade flows are regressed on $\boldsymbol{\alpha_{BA}}$ and a set of origin and destination fixed effects (see Donaldson (2018) for a very similar procedure). This produces an estimate of $\boldsymbol{\alpha_{BA}} = (1, 2, 6)$. We estimate Stone Age-specific relative transport costs using the same procedure. The only difference being that we use goods transported during the Stone Age to infer costs. The resulting transport mode-specific per-unit shipping cost estimates for the Stone Age are: $\boldsymbol{\alpha_{SA}} = (1, 1/14, 2/7)$. More details on the estimation procedure are provided in Appendix B.

Comparing the transport cost vectors of the Stone and Bronze, our estimates suggest that the relative costs of shipping goods changed dramatically across modes. Most strikingly, transport by sea evolved from being the most expensive way of moving goods during the Stone Age to being the cheapest one in the Bronze Age. This implies that technological progress was heavily biased towards seafaring in the latter period. Reassuringly, this aligns well with archaeological evidence. During the Stone Age, waterborne transport depended entirely on dugout canoes. These canoes had shallow hulls and were propelled by men using oars or paddles. They were therefore neither suited for (or capable of) long-distance journeys nor large-scale cargo transport (Rahmstorf, 2010). As a result, long-distance trade took place overland. For example, goods exchanged between the Near East and Mediterranean Europe were most likely transported via the Anatolian land bridge (Rahmstorf, 2010). This pattern overland-dominated transport changed with the development of deep-hulled boats alongside the invention of sails at the beginning of the Bronze Age. The plank boats with deep hulls had the capacity to carry several tonnes of goods and were stable enough to be used for coastal shipping. The sailing technology further contributed to a reduction in seaborne transport by increasing the manoeuvrability and speed of boats (e.g. Nessel, Neumann and Bartelheim, 2018). Together, these technological innovations facilitated large-scale transport of goods via sea routes, making seaborne transport the most cost-effective mode of shipping goods over long distances (e.g. Nessel, Neumann and Bartelheim, 2018). This resulted in the economic integration of the Mediterranean and Mesopotamia as well as flourishing long-distance trade between Mesopotamia and the Indus civilization via the Indian Ocean (e.g., Rahmstorf (2010), Cunliffe (2011, p.189) or Vogt (1996)).

[32] The relatively coarse size of cells is chosen to account for the fact that coastlines as well as river courses can shift over time.

Our estimates further suggest that there was a moderate decline in overland transport costs relative to river transport between the Stone and the Bronze Age.[33] Again this finding aligns well with the archaeological. During the Stone Age, goods were transported overland by humans or ox wagons, implying limited cargo carrying ability and slow progress across space. A number of important innovations increased both the speed and freight capacity during the Bronze Age. For example, the spoked wheel was invented along with chariots and other transport vehicles (Uckelmann, 2013). Furthermore, the Bronze Age saw the domestication of horses which subsequently allowed harnessing them to vehicles. Similarly, the domestication of the camel made overland transport of bulk commodities in arid regions feasible.

Summing up, our transport cost vector estimates map well onto the findings of the archaeological literature. They suggest that coastal and river transport was relatively less expensive than overland shipment during the Bronze Age. A further take-away—not directly deducible from our estimates—is that transport costs dropped dramatically across all modes during the Bronze Age, thus further facilitating long-distance trade.

4.2 Transit trade

Combining the information on location of metal mines with our estimates on Bronze Age-specific transport costs, we construct our main explanatory variable: the grid cell's predicted transit trade intensity in bronze inputs. We subsequently refer to this variable as the 'transit trade index'. Throughout, we implicitly assume that the input factors are directly transported from the mines to the final destination (consumer market), where they are then further processed into final goods. This implies that bronze casting takes place at the final destination. That is, copper and tin are imported by the 'destination' grid cell and then combined at a ratio of 90% to 10% to form bronze.

We also assume that a consumer grid cell imports a given input factor from the mine associated with the lowest shipping costs. In other words, a grid cell draws copper (tin) only from the copper (tin) mine to/from which transport is cheapest. The cost-minimising mine (separate for each metal) is identified in a two-step procedure. First, we identify the least-cost paths and the associated transport costs from all mines to a given destination grid using Dijkstra (1959)'s algorithm and the Bronze-Age-specific shipping costs $\boldsymbol{\alpha_{BA}}$.[34] Second,identify the mine for which the transport costs are lowest. In the following, we denote the least-cost path (i.e. the route) connecting a destination grid d to the transport cost-minimising mine producing metal m as LCP_d^m. The cost associated with this path is represented by C_d^m.

[33] However, it is important to note that river transport is relatively cheaper (compared to overland transport) during both the Stone Age and the Bronze Age.

[34] In analogy to the inference of transport costs, we use a transport cost surface of 0.25×0.25 degrees to identify least-cost paths. Sea transport is restricted to coastal regions (where the maximum permissible distance from the coast is 50 kilometres).

Transit trade index

Based on the assumptions outlined above, we define the transit trade index as the number of least-cost paths that connect the mines to destinations and intersect grid cell g. We weight each least-cost path taking into account the importance of the destination (i.e., size of consumer market) and the input metal. The weight of the destination is based on the total cropland area ($crop_d$), where destinations with more extensive croplands receive higher weights.[35] The cropland data are drawn from Klein Goldewijk, Beusen and Janssen (2010) who provide estimates on land use at 1000 year intervals. Throughout, we use values for the year 3000 BCE. Figure A.4 visualises the spatial distribution of the croplands for that year. The weighting of inputs reflects the ratio at which copper and tin are combined to produce bronze. Accordingly, we set $w_{\text{copper}} = 0.9$ and $w_{\text{tin}} = 0.1$.

Combining all building blocks, we compute our measure of transit trade:

$$T_g = \sum_{\substack{m \in \\ \text{copper, tin}}} \sum_{LCP_d^m \cap g} w_d \times w_m, \tag{1}$$

where T_g represents our transit index of grid cell g. The least-cost paths that intersect the grid are symbolised by $LCP_d^m \cap g$, the metal input weights by w_m, and the destination weights by w_d. Equation (1) illustrates that variation in T_g is generated from four sources: (a) the location of mines and (b) the relative transport costs. These two factors determine the course of the least-cost paths. The metal weights (c) and destination weights (d), in turn, determine the mass assigned to each path.

A natural interpretation of our transit index is that it captures the volume of metal that crosses a given region on its way from mining sites to population centres. This implies that the higher the volume, the greater the cell's scope to exploit the gains of trade—including the taxation of transit trade—and the more likely it becomes that civilizations emerge.[36] Also noteworthy is that our transit trade index is closely related to the concept of betweenness centrality.[37]

Figure 1 visualises the spatial distribution of the transit trade index, where darker shadings indicate a greater trade intensity. Also depicted is the location of cities, as represented by the dots. Consistent with the archaeological evidence that transit trade in bronze inputs was an important driver of the Urban Revolution (see Section 1), Figure 1 suggests that most cities emerged along clearly discernible trade corridors. In the subsequent sections, we formally test

[35] The use of croplands as proxy for the demand/market size is based on the observation that copper and tin were often exchanged for crops (e.g. Earle et al., 2015).

[36] Ultimately, however, how much tax can be raised depends not only on the volume of transit trade (as measured by our index), but also on how costly it is to reroute trade through other cells. In Section 6 we introduce the measure of Modified Efficiency Centrality which allows us to gauge the importance of taxation in explaining our results.

[37] Betweenness centrality represents the number of least-cost paths connecting node-pairs within a network that pass through a given node.

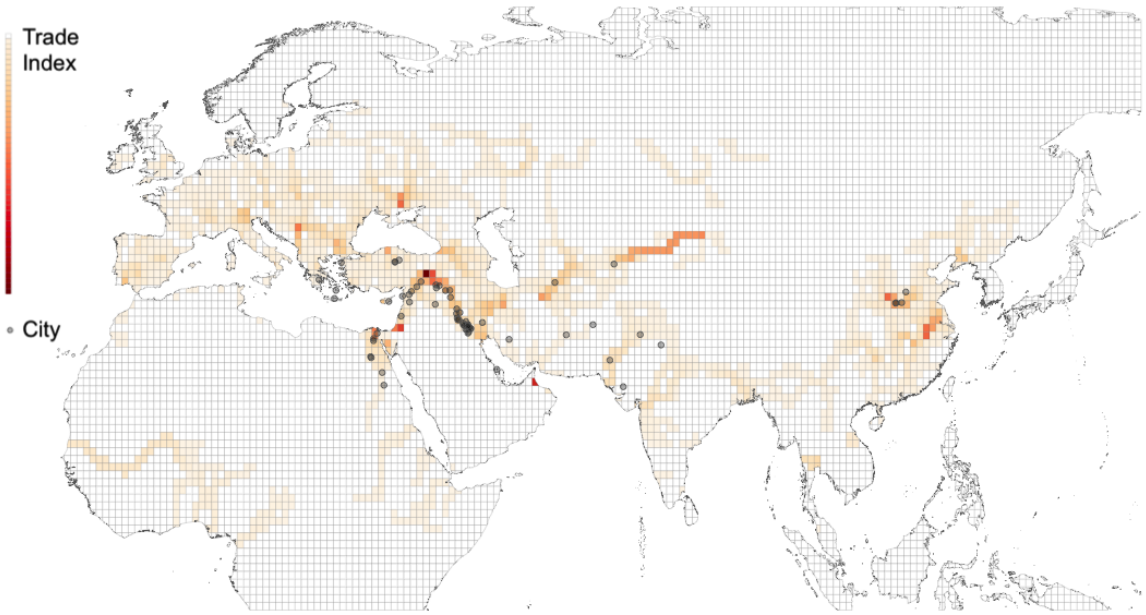


Figure 1: Geographic scope of analysis, location of cities, and transit potential.
Figure depicts the location of cities up to 1300 BCE (Reba, Reitsma and Seto, 2016) along with the predicted transit trade intensity in bronze inputs of grid cells. Cities are represented by dots. The shading represents predicted transit intensity in 3000 BCE, where darker shadings imply greater intensity.

for the existence of this relationship.

Deposit and climate-based instrumental variable

The main threats to the validity of our empirical analysis are the presence omitted variables, measurement error as well as the possibility that the location of mines and croplands are endogenous to outcomes (see Section 5 for a more detailed discussion). In order to address these threats, we construct an instrumental variable in analogy to Equation (1). The difference being that we replace the location of mines as well as the destination weights with factors that are plausibly exogenous to economic activity during the Bronze Age. More specifically, we exchange the location of known Bronze Age mining sites with the location of tin and copper deposits. These data come from U.S. Geological Survey (2011) and represent all known deposits as of 2011—irrespective of whether they are exploited or not. In analogy to the procedure described above, we then identify the least-cost paths (and associated costs) that connect each grid cell to the cost-minimising copper and tin deposit, respectively. When assigning destination weights, we use local net primary production (NPP) rather than cropland areas. NPP is a measure of agricultural potential that is constructed using solely exogenous temperature and precipitations as inputs.[38] The climate data required for the computation

[38]More technically, NPP is defined as the difference between the energy fixed by autotrophs and their respiration. We construct NPP following the Miami model (Lieth, 1975):

$$NPP_d = \min(NPP_d^T, NPP_d^P),$$

of the NPP come from Karger et al. (2021). Combing the deposit and climate data, our instrument for transit trade intensity—D_g—is given by:

$$D_g = \sum_{\substack{m \in \\ \text{copper, tin}}} \sum_{LCP_d^{D_m} \cap g} \omega_d \times \omega_m, \tag{2}$$

where $LCP_d^{D_m} \cap g$ are least-cost paths that connect destinations to cost-minimising deposits of metal m and intersect grid cell g, ω_d are the NPP-based destination weights for period, and ω_m are the metal input weights. In keeping with our transit trade index we use climate values for the year 3000 BCE to construct the destination weights ω_d. Figure A.5 illustrates the distribution of deposits and NPP along with the resulting values of the instrumental variable.

5 Metal trade and Urban Revolution

5.1 Cross-sectional evidence: Cities by 1300 BCE

This subsection examines the link between metal trade and Bronze-Age urban settlements. The goal is to assess whether cities arose in the road knots of the metal trade network and suggest a causal relationship. Figure 1 shows the spatial distribution of the potential transit trade, as dictated by both the natural topography and the distribution of Bronze-Age metal mines and cropland, against the cities that emerged before the collapse of the Bronze Age. A visual inspection provides a first clue of the positive correlation between the location of Bronze-Age road-knots and cities. We formally test for this correlation by estimating the following equation:

$$y_g = \theta \; IHS(T_g) + X_g' \, \phi + \varepsilon_g, \tag{3}$$

y_g is a dummy indicating whether a city had emerged in grid cell g during the Bronze Age.[39] The main regressor of interest is T_g, the transit trade index of grid cell g, transformed using the inverse hyperbolic sine (IHS) transformation. The IHS transformation behaves like a log (thus filtering out scale effects) but it allows to retain the zero-value observations. In Appendix C, we show the empirical results without applying this transformation (i.e., using the raw values). The vector X_g represents a set of geographical controls.

To correct for spatial autocorrelation of the error term we estimate standard errors in two different ways: we allow either for clustering at the 5×5 grid cell level or for spatial autocorrelation, using Conley (1999) standard errors, with distance cutoffs of 1000 Km. In Appendix

where NPP_d represents net primary production in destination grid d, and $NPP_d^T = 3000/(1 + e^{1.315 - 0.119\,T})$, and $NPP_d^P = 3000/(1 - e^{-0.000664\,P})$. Average annual temperature is symbolised by T and the sum of annual precipitation by P.

[39] For ease of interpretation, we multiply the dummy by 100.

Figures C.1a–C.1b we show how results are affected by varying the size of the clustering grid (from 1×1 to 20×20) or the Conley cutoff (from 100km to 2,000km). The takeaway is that the size of standard errors is practically unchanged when relaxing the boundaries of spatial correlation above those that we chose as benchmarks.

Table 1: OLS cross-sectional evidence: Reba, Reitsma and Seto (2016) city data

	Any City by 1300 BCE (×100)					# Cities (×100)
	(1)	(2)	(3)	(4)	(5)	(6)
Transit Index	0.388	0.392	0.360	0.436	0.377	0.528
	(0.112)***	(0.115)***	(0.106)***	(0.121)***	(0.109)***	(0.156)***
	[0.150]***	[0.154]**	[0.140]**	[0.164]***	[0.142]***	[0.214]**
Proximity mines		-0.018			-0.939	-1.627
		(0.049)			(0.329)***	(0.714)**
		[0.056]			[0.434]**	[0.977]*
Proximity croplands			0.211		1.289	2.123
			(0.092)**		(0.419)***	(0.867)**
			[0.124]*		[0.545]**	[1.166]*
Land productivity				-0.039	-0.012	-0.011
				(0.013)***	(0.013)	(0.020)
				[0.018]**	[0.017]	[0.027]
Geography controls	No	No	No	No	Yes	Yes
Continent fixed effects	Yes	Yes	Yes	Yes	Yes	Yes
Observations	9,426	9,426	9,426	9,426	9,426	9,426
Mean dependent variable	0.477	0.477	0.477	0.477	0.477	0.668
R^2	0.021	0.021	0.022	0.022	0.032	0.024

Notes: This table reports estimates of Equation (3) using OLS. Standard errors clustered at the level of 5×5 degree grid cells reported in parentheses. Standard errors computed using the approach of Conley (1999) (cut-off 1000km) are reported in square brackets. 'Any city by 1300 BCE' is a dummy equal to one if a city was present in a given 1×1 degree grid cell by 1300 BCE. Variable is multiplied by hundred to facilitate interpretation. '# Cities' is the total number of cities that had emerged in a grid grid cell by 1300 BCE. Variable is multiplied by hundred to facilitate interpretation. 'Transit trade index' is the cropland and metal input weighted number of least-cost paths that intersect a grid cell, as defined in Equation (1). 'Proximity mines' is the inverse input weighted average transport costs to metal mines. 'Proximity croplands' represents the grid's proximity to croplands, defined as the inverse transport cost weighted distance to croplands. 'Land productivity' is the cell's agricultural potential, measured by the caloric suitability index of Galor and Özak (2016). 'Geography controls' include latitude, elevation, precipitation, temperature, Strahler index, log distance to the coastline, and a dummy variable indicating whether a grid cell lies at the coast.* $p < 0.10$, ** $p < 0.05$, *** $p < 0.01$.

Table 1 reports the OLS estimates. The data source for the location of Bronze-Age cities is Reba, Reitsma and Seto (2016). The dependent variable captures all cities in the database that emerged before the end of the Bronze Age (1300 BCE). In the benchmark specification, the transit trade index is computed using the distribution of cropland in 4000 BCE, the first data point available before the beginning of the Bronze Age. Column 1 shows the most parsimonious specification, in which the only controls are a set of continent fixed effects. The estimated coefficient on T_g is positive and statistically significant. To interpret its magnitude, consider a grid cell crossed by one optimal path connecting a mine with a fully cultivated cell. Assume that a second optimal path crosses the same grid cell: this will imply an increase in the transit index by approximately 67 percentage points, which translates in an increased probability of having a city in the cell of 0.26 percentage points. This is a remarkably large

number: only 0.48 percent of grid cells have a city by 1300 BCE. A natural conjecture, when looking at this correlation, is that it might be explained by the fact that cells with higher transit trade index are also generally closer to metal mines or large cropland areas (and therefore populations). In columns 2-3 of Table 1, we run a horse-race exercise between three potential explanations of an early civilization process that might be captured by our trade potential measure: the potential for transit trade, the proximity to sources of metals, the proximity to densely populated area (or a cultivated land). It turns out that: 1) The correlation between the transit trade index and the location of Bronze-Age cities is unaffected when controlling for proximity to either mines or cropland. 2) Proximity to metal mines is negatively correlated with cities: this is explained by the fact that Bronze-Age copper and tin mines are generally located in far-away mountainous areas 3) Proximity to croplands is positively correlated with cities, which is in line with our prior that cities cannot be located too far away from agricultural areas. In column (4) we control for land productivity, as measured by the potential caloric yield of a given grid cell attainable given the set of crops that were suitable for cultivation in the pre-1500 period (c.f. Galor and Özak, 2015; Galor and Özak, 2016). Land productivity is commonly mentioned as a determinant of early urbanisation and hierarchy. However, conditional on the transit trade index, land productivity is negatively associated with the presence of cities, a first hint that the conventional productivity theories behind the rise of Urban Revolution do not seem to be confirmed in the data. More importantly, the inclusion of land productivity does not influence the point estimate of our transit trade index. To identify the passage points in the metal trade network, we rely not only on the distribution of mines and cropland, but also on three geographical features: the location of major rivers, coastal lines and land elevation. In column 5, we control for these three features in addition to proximity to mines, proximity to croplands, and land productivity. One more time, the estimated coefficient on the T_g is practically unaffected. In the final column of Table 1 we use the number of cities rather than a simple indicator variable as outcome. Reflecting previous results, we find that potential transit trade is positively correlated with the number of cities located in a grid cell.

The OLS estimates of equation 3 are far from having a causal interpretation. While the stability of point estimates across the regression specifications in columns (1)–(5) goes some way in mitigating concerns related to omitted variables, endogeneity remains a worry. Variation in the trade potential is inter alia driven by the spatial distribution of croplands and mines, both of which are likely to be affected by the location of Bronze-Age cities and civilizations. To get closer to a causal link between metal transit trade and the rise of cities, we use a 2SLS panel estimation framework. The instrumental variable, which was described in detail in the previous section, is an alternative measure of potential transit trade, which captures the passage regions connecting mineral deposits and productive land, two objects unaffected by human intervention (differently than mines and cropland). We remind the reader that the

specific measure of land productivity we use to construct this variable captures the potential biomass that can be produced in a certain region (as dictated by the climate): it does not depend on the exploitation strategy of the land (i.e., it works for both hunting-gathering and agriculture). In addition to endogeneity concerns, the IV approach also allows us to address the possibility that measurement error in our transit trade index—e.g., induced by incomplete information on location of tin and copper mines—creates an attenuation bias. Formally, the first stage of our 2SLS-instrumental variable approach is represented by:

$$IHS(T_g) = \delta\, IHS(D_g) + X_g'\,\eta + \zeta_g, \tag{4}$$

where D_g is the instrumental variable.

The 2SLS estimates are presented in Table 2. Panel A reports the second-stage estimates, while Panel B reports the first-stage. Looking at panel B first, we can see that our instrument successfully predicts transit trade. The first-stage F-statistic ranges between 276 and 67. The estimated coefficient on the IV is positive (as expected), statistically significant and stable across regression specifications. The second-stage estimates support the validity of our earlier results. Practically, there are no changes between the OLS and IV estimates on the estimated coefficient on T_g.

A potential concern, related with our excluded instrument, comes from the mode-specific relative transportation costs that are used for its construction. As discussed in section 4.1, these relative costs are estimated from Bronze-Age bilateral trade relationships in Europe and the Middle East. This implies an important threat to our identification strategy. Bronze-Age transportation technologies might have been developed to serve the specific needs of Bronze-Age civilizations (in Europe and the Middle East): cities might be central in the metal trade network not because they are in natural passage regions between mines and cropland but because they develop specific transportation technologies to gain easy access to cropland and mines. To alleviate this concern, we run two robustness checks. First, we document that our estimates remain stable if we restrict the spatial extent of our analysis to areas that are not used in the estimation of the relative transportation costs (see column (1) in Appendix Table C.1). Second, we use relative transportation costs estimated for the Stone Age (rather than the Bronze Age) in the construction of our instrument (see column 2). In both cases, results are virtually unchanged although, as expected, the first stages become slightly less powerful.

The second main concern is that our transit trade index (partially) picks up effects of geographical factors that themselves influence the outcome variable. In column (3) of Appendix Table C.1, we show that our estimates remain stable when we account for a wide variety of observable characteristics. To tie our hands, we extend the set of controls to include all natural characteristics employed in Henderson et al. (2018)'s article which investigates the historical

Table 2: 2SLS-IV cross-sectional evidence: Reba, Reitsma and Seto (2016) city data

	Any City by 1300 BCE (×100)					# Cities (×100)
	(1)	(2)	(3)	(4)	(5)	(6)
	Panel A: Second stage					
Transit Index	0.403	0.419	0.326	0.473	0.367	0.352
	(0.133)***	(0.162)**	(0.135)**	(0.154)***	(0.160)**	(0.166)**
	[0.178]**	[0.213]**	[0.175]*	[0.207]**	[0.179]**	[0.175]**
Proximity mines		-0.040			-0.930	-1.475
		(0.111)			(0.360)**	(0.652)**
		[0.133]			[0.456]**	[0.889]*
Proximity croplands			0.242		1.283	2.022**
			(0.132)*		(0.433)***	(0.823)**
			[0.167]		[0.556]**	[1.110]*
Land productivity				-0.044	-0.011	0.010
				(0.019)**	(0.017)	(0.028)
				[0.025]	[0.019]*	[0.038]
	Panel B: First stage					
IV Transit Index	0.600	0.453	0.478	0.488	0.396	0.396
	(0.036)***	(0.036)***	(0.035)***	(0.032)***	(0.033)***	(0.033)***
	[0.055]***	[0.053]***	[0.051]***	[0.048]***	[0.048]***	[0.048]***
Geography controls	No	No	No	No	Yes	Yes
Continent fixed effects	Yes	Yes	Yes	Yes	Yes	Yes
Observations	9,426	9,426	9,426	9,426	9,426	9,426
Mean dependent variable	0.477	0.477	0.477	0.477	0.477	0.668
First-stage F-statistic (5×5 grids)	275.6	161.8	187.1	237.3	141.1	141.1
First-stage F-statistic (Conley 1000km)	118.7	71.09	85.95	102.8	66.82	66.82

Notes: Panel A of this table reports the second-stage estimates of Equation (3) using 2SLS-IV. Panel B reports the corresponding first-stage estimates (Equation (4)). Standard errors clustered at the level of 5×5 degree grid cells reported in parentheses. Standard errors computed using the approach of Conley (1999) (cut-off 1000km) are reported in square brackets. 'Any city by 1300 BCE' is a dummy equal to one if a city was present in a given 1×1 degree grid cell by 1300 BCE. Variable is multiplied by hundred to facilitate interpretation. '# Cities' is the total number of cities that had emerged in a grid grid cell by 1300 BCE. Variable is multiplied by hundred to facilitate interpretation. 'Transit trade index' is the cropland and metal input weighted number of least-cost paths that intersect a grid cell, as defined in Equation (1). 'IV Transit trade' is the NPP and metal input weighted number of least-cost paths that intersect a grid cell, as defined in Equation (2). 'Proximity mines' is the inverse input weighted average transport costs to metal mines. 'Proximity croplands' represents the grid's proximity to croplands, defined as the inverse transport cost weighted distance to croplands. 'Land productivity' is the cell's agricultural potential, measured by the caloric suitability index of Galor and Özak (2016). 'Geography controls' include latitude, elevation, precipitation, temperature, Strahler index, log distance to the coastline, and a dummy variable indicating whether a grid cell lies at the coast. * $p < 0.10$, ** $p < 0.05$, *** $p < 0.01$.

and current determinants of the spatial distribution of economic activity worldwide.[40] We also show that our results remain stable if we include transit trade indices constructed for all (other) metals discovered by the end of the Bronze Age (see, e.g. Murr, 2015). This specifically speaks to the concern that metal deposits could be spatially clustered, in which case the bronze trade index could be partially capturing the effects of trade in other metals. In analogy to our instrumental variable approach, we construct transit trade measures for

[40]Specifically, we add controls for the length of growing period, ruggedness, Kiszewski et al. (2004)'s malaria index, a set of 14 biome indicators as well as separate dummy variables indicating whether a navigable river, a lake, or a natural harbour lies within 50 km of the grid cell centroids.

gold, iron, lead, mercury, and silver.[41] Reassuringly, the point estimates of our transit trade index remains stable when we control for (potential) trade in these alternative metals (see column (4) of Appendix Tables C.1).

Finally, a concern related with our main results comes from the data sources on Bronze-Age cities. As discussed in the data section, the data in Reba, Reitsma and Seto (2016) are constructed from two rather old sources dating back from the 1980s. For this reason, in Appendix Table C.2., we repeat the analysis using an alternative more modern source: HYDE 3.1. (Goldewijk, Beusen and Janssen (2010)). Rather than capturing the cities, this source reports the urban built-up area in each grid-cell in each BCE millennium since the Neolithic. The dependent variable is now an indicator for whether there is any urban built up area in the cell in 2000 BCE (the latest data point available before the Bronze Age collapse). Once again, all main results are confirmed.

Overall, the results presented in this subsection provide evidence in support of the hypothesis that long-distance metal trade plays a central role in explaining the spatial distribution of the Urban Revolution. Cities were much more likely to be established along trade corridors connecting cropland with tin and copper mines. The 2SLS estimates suggest a causal link but, due to the cross-sectional nature of the data, we cannot exclude that potential omitted geographic factors that might be driving the results (though we do control for a large number of confounders). To overcome this limitation, we next turn to the use of panel data, which allows us to account for time-invariant geographic factors.

5.2 Difference-in-Differences evidence: Archaeological sites

In this subsection, we use information on the location of archaeological sites during the Stone Age and Bronze Age, respectively, to test for the effects of metal transit trade. More specifically, we analyse if transit trade influences the probability that an archaeological site emergences during the Bronze Age using the following difference-in-differences regression model:

$$y_{g,p} = \beta \; IHS(T_g) \times I_p^{BA} + X'_{g,p}\,\Phi + \mu_g + \tau_p + \psi_{g,p}. \tag{5}$$

In analogy to the cross-sectional regressions, outcome $y_{g,p}$ captures whether a given measure of civilisation or hierarchy is present in grid cell g and period p (where p is either the Stone Age or Bronze Age). As before T_g is the transit index. The indicator variable I_p^{BA} is equal to one during the Bronze Age and zero otherwise. As an important improvement over the cross-sectional setting, the use of panel data allows us to include grid cell fixed effects (μ_g). These absorb any time-invariant characteristics that influence our measures of civilisation. Possible aspects include waterways, ruggedness or geographical position of the cell. Additionally, we can account for regional trends by including continent×period fixed effects τ_p. We further

[41] That is, for each metal we combine the location of deposits with the climate-based net primary production to construct the transit trade measure according to equations (4) and (6).

extend the regression setup to include time varying geographic control variables $X_{g,p}$.[42]

The critical identifying assumption in the regression equation (5) is that there are no unobserved factors that are correlated with changes in transit trade and the outcome variables. While the threat of time-invariant unobservables is substantially mitigated by the inclusion of grid cell fixed effects, endogeneity remains an important concern. To address this issue, we again rely on our instrumental variable approach. In the first stage the transit index ($T_{g,p}$) is predicted using our instrumental variable (D_g). The first-stage regression is given by:

$$IHS(T_g) \times I_p^{BA} = \sigma \, IHS(D_g) \times I_p^{BA} + X'_{g,p} \, \psi + \rho_g + \nu_p + \xi_{g,p}. \tag{6}$$

Table 3 presents the difference-in-differences results. In Panel A we use the Whitehouse and Whitehouse (1975) data as outcomes, in Panel B the data from the Pleiades Gazetteer.

We start by investigating whether the probability of finding a site in a given cell increases in bronze transit trade intensity. Column (1) presents the results of a parsimonious regression specification that only accounts for grid cell and period fixed effects. For both, the Whitehouse and Whitehouse (1975) and the Pleiades data, we find that transit trade statistically significantly increases the likelihood that an archaeological site was created during the Bronze Age. The point estimates in Panel A and B imply that a one percent increase in our transit trade index raises the probability of finding a Bronze Age Site by 1.6 (Panel A) and 0.85 (Panel B) percentage points, respectively. The size of the coefficients drop somewhat in column (2) where we include the full set of controls. However, the effects remain significant at conventional confidence levels. In columns (3)–(5) we replace the dependent variable with the number of archaeological sites, the presence of settlements, and the number of settlements, respectively. Our transit trade measure increases all three alternative measures of civilisation, thus confirming previous results.

In keeping with the structure of the previous analysis we re-run all regressions using our 2SLS-IV approach (columns (6)–(10)). The first-stage F-statistics range between 276 and 132, documenting the relevance of our instrument. Throughout, we find that bronze transit trade intensity increases the probability of discovering an archaeological site created during the Bronze Age, relative to a site created during the Stone Age (columns (6)–(8)). Similarly, we find a positive effect on the establishment of settlements in the following two columns in all but one regression model (column (9), Panel B). As in the cross-sectional analysis, the size of the IV estimates are very close to their OLS counterparts. The results of our preferred regression setup in Panel A column (7), for example, imply that the likelihood of a site emerging during the Bronze Age increases by 1.36 percentage points when transit trade intensity rises by one percent. This size of the effects are economically meaningful. Moving

[42] Where characteristics are time-invariant, we interact them with the time-period specific dummy I_p^{BA} to allow for differential effects over time.

Table 3: Difference-in-differences (Stone Age vs Bronze Age): Archaeological sites

	OLS					2SLS-IV				
	Any Site (×100)		#Sites (×100)	Any Settlement (×100)	#Settlements (×100)	Any Site (×100)		#Sites (×100)	Any Settlement (×100)	#Settlements (×100)
	(1)	(2)	(3)	(4)	(5)	(6)	(7)	(8)	(9)	(10)
Panel A: Second stage Whitehouse and Whitehouse (1975) archaeological sites										
Transit Index×Bronze Age	1.604	1.211	9.212	1.031	4.059	1.302	1.355	7.954	1.263	4.802
	(0.204)***	(0.205)***	(1.815)***	(0.199)***	(0.819)***	(0.248)***	(0.444)***	(3.195)**	(0.461)***	(1.725)***
	[0.223]***	[0.199]***	[1.959]***	[0.192]***	[0.901]***	[0.241]***	[0.353]***	[2.422]***	[0.359]***	[1.471]***
Panel B: Second stage Pleiades Gazetteer (Bagnall, 2022)										
Transit Index×Bronze Age	0.846	0.712	4.015	0.608	2.356	0.374	0.643	4.194	0.373	2.325
	(0.147)***	(0.144)***	(1.185)***	(0.121)***	(0.629)***	(0.165)**	(0.326)**	(1.803)**	(0.261)	(1.153)**
	[0.153]***	[0.141]***	[1.148]***	[0.121]***	[0.672]***	[0.144]***	[0.268]**	[1.504]***	[0.210]*	[1.051]**
Panel C: First stage										
IV Transit trade×Bronze Age						0.600	0.396	0.396	0.396	0.396
						(0.036)***	(0.033)***	(0.033)***	(0.033)***	(0.033)***
						[0.039]***	[0.034]***	[0.034]***	[0.034]***	[0.034]***
Proximity to metal mines	No	Yes	Yes	Yes	Yes	No	Yes	Yes	Yes	Yes
Proximity croplands	No	Yes	Yes	Yes	Yes	No	Yes	Yes	Yes	Yes
Land productivity	No	Yes	Yes	Yes	Yes	No	Yes	Yes	Yes	Yes
Geography controls	No	Yes	Yes	Yes	Yes	No	Yes	Yes	Yes	Yes
Grid cell fixed effects	Yes	Yes	Yes	Yes	Yes	Yes	Yes	Yes	Yes	Yes
Continent×period fixed effects	Yes	Yes	Yes	Yes	Yes	Yes	Yes	Yes	Yes	Yes
Observations	18,852	18,852	18,852	18,852	18,852	18,852	18,852	18,852	18,852	18,852
Mean dependent variable Panel A	8.498	8.498	23.12	5.617	10.180	8.498	8.498	23.12	5.617	10.180
Mean dependent variable Panel B	2.376	2.376	6.265	1.851	3.962	2.376	2.376	6.265	1.851	3.962
First-stage F-statistic (5×5 grids)						275.7	141.2	141.2	141.2	141.2
First-stage F-statistic (Conley 1000km)						234.7	132	132	132	132
R^2 Panel A	0.090	0.108	0.080	0.097	0.088					
R^2 Panel B	0.046	0.066	0.030	0.055	0.054					

Notes: This table reports panel OLS estimates (Equation (5)) and panel 2SLS-IV estimates (Equation (6)). Panel A uses data from Whitehouse and Whitehouse (1975) as outcomes and Panel B data from (Bagnall, 2022). Panel C reports first-stage estimates. Standard errors clustered at the level of 5×5 degree grid cells reported in parentheses. Standard errors computed using the approach of Conley (1999) (cut-off 1000km) are reported in square brackets. 'Any Site' is a dummy equal to one if an archaeological site was present in a given 1×1 degree grid and period. Variable is multiplied by hundred to facilitate interpretation. '#Sites' represents the number of archaeological sites located within a grid cell and period. 'Any Settlement' is a dummy equal to one if a settlement was present in a given 1×1 degree grid and period. Variable is multiplied by hundred to facilitate interpretation. '#Settlements' represents the number of settlements located in a within grid cell and period. 'Bronze Age' is an indicator that takes that is equal to one during the Bronze Age and zero during the Stone Age. 'Transit trade index' is the cropland and metal input weighted number of least-cost paths that intersect a grid cell, as defined in Equation (1). 'IV Transit trade' is the NPP and metal input weighted number of least-cost paths that intersect a grid cell (defined in Equation (2)). 'Proximity mines' is the inverse input weighted average transport costs to metal mines. 'Proximity croplands' represents the grid's proximity to croplands, defined as the inverse transport cost weighted distance to croplands. 'Land productivity' is the cell's agricultural potential, measured by the caloric suitability index of Galor and Özak (2016). 'Geography controls' include latitude, elevation, precipitation, temperature, Strahler index, log distance to the coastline, and a dummy variable indicating whether a grid cell lies at the coast. * $p < 0.10$, ** $p < 0.05$, *** $p < 0.01$.

from a cell without transit trade to a cell that is intersected by a path destined for a cell that utilises 100 percent of its area for growing crops, makes it 12.6 percentage points more likely to observe a site. Evaluated at the sample mean this corresponds to 1.5 fold increase.

In Appendix Tables C.3–C.4 we conduct robustness tests in analogy to the cross-sectional regressions to support the validity of our difference-in-differences results. Specifically, we show that our estimates change little if (i) we restrict our sample to cells not used in the estimation of the transport cots vector $\boldsymbol{\alpha_{BA}}$, (ii) use relative transportation costs estimated for the Stone Age (rather than the Bronze Age) in the construction of our instrumental variable, (iii) extent the set of control variables, (iv) account for transit trade in other metals, and (v) control for transit trade constructed using transport cost estimates not specific to the Bronze Age. Finally, we show that our results do not depend on the standard error clustering approach (Figures C.2a–C.2d)

Pre-trends

We use estimates on start and end date of sites available from the Pleiades database to trace out the effects of transit trade over time in more detail and test for pre-trends. Our identifying assumption in our difference-in-differences setup requires that bronze transit trade did not exhibit a differential effect prior to the onset of the Bronze Age. To investigate the plausibility of this assumption, we construct a grid cell panel dataset on the presence of archaeological sites that spans the period [6000,1300] BCE at 1,000 year intervals (see Section 3 for more details). To investigate if our transit trade index exerts different effects over time, we interact the (time-invariant) index with time period fixed effects. In the subsequent analysis, we take the time period [4000,3000) as the reference category. The time-period interacted coefficients of the transit trade index thus capture the differential effect of the transit trade on the outcome in a given period relative to the base period. The inclusion of grid cell fixed effects and time period dummies implies that time-invariant cell-specific differences as well as general time-specific changes are washed out.

Formally, the second-stage can be represented as:

$$y_{g,p} = \sum_{p=6000}^{1300} \psi_p T_g \times I_p + \gamma_g + \tau_p + \varepsilon_{g,p}. \tag{7}$$

The dependent variable $y_{g,p}$ is an indicator for the presence of any archaeological site in grid cell g in millennium t. Grid-cell-level fixed effects are represented by γ_g, time-period fixed effects by τ_t, and the idiosyncratic error term by $\varepsilon_{g,p}$. The coefficients ψ_p capture the additional effect of the transit trade index in a given period relative to the reference millennium [4000,3000) BCE. For the first-stage regressions, we use the transit index as dependent variable and instrument as the main explanatory variable.

Figure 2 visualises the resulting 2SLS-IV point estimates along with the 90 percent confidence

intervals. The figure documents that the transit trade only starts to exert a differential effect on the probability of finding an archaeological site after the onset of the Bronze Age (i.e., after 3000 BCE). Point estimates for earlier time spans are not statistically significantly different compared to the reference millennium [4000, 3000). This absence of pre-trends provides further evidence that our estimates capture Bronze Age-specific effects of transit trade in input metals.

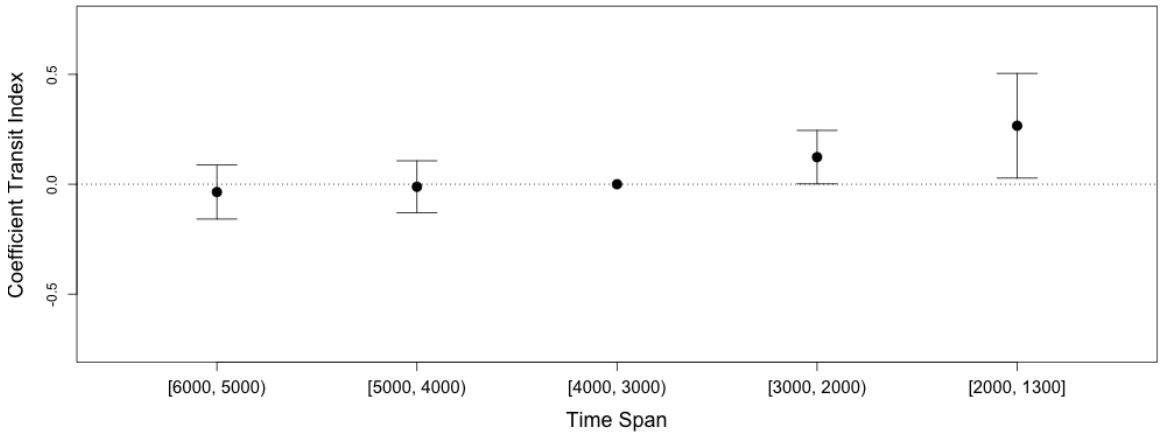


Figure 2: Effect of transit trade index over time
Figure depicts 2SLS-IV point estimates and 90% confidence intervals of time-period interacted effect of transit trade relative to the time span $[4000, 3000)$ BCE. Standard errors are clustered at the level of 5×5 degree grid cells. Dependent variable is a dummy equal to one if an archaeological site was present in a given 1×1 degree grid and period. Variable is multiplied by hundred to facilitate interpretation. See Section 3 for details on definition and construction of variables.

Taken together, our analysis so far corroborates the hypothesis that the discovery of the bronze casting process led to long-distance trade in the two input factors. The resulting trade patterns, in turn, influenced the spatial distribution of civilization. Regions located along trade corridors were more likely to see the emergence of hierarchical structures. Consistent with archaeological evidence, the implied magnitude of our estimates is substantial. An important note of caution relates to the quality of our outcome variables employed so far. As outlined in Section 3, these come with various caveats. Specifically, the Whitehouse and Whitehouse (1975)'s data are rather outdated, while the Pleiades data are skewed towards Eurasia and Mediterranean Africa.

In the last part of this empirical section, we reproduce our main insights focusing on two regions for which high-quality data are available: China and Europe.

5.3 China

Bronze metallurgy in China originated around 2000-1900 BCE and it probably developed inside China separately from outside influence. The archaeological site of Erlitou is the largest among the sites dating from these years. It is located at an important transportation

node, at the point in which the Yi River connects the Yellow River, the second longest river in Asia, with the Yangtze River, the longest one. We discuss in detail this site in section 7.6. Essentially, a recent archaeological literature argues that Erlitou took advantage of his strategic position to direct the metal trade in the region, eventually becoming the capital of a trade civilization. In this subsection, we show that the link between trade and the Urban Revolution in China extends beyond the Erlitou civilization.

The advantage of focusing on China is that we can rely on a comprehensive and detailed catalogue of Chinese archaeological sites, which we digitised to capture the rise and spread of the Urban Revolution in the Chinese context. As described in the data section, we use a text algorithm to identify sites indicative of (1) urban settlements, (2) full-time specialists in non-subsistence activities, (3) ruling class exempt from manual tasks, (4) monumental building, (5) a standardised system of measures and recordings used in exchange and production, (6) writing, (7) highly developed art forms.

We aggregate these artefacts in 1×1 degree grid-cells for three periods: Palaeolithic, Neolithic and Bronze Age. We assume that the Bronze Age starts in 2070 BCE with the first Chinese dynasty (Xia) and ends in 771 BCE with the Western Zhou dynasty. The result is a panel dataset that illustrates the rise of different aspects that have been associated with the Urban Revolution in China.

Empirical analysis

To study how metal trade fostered the Urban Revolution in this context, we estimate the difference-in-differences regression model in equation (5). The main results are illustrated in Table 4. In this table we use two variables to capture the Urban Revolution. The first one is an indicator variable, which identifies the presence of archaeological sites that feature at least one of the seven criteria associated with the Urban Revolution. The second one is a count variable of these sites.

Both the OLS and 2SLS estimates point towards a large and statistically significant association between the transit index measure and the Chinese relics indicative of the Urban Revolution. The 2SLS estimates imply that an exogenous doubling of the number of transiting paths connecting metal mines with cropland implies an increase in the probability of featuring sites indicative of the Urban Revolution during the Bronze Age in the order of 600 log points. The magnitude of the estimated coefficient does not change if we run the parsimonious specifications, with only grid-cell and period fixed effects, or if we consider our benchmark specifications with the usual full set of controls.

The richness of the data further allows us to investigate if transit trade differentially fostered specific aspects of the Urban Revolution. To this end, we define seven dummy variables, each capturing if a specific urban revolution criterion is present in a given grid cell and period. We then separately run our 2SLS difference-in-difference regressions with the full set of controls

Table 4: Difference-in-differences (Stone Age vs Bronze Age): Atlas of Chinese Relics

	OLS			2SLS-IV		
	Any Criteria (×100)		IHS #Criteria	Any Criteria (×100)		IHS #Criteria
	(1)	(2)	(3)	(4)	(5)	(6)
	Panel A: Second stage					
Transit Index×Bronze Age	4.275	2.678	0.078	6.359	6.585	0.176
	(0.552)***	(0.567)***	(0.021)***	(1.230)***	(2.389)***	(0.055)***
	[0.357]***	[0.441]***	[0.015]***	[1.052]***	[2.257]***	[0.053]***
	Panel B: First stage					
IV Transit trade×Bronze Age				0.929	0.657	0.657
				(0.133)***	(0.102)***	(0.102)***
				[0.115]***	[0.081]***	[0.081]***
Proximity mines	No	Yes	Yes	No	Yes	Yes
Proximity to croplands	No	Yes	Yes	No	Yes	Yes
Land productivity	No	Yes	Yes	No	Yes	Yes
Geography controls	No	Yes	Yes	No	Yes	Yes
Grid cell fixed effects	Yes	Yes	Yes	Yes	Yes	Yes
Period fixed effects	Yes	Yes	Yes	Yes	Yes	Yes
Observations	2,138	2,138	2,138	2,138	2,138	2,138
Mean dependent variable	15.110	15.110	0.325	15.110	15.110	0.325
First-stage F-statistic (5×5 grids)				48.63	41.10	41.10
First-stage F-statistic (Conley 1000km)				64.08	64.39	64.39
R^2	0.251	0.270	0.349			

Notes: This table reports panel OLS estimates (columns (1)–(3)) and panel 2SLS-IV estimates (columns (4)–(6)). Panel A reports the main and second-stage estimates (Equation (5)) , while panel B reports the first-stage estimates (Equation (6)). Standard errors clustered at the level of 5×5 degree grid cells reported in parentheses. Standard errors computed using the approach of Conley (1999) (cut-off 1000km) are reported in square brackets. 'Any Criteria' is a dummy equal to one if at least one of Childe (1950)'s criterion of urban revolution was present in a given 1×1 degree grid and period. Variable is multiplied by hundred to facilitate interpretation. 'IHS #Criteria' represents the IHS of number of archaeological sites located in a within grid cell and period (transformed using the inverse hyperbolic sine function). 'Bronze Age' is an indicator that takes that is equal to one during the Bronze Age and zero during the Stone Age. 'Transit trade index' is the cropland and metal input weighted number of least-cost paths that intersect a grid cell, as defined in Equation (1). 'IV Transit trade' is the NPP and metal input weighted number of least-cost paths that intersect a grid cell (defined in equation (2)). 'Proximity mines' is the inverse input weighted average transport costs to metal mines. 'Proximity croplands' represents the grid's proximity to croplands, defined as the inverse transport cost weighted distance to croplands. 'Land productivity' is the cell's agricultural potential, measured by the caloric suitability index of Galor and Özak (2016). 'Geography controls' include latitude, elevation, precipitation, temperature, Strahler index, log distance to the coastline, and a dummy variable indicating whether a grid cell lies at the coast. * $p < 0.10$, ** $p < 0.05$, *** $p < 0.01$.

using these dummies as outcomes. Figure 3 visualises the results: metal transit trade seems to affect every aspect of the Urban Revolution.

The results presented in this subsection corroborate the findings of our previous 'global' analysis for the case of China, where very detailed outcome variables are available. In a final step, we provide further evidence for the general validity of our results by testing for the existence of pre-trends. In analogy to the main part, we then analyse if metal transit trade had a differential impact during the Bronze Age by interacting the transit trade index with time period fixed effects (see Section 5.2 for more details). Figure 4 depicts the results. Reassuringly, we fail to detect any pre-trends. The transit index measure produces an increase in the sites indicative of the Urban Revolution only in the Bronze Age.

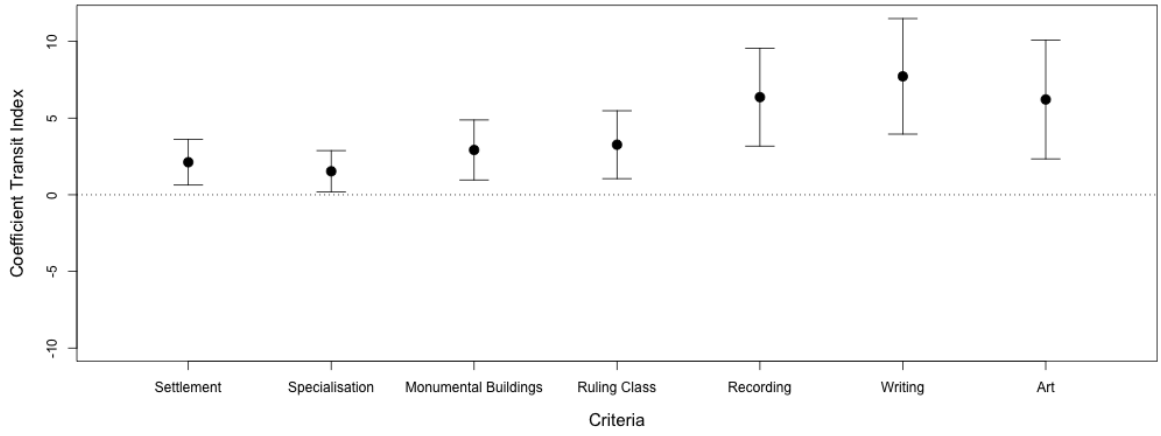


Figure 3: Effect of transit trade index on Childe's criteria of Urban Revolution
Figure depicts 2SLS-IV point estimates and 90% confidence intervals of the effect of transit trade on individual Urban Revolution criteria relative to the Stone Age. Dependent variables are dummies equal to one if a given criterion was present in a given 1×1 degree grid and period. Variable is multiplied by hundred to facilitate interpretation. See Section 3 for details on definition and construction of variables.

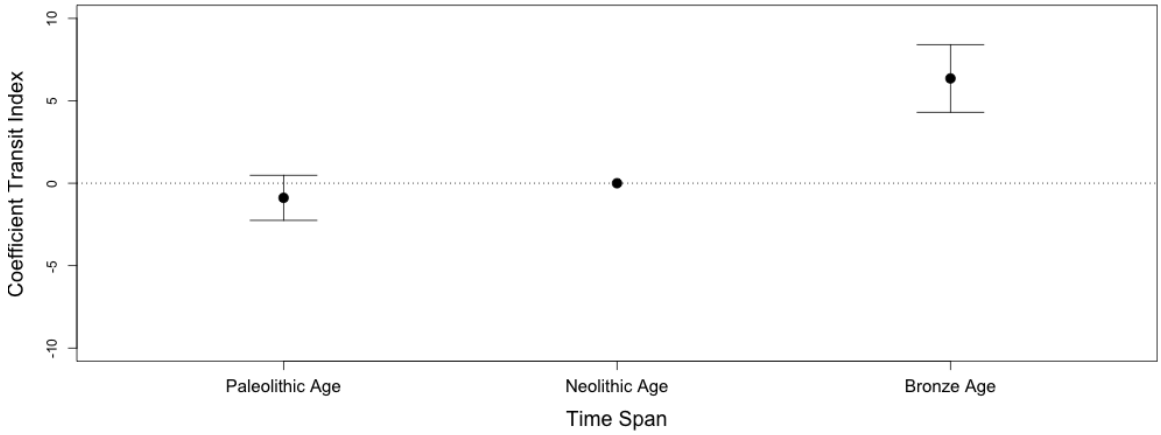


Figure 4: Effect of transit trade index over time
Figure depicts 2SLS-IV point estimates and 90% confidence intervals of time-period interacted effect of transit trade relative to the Neolithic Age. Standard errors are clustered at the level of 5×5 degree grid cells. Dependent variable is a dummy equal to one if at least one of Childe's Urban Revolution criteria was present in a given 1×1 degree grid and period. Variable is multiplied by hundred to facilitate interpretation. See Section 3 for details on definition and construction of variables.

5.4 Europe

In this subsection, we focus on the European Bronze Age which represents the most extensively studied episode in world archaeology Radivojević et al. (2019). The rich archaeological record, combined with radiocarbon dating, enables us to track socio-economic development during this period at a detailed level of spatial and temporal aggregation. In the following, we will focus on Central and Western Europe. Importantly, this excludes the Aegean and the Eastern

Mediterranean. There the Bronze Age started around 2700 BCE and is characterised by the emergence of the first European civilisations and cities.[43] In our study region—depicted in Figure F.1—the Bronze Age started around 2200 BCE. Similar to other regions of the world, the diffusion of the new technology—bronze—was pervasive and happened within a few centuries (Hänsel, 2014, pp.114, Kristiansen and Larson, 2005, pp.112). The ensuing demand for bronze led to the establishment of interregional trade networks in order to secure tin and copper in large quantities from mines, which were primarily located in Europe. However, demand for metals from these mines extended beyond Central and Western Europe to regions such as Anatolia or the Eastern Mediterranean (OBrien, 2013). For example, large-scale mining of copper during the Bronze Age is well-documented in Mittenberg, where a total of 18,000 tons is estimated to have been mined during the Bronze Age. Important tin mines were located in Cornwall and Western Iberia (OBrien, 2013, Earle et al., 2015). Noteworthy for the subsequent empirical analysis, for Europe we have detailed information on location of mines along with the approximate period during which they were operational (e.g. O'Brien, 2015).

In contrast to the Aegean and the Eastern Mediterranean, civilisations or cities did not emerge during the Bronze Age. However, Central and Western Europe witnessed the start of the precursory process of socio-economic stratification—the formation of local elites—during this period (Earle et al., 2015, Harding, 2000, pp.388). Previously typically organised as classless bands and tribes, the Bronze Age saw the emergence of hierarchically organised societies, i.e., chiefdoms, with local leaders having some centralised decision-making power (Earle et al., 2015). The archaeological literature directly links this development to long-distance trade in copper and tin (Cunliffe, 2011, pp.221,Earle et al., 2015). Control over inter-regional commodity flows led to the emergence of chiefdoms and a warrior class that was able to defend territories and hence secure trade corridors and associated revenues (Earle et al., 2015). Archaeological evidence for the presence of chiefdoms is found in graves. Valuable grave goods, and bronze artefacts in particular, are indicative of an elite status of the deceased (Harding, 2000, p.389, Hänsel, 2014, pp.113). Weapons (partly) made out of bronze, e.g., battle axes and swords, represent the strongest evidence for the existence of local elites (Earle et al., 2015,Hänsel, 2014, pp.118,Harding, 2015).

In addition to the establishment of long-distance trade networks and chiefdoms, the European Bronze Age was also characterised by increased regional and supra-regional cultural integration. That is, the formation and evolution of regional cultural groups or ethnicities. The presence of these groups, such as the Bell Beaker culture, can be identified in archaeological records by the recurrence of specific artefact types (e.g., particularly shaped drinking vessels), housing types or burial traditions in a given region (Harding, 2000, ch.1). Importantly, the relative chronology of different cultural groups across Europe is well-established in the

[43] See Section 1 for more details.

literature (Harding, 2000, p.10). For our empirical analysis, this implies that we can map artefacts—grave goods in particular—to different time periods within the European Bronze Age.

In sum, the defining features of the European Bronze Age are the large-scale use of bronze across all of Europe, interconnected regional economies as well as the emergence of socio-economic stratification (Cunliffe, 2011, pp.179). The presence of local elites can be identified and periodized using bronze grave goods.

Empirical analysis

As described in Section 3.4, we construct a two-period panel data set that spans the Early/Middle Bronze Age [3000 BCE, 1300 BCE) and Late Bronze Age [1300 BCE, 500 BCE]. For each period, we have information on the presence of hierarchy, as measured by bronze weapons discovered at a Bronze Age burial site. Hence our dataset represents a *within*-Bronze Age panel. As an important improvement over the previous analysis, the high-quality information on the start and end periods of the European mines allows us to exploit the temporal dimension in mining activity *within* the Bronze Age. More specifically, we can construct a transit trade index that varies within the Bronze Age by taking into account which mines are active during the Early/Middle and the Late Bronze Age.[44,45] For each grid cell we thus have two values of the transit trade index: one for the Early/Middle Bronze Age and one for the Late Bronze Age.

For our empirical analysis, we restrict the sample to grid cells in which artefacts were ever excavated. This addresses potential issues regarding the selective coverage of the *PBF* publications (i.e. the various volumes only cover specific regions). Restricting our sample to the 'intensive' margin further mitigates concerns related excavation biases (e.g., more excavation near known metal mines). The cells included in our analysis are shaded grey in Figure F.1.[46] Using this sample, we run the following panel data model to test if social stratification is more likely to emerge when transit trade intensifies:

$$y_{g,p} = \beta \; IHS(T_{g,p}) + X_{g,p}\,\chi + \mu_g + \tau_p + \psi_{g,p}, \tag{8}$$

where $y_{g,p}$ is the presence of bronze weapons in graves. The main explanatory variable $IHS(T_{g,p})$ is the IHS of the transit trade index for cell g in period p. As outlined above, $T_{g,p}$ now exhibits within-Bronze Age variation. The vector $X_{g,p}$ represents control variables. Grid

[44] That is, we construct the transit trade index as described in Section 4.2 separately for the Early/Middle and the Late Bronze Age. Thereby, we only use the subset of mines that were active in the respective period in the construction process.

[45] A drawback of focussing on within-Bronze Age variation is that we cannot employ our instrumental variable strategy due to the fact that we do not have temporal variation in the location of metal deposits (within the Bronze Age).

[46] Our results, however, do not depend on this restriction. Including all grid cells within Europe produces very similar estimates.

cell fixed effects and period fixed effects are symbolised by μ_g and τ_p. Finally, $\psi_{g,p}$ is the error term.

Table 5 reports the results of regression model (8). The point estimate in column (1) implies that the probability that an individual was buried with a bronze weapon rises by 4.5 percentage points when transit trade grows by one percent. This translates into a 43 percent increase when moving from a cell without transit trade to one cell intersected by a path that connects a mine to a cell that devotes all of its area to crop cultivation. The size of the point estimate drops somewhat—to 3.565—when we add our standard set of control variables in column (2). The statistical significance of our results, however, is unaffected.

In columns (3)–(4) we use the IHS number of weapons excavated in graves as a measure of hierarchy whereas we use the proportion of all weapons excavated in a given grid cell found in graves as the dependent variable in column (5)–(6). Regardless of outcomes and controls used, we consistently find that increased transit volumes raise the probability of hierarchy emerging. transit trade index: one for the Early/Middle Bronze Age and one for the Late

Table 5: OLS panel evidence: Weapons as Grave Goods

	Any Weapons in Grave (×100)		IHS Number of Weapons in Grave		IHS Share Weapons in Grave	
	(1)	(2)	(3)	(4)	(5)	(6)
Transit Index	4.495	3.565	0.103	0.054	0.143	0.114
	(1.772)**	(1.497)**	(0.032)***	(0.026)**	(0.067)**	(0.061)*
	[1.971]**	[1.475]**	[0.037]***	[0.019]***	[0.072]**	[0.055]**
Proximity mines	No	Yes	No	Yes	No	Yes
Proximity croplands	No	Yes	No	Yes	No	Yes
Land productivity	No	Yes	No	Yes	No	Yes
Geography controls	No	Yes	No	Yes	No	Yes
Continent fixed effects	Yes	Yes	Yes	Yes	Yes	Yes
Observations	726	726	726	726	726	726
Mean dependent variable	38.150	38.150	0.766	0.766	1.477	1.477
R^2	0.028	0.182	0.036	0.272	0.018	0.104

Notes: This table reports estimates of Equation (8) using OLS. Standard errors clustered at the level of 1×1 degree grid cells reported in parentheses. Standard errors computed using the approach of Conley (1999) (cut-off 1000km) are reported in square brackets. 'Any Weapons in Grave' is a dummy equal to one if a weapon was present in a grave in a given 1×1 degree grid and period. Variable is multiplied by hundred to facilitate interpretation. 'IHS Number of Weapons in Grave' is the IHS of the total number of weapons found in graves in a given 1×1 degree grid and period. 'IHS Number of Weapons in Grave' is the IHS of the total number of weapons found in graves in a given 1×1 degree grid and period. 'IHS Share Weapons in Grave' is the IHS of the proportion of total weapons excavated in a given 1×1 degree grid and period that were found in graves. Variable is multiplied by hundred to facilitate interpretation. 'Transit trade index' is the cropland and metal input weighted number of least-cost paths that intersect a grid cell, as defined in Equation (1). 'Proximity mines' is the inverse input weighted average transport costs to metal mines. 'Proximity croplands' represents the grid's proximity to croplands, defined as the inverse transport cost weighted distance to croplands. 'Land productivity' is the cell's agricultural potential, measured by the caloric suitability index of Galor and Özak (2016). 'Geography controls' include latitude, elevation, precipitation, temperature, Strahler index, log distance to the coastline, and a dummy variable indicating whether a grid cell lies at the coast.* $p < 0.10$, ** $p < 0.05$, *** $p < 0.01$.

Bronze Age.

6 Appropriability mechanism

The results so far indicate that trade in bronze inputs was an important driver of the Urban Revolution. Social stratification, complex hierarchies, states, and cities were more likely to emerge in regions central in the metal trade network. In this section, we study the mechanism underlying this result. The first subsection spells down a theoretical framework which emphasises the appropriability nature of transit metal trade. While some optimal routes connecting populations with mining regions could be easily circumvented, some others could not be avoided unless traders were willing to face disproportionate transportation costs. We argue that it is exactly in these latter regions that a new elite, relying on taxing transit traders, could rise. Sufficient fiscal revenues allowed this elite to pay the fixed cost needed to establish the monopoly of power and commit to a revenue-maximising tax rate. In turn, this arrangement was beneficial to metal traders, who avoided higher expropriation rates by unorganised roving bandits. The main insight from the model is that a trade-taxing elite, and associated civilisation, is more likely to emerge in the bottlenecks to the metal trade network - regions that (a) have high transit trade volumes and (b) are costly to circumvent. In the second subsection, we bring the theory to the data. We construct a measure of the potential tax revenues that could be extracted by a would be elite in a grid-cell, by calculating the additional trade costs to metal traders to avoid that cell. We then run a horse race between this measure, which identifies the bottlenecks in the metal trade network, and the transit trade index, which identifies the road-knots. It turns out that the bottlenecks were indeed the ultimate cradle of civilization.

6.1 Theory

IN PROGRESS

6.2 Empirical evidence

To gauge the extent to which the rise of a tax-levying elite drives our results, we construct a transit trade centrality measure that incorporates the scope for taxation. We build on the intuition, developed in our theoretical framework, that revenues from taxing transit trade in a certain region depends not only on the optimal routes passing by the region, but also on the absence of valid alternatives to these routes. In order to translate this insight to the data we construct a measure of the trade costs that metal traders would have to incur to avoid a certain region. To this end, we compute the Modified Efficiency Centrality (Wang, Wang and Deng, 2019) in the metal trade network. This centrality index captures how much the total transport costs in the global metal trade increases if a given cell is blocked for transit (i.e., if we do not allow paths to intersect the cell). That is, it represents the difference in global transport costs between the unrestricted case—which is equal to the total transport costs associated with our main transit trade index—and the situation in which a given cell is

blocked for transit trade (see Appendix D.2 for more details). Subsequently, we refer to this increase in transport cost as 'blockage cost'. The higher the blockage cost, the more costly it is to circumvent a cell, and—consequently—the greater is the potential tax revenue. Figure 5 visualises the geographic variation in these costs.

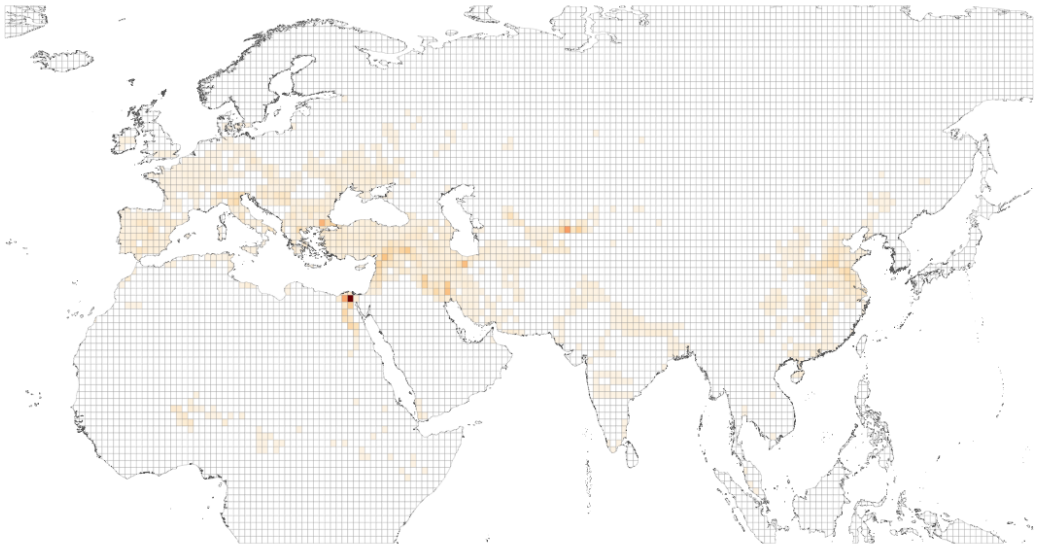


Figure 5: Blockage cost.
Figure depicts the global cost of blocking a cell for transit trade in 3000 BCE (see Appendix D.2 for more details). Darker shadings imply greater costs.

We test if the rise of a trade-taxing elite is a plausible mechanism by running a horse race between our main transit trade index and the blockage cost.[47] If taxation plays a role, we would expect the blockage cost coefficient to be statistically significant, positive and sizable.

Table 6 presents the findings of the horse race regressions. In analogy to the structure of Section 5 we first look at cross-sectional city data from Reba, Reitsma and Seto (2016). For reference, column (1) replicates the results of our preferred specification (Table 1, column (5)). This produces a point estimate of 0.377. The size of the transit trade index drops by 46% (column (2)), when we account for the blockage cost. More importantly, the latter is statistically significant, positive and of considerable economic magnitude. This suggests the rise of a trade-taxing elite is one important reason why civilisation emerged in regions central to the metal trade.

In columns (3)–(4) we run the horse race using Whitehouse and Whitehouse (1975)'s panel data, whereas we use the Pleiades Gazetteer panel in columns (5)–(6). The pattern of results does not change compared to the cross-sectional setup. In both cases the difference-

[47]Subsequently, we restrict our analysis to OLS regressions. With IV regressions, we are not able to disentangle the relative importance of the trade versus taxation channel because both instruments (the one for our main transit index and the one for the blockage cost) have predictive power for both potentially endogenous variables. See Appendix D.2 for more details.

Table 6: Controlling for blockage costs

	Any City 1300 BCE (×100) Reba, Reitsma and Seto (2016)		Any Site (×100) Whitehouse and Whitehouse (1975)		Any Site (×100) Bagnall (2022)	
	(1)	(2)	(3)	(4)	(5)	(6)
Transit Index	0.377	0.202				
	(0.109)***	(0.073)***				
	[0.142]***	[0.089]**				
Blockage cost		0.193				
		(0.066)***				
		[0.077]**				
Transit Index×Bronze Age			1.211	0.601	0.712	0.339
			(0.205)***	(0.231)***	(0.144)***	(0.148)**
			[0.199]***	[0.162]***	[0.141]***	[0.106]***
Blockage cost×Bronze Age				0.671		0.410
				(0.206)***		(0.144)***
				[0.177]***		[0.137]***
Proximity to metal mines	Yes	Yes	Yes	Yes	Yes	Yes
Proximity croplands	Yes	Yes	Yes	Yes	Yes	Yes
Land productivity	Yes	Yes	Yes	Yes	Yes	Yes
Geography controls	Yes	Yes	Yes	Yes	Yes	Yes
Continent fixed effects s	Yes	Yes	Yes	Yes	Yes	Yes
Observations	9,426	9,426	18,852	18,852	18,852	18,852
Mean dependent variable	0.477	0.477	8.498	8.498	2.376	2.376
R^2	0.032	0.034	0.108	0.111	0.066	0.068

Notes: This table reports estimates of Equation (3) using OLS. Standard errors clustered at the level of 5×5 degree grid cells reported in parentheses. Standard errors computed using the approach of Conley (1999) (cut-off 1000km) are reported in square brackets. 'Any city by 1300 BCE' is a dummy equal to one if a city was present in a given 1×1 degree grid cell by 1300 BCE. Variable is multiplied by hundred to facilitate interpretation. 'Any Site' is a dummy equal to one if an archaeological site was present in a given 1×1 degree grid and period. Variable is multiplied by hundred to facilitate interpretation. 'Bronze Age' is an indicator that takes that is equal to one during the Bronze Age and zero during the Stone Age. 'Transit trade index' is the cropland and metal input weighted number of least-cost paths that intersect a grid cell, as defined in Equation (1). 'Blockage cost' are the globally incurred additional transport costs to the closest copper and tin mines resulting from blocking a given grid cell. 'Proximity mines' is the inverse input weighted average transport costs to metal mines. 'Proximity croplands' represents the grid's proximity to croplands, defined as the inverse transport cost weighted distance to croplands. 'Land productivity' is the cell's agricultural potential, measured by the caloric suitability index of Galor and Özak (2016). 'Geography controls' include latitude, elevation, precipitation, temperature, Strahler index, log distance to the coastline, and a dummy variable indicating whether a grid cell lies at the coast. * $p < 0.10$, ** $p < 0.05$, *** $p < 0.01$.

in-differences regressions document that blockage cost exert a statistically significant and economically sizeable effect. That is, the likelihood that a site emerges during the Bronze Age increases considerably in a cell that is costly to circumvent in the metal trade. The coefficient of transit trade drops by around 50% when we control for variation in blockage costs.

Taken together, the results presented in 6 provide strong evidence that the emergence of a metal trade-taxing elite is an important driver of the Urban Revolution.

7 Archaeological case studies

7.1 Ancient Sumer in the Early Dynastic Period (2900 BCE-2334 BCE)

The Urban Revolution started with the Sumerian Civilization. After a long transition during the Uruk period, full urban life flowered during the Early Dynastic Period. At this point, all the 10 formal criteria that Childe use to define Urban Revolution can be traced in South Mesopotamia: increased settlement size, concentration of wealth, large-scale public works, writing, representational art, knowledge of science and engineering, foreign trade, full-time specialists in non-subsistence activities, class-stratified society, and a political organisation based on residence rather than kinship. A thesis with a long-standing tradition in anthropology and archaeology is that long-distance trade was the main driving factor of this "Revolution". The first Sumerian cities emerged along the coast of the Persian Gulf, in the alluvial delta of the Tigris and Euphrates. These cities were located in a nodal point connecting Anatolia, Mesopotamia, and Iran with the Persian Gulf, through an enormous dendritic transportation system created by the north-to-south flowing rivers. In the words of Guillermo Algaze: "That emergence of early cities in the southern Mesopotamian alluvium must be understood in terms of the unique ecological conditions that existed across the region during the fourth millennium, and the enduring geographical framework of the area, which allowed for the efficient movement of commodities via water transport and facilitated interaction between diverse social units alongside natural and artificial river channels. These conditions promoted evolving long-term trade patterns that, inadvertently, differentially favoured the development of polities in the southern Mesopotamian alluvium over contemporary societies in neighboring regions."

The principal commodities referred to in commercial documents during the Early Dynastic Period are copper, tin, and tin-bronze, which were normally purchased in exchange of silver, barley and wool (Lambert (1953), Leemans (1975), Foster (1997), Dercksen (1999), Prentice (2010) and Foster (2016)).

Ancient Sumerian cities were the first to show evidence of copper alloys utilisation. Sumer was the birthplace of both arsenic copper, which became prevalent in the second half of the 6th millennium BCE, and the bronze technology. The rise of bronze production coincides with the rise of the Urban Revolution among the Sumerians: tin bronze is thought to have been introduced in Mesopotamia at the very end of the 4th millennium BCE, with the first known bronze object dating from around 3000 BCE.

Notice, however, that South Mesopotamia has no local sources of metals. The focus of much documented commercial activity of Sumerian cities is the acquisition of copper and tin, through both land routes connected to the rivers or sea routes[48].

[48] Curiously, a famous tablet, excavated in Ur, contains the oldest known customer complaint. The complaint refers to the quality of the copper sold from a merchant coming from Dilmun, a polity almost certainly

Regarding copper, there were two well-documented routes used to bring this metal to Mesopotamia. The first was a land route, which was connecting the mines in the Zagros (Iran) and the Taurus (Turkey) mountains with Southern Mesopotamia, and was facilitated by the rivers and canals in the water system formed by the Tigris and the Euphrates (Muhly (1973), Morr et al. (2013)). The second route was a sea route, which was connecting Ur and the other Sumerian ports in Southern Mesopotamia, through the Persian Gulf, to three exporters of copper: Magan, Dilmun and Meluhha. Magan was a polity located in present-day Oman and a major source of copper ores. Recent estimates report that approximately half of the Sumerian copper was coming from there (Giardino, 2019)[49]. Dilmun is already cited in archaic texts dealing with the copper trade in Uruk from the late fourth millennium BCE. The importance of this trade post is confirmed by the fact that copper trade in the Persian Gulf was carried out by the "Dilmun boats" and transactions in Ur were conducted using the "Dilmun weight standard". Dilmun probably served only as a trading post and it was never the ultimate origin of the traded products. Based on epigraphic and archaeological evidence, it seems that the ultimate source of copper trade through Dilmun was Meluhha (Begemann et al. (2010)), which is generally believed to be located in the present-day Indus Valley (Muhly (1973)), where the Harappan Civilization flourished starting from the mid third millennium BCE. In particular, lead isotope studies have suggested that the ultimate source of copper travelling through Dilmun in Mesopotamia might be the Aravalli Hills in southern Rajasthan (Begermann and Schmitt-Strecker (2008)).

As opposed to copper, the sources of tin for Mesopotamia during the Bronze Age are not as well defined. The cuneiform texts seem to indicate that all the major tin sources used in the region in the early bronze age were located east of Mesopotamia. Tin imported in Mesopotamia is believed to mainly originate from western Afghanistan and the Zagros mountains in current-day Iran. Tin from Afghanistan was probably transported through a sea-route passing by Magan (Cleuziou and Berthoud (1982)), while a land route from the Zagros mountains was probably opened later. Limited evidence of tin mining during the Bronze Age is also present in Goltepe, in Anatolia, which led to the hypothesis that some of the tin used in Mesopotamia might have come also from Anatolia (Yener and Vandiver (1993) and Yener (2021)).

The trade vocation of Sumerian cities is evidenced in the Epic of Gilgamesh, the first known piece of literature in history. The story opens with a description of Uruk (probably the first

corresponding to present-day Bahrein: "When you came, you said to me as follows : I will give Gimil-Sin (when he comes) fine quality copper ingots. You left then but you did not do what you promised me. You put ingots which were not good before my messenger (Sit-Sin) and said: If you want to take them, take them; if you do not want to take them, go away! [..] Is there anyone among the merchants who trade with Dilmun who has treated me in this way? You alone treat my messenger with contempt!"

[49]Moreover, excavations from the 1970s have yielded clear evidence of large-scale production of copper throughout the mountainous region of eastern Oman that can be traced back at least to the middle of the third millennium BCE (Weisgerber (1981, 1983)).

city in human history), emphasising the beauty of its walls and its markets. The city itself is referred to as "the great market". The cuneiform texts indicate that ancient Sumerian cities were not only a trading hub for tin and copper, but also important manufacturing centres with stratified classes of metal workers.

7.2 The Harappan civilization in the Indus valley (2600 BCE-1900 BCE)

The second half of the third millennium BCE marked the birth of the first urban civilization in southern Asia, in the Indus Valley. Rather than emerging from a slow period of gradual growth and modification as in the Sumerian case, the Harappan civilization seems to have resulted from a very short period of transformation (Possehl, 1990). During the Urban Phase (or Mature Harappan), within 100-150 years, both writing and a widely used of system of weights and measures appeared, towns start displaying monumental buildings, signs of centralised urban planning (e.g. massive brick platforms, well-digging, drainage systems, gird plans) and unprecedented levels of social differentiation emerged (e.g. big/small houses, brick/mud houses, growth in the use of precious metals for personal adornments etc.). Several scholars have suggested that external trade was a major factor in the rise and maintenance of the urban centres (Possehl (1990), Ratnagar (1981)). Trade was facilitated by two major river systems, the Indus and the Ghaggar-Hakra (now dry), which were connecting regions rich in tin and copper in Balochistan and Afghanistan, through the Gulf of Oman, to the Persian Gulf and Mesopotamia. In the words of Gregory Possehl (1996): "The Indus-Mesopotamia trade developed in part because ships had many advantages over caravans for the long-distance transport of products that were also theoretically available from alternative sources, and in part because, for some desirable products, there was no readily available alternative source". Archaeological traces of the pivotal role of the Harappan civilization in moving raw materials from the centre of Asia to Mesopotamia through the Persian gulf can be found throughout the route. Several Harappan-related sites have been found in Southern Baluchistan and in Afghanistan: these were apparently trading colonies near major sources of lapis lazuli, copper, and tin. Moreover, a series of archaeological findings point towards the presence of Harappan colonies or trade posts throughout the Persian Gulf. In Oman, archaeologists found a series of metal tools of clear Indus origin, several Indus trade tools used to normalise exchanges (e.g., the Indus type stamp seals and cubical weights) and a number of Indus-type artefacts made in Oman by Indus or Indus-trained craftspeople using local raw materials. Moreover, more and more Indus pottery is steadily being recognized at sites in Oman and the Persian Gulf and Indus products were imitated in the Arabian coast (Edens (1993, p.354)).

As discussed in the previous subsection, although the tin sources in Mesopotamia are still not fully understood, several scholars have suggested that the Harappan civilization provided a major source. The supply of tin by this sea route is suggested, for instance, in a passage in one of the texts of Gudea, a priest king reigning in Southern Mesopotamia, who describes the

trove of objects reserved for the god and placed in the temple:

"Along with copper, tin, slabs of lapis lazuli, shining metal (and) spotless Meluhha cornelian" (RIME 3/1,96).

People of Meluhha are described as traders in the Sumerian texts and there are frequent references to their ships. Harappan-style artefacts, including seals, beads, and shell objects, have been recovered from sites in Mesopotamia dating from 2550 BCE. On the other side, there is no archaeological evidence of Mesopotamian goods in Indus cities. This has been interpreted as a sign that either imports from Mesopotamia were perishable goods, or that Indus-Mesopotamia trade was mainly indirect, via Dilmun and Magan.

7.3 Assur in the Old Assyrian period (2000 BCE-1800 BCE)

The city of Assur was built on a sandstone cliff, a rather unproductive agricultural land, on the wrong edge of Mesopotamia productive zone. It was, however, an important trading node connecting Anatolia to Sumer and Iran as it lay between the Tigris and two of its largest affluents, the Great and the Little Zab rivers. The local kings leveraged the commercial potential and geographic position. Eventually, it became a superpower in the region, giving the name to the Assyrian empire. Texts of kings Ilushuma and his son, Erishum I (1939-1900 BCE) give a hint on how the city emerged on the international stage. The longer known text, which is present in numerous copies on bricks runs as follow:

"Ilushuma, vice-regent of Ashur, built the temple for the goddess Ishtar, his mistress, for his life. A new wall [..] I constructed and subdivided for my city house-plots. The god Ashur opened for me two springs in Mount Ebih and I made bricks for the wall by the two springs. [..] The freedom of the Akkadians and their children I established. I purified their copper. I established their freedom from the border of the marshes and Ur and Nippur, Awal and Kismar, Der of the god lshtaran, as far as the City (i.e. Ashur)."

This text has been argued to reflect the commercial nature of the city and the efforts by Ilushuma to attract traders from south Mesopotamia to the Ashur market by giving them certain privileges (Larsen (1976), Kuhrt (1995)). Ashur was a central node in the tin trade serving as an entrepot, where traders coming from South Mesopotamia would go to buy tin and sell copper coming from the Gulf. In particular, in the final part the text refers to the three major caravan routes coming from south Mesopotamia: one ran from Ur (the point of entry for copper from the Gulf) to Nippur then up to Ashur; the second ran along the Tigris; and the third went from Elam through Der, east of the Tigris, and then across to Ashur. Erishum I, Ilushuma's successor, made tax-exempt trade in copper, tin, and barley, the most relevant commodities in the local markets, a policy intended to maximise the profits of their nodal position in trade (Grayson (1972, p.62) and Kuhrt (1995, p.87)).

The Assyrian texts depict a flourishing market economy based on free enterprise and private initiative, profit-seeking and risk-taking merchants, backed by elaborate financial contracts,

and a well-functioning judicial system. Assyrian merchants established trading colonies or "ports" among the small city-states of Anatolia. These trade posts had their own legal and financial institutions and played a crucial role in fostering the economic, institutional, and demographic development of Anatolian city-states. They were also instrumental to the rise of a local elite of Anatolian kings, which were both guaranteeing protection for passing merchant caravans and maintaining roads and bridges in exchange for tolls and taxes on transit trade. The bulk of our information on Assyrian trade comes from documents found in one of these "ports", Kanesh, located in central Anatolia about 1200 km away. Kanesh was an important Assyrian trading post in Anatolia, which had evolved into a full-fledged city with its own institutions, an assembly and specialised bureaucrats, modelled mirroring those of Ashur.

Goods were transported from Ashur to Anatolia through caravans of donkeys. Interestingly, each donkey always carried some tin (Landsberg (1965), Larsen (1976, 1987)), together with other goods. This suggests that trade arrangements to provide the inputs for bronze production in Anatolia, might have led to the development of long-distance trade not only in tin, copper and barley but also in other manufactures like textile, pottery and precious stones. In the words of Emilie Kurth:

"Ashur played a major role at this time in the acquisition and distribution of this metal [tin] from the east. On arrival in Anatolia everything, including the donkeys, was sold, and the main import back to Ashur was silver and some gold. Within Anatolia itself the Assyrians, given their sophisticated and developed system of trading stations, were able to increase their profits by playing the dominant role in the internal carrying trade. They probably also organised the Anatolian inter-state trade in copper (Larsen (1967)), which may have been mined at the rich deposits of Ergani Maden (near Elazig, Turkey). The tin was, bulk for bulk, more valuable than the textiles, but it was the textiles which provided the main volume of the trade (Vecnhof (1972), Larsen (1987)), and the documents show that they were centrally imposed to Assyrian commerce and highly valued in Anatolia."

7.4 The city of Mary (1810 BCE-1760 BC)

The city of Mari was located on the Euphrates, just downstream from its confluence with the Khabur River. It was an important political power already starting from the 2600 BCE, but we have considerable information dating from 1810-1760 BCE thanks to a large archive of documents excavated starting from the 1930s. These documents reveal that the rise of Mari was essentially driven by its strategic geographical position on major metal routes (Kristiansen and Larsson (2005, p.93)). The archives show that Mari was the main supplier of tin (coming from the further east) for much of the Levant and the Eastern Mediterranean, including Crete (Morris (1992, p. 102)). The tin trade, transiting through Mari, directly involved kings from far away regions. For instance, in Mari's archive, we find a letter from the king of Qatna, a city located 400 km east of Mari, addressed to the King of Ekallate, a city located to the

west of Mari:

"This matter is unspeakable, yet I must speak and relieve my feelings: you are a great king; you asked me for two horses, and I had them sent to you. And now you sent me (only) 20 minas (c. 10 kilos) of tin. Is it not the case that, without any quibbling and in full, you got (what you wanted) from me? And you dare to send me this paltry amount of tin! If you had sent nothing at all, by the god of my fathers, I could not have been so angry¡'

A series of tablets deciphered by Dossin (1970) suggests that tin was transported east to west, using Mari as a nodal point. Tin came from unspecified sources in the east, transiting through Babylon and Susa. Once arrived in Mari, it would then transshipped to various sites in Syria and Palestine and, through the port of Ugarit, even across the Mediterranean sea to Crete[50].

The hub nature for the tin long-distance commerce was also providing the majority of the state income in Mari. Main sources of fiscal revenues were taxes on transit trade, crossing-dues, tolls, and taxes on boats (Kuhrt, 2020). Diplomatic gifts were another source of royal wealth (Zaccagnini, 1983). The state actively took part in trade and. at times, had a dominant role. Still, there is also evidence for private commercial ventures and an extensive private commercial network starting from the Ur III period (2112 BCE-2004 BCE) up until the Old Babylonian period (1894-1595 BCE)[51] .

7.5 The Bronze Age Aegean

The Bronze Age Aegean in the eastern Mediterranean encompassed several powerful entities: the Minoans on Crete; the Mycenaeans on mainland Greece, and the Cypriots in Cyprus.

During the third millennium BCE, the Minoans were already at the centre of the Aegean trade network, with close contacts with the Cyclades. This is testified by imports from these islands, trade in raw materials (e.g., obsidian, copper, lead, silver), the local production of material culture in Cycladic styles or technologies, and a relocation of Cycladic groups along the northern coast of Crete (Renfrew (1964), Warren (1984), Karantzali (1996), Day, Wilson and Kiriatzi (1998); Papadatos (2005); Dimopoulou-Rethemiotaki Wilson, and Day (2007)). It is during the Middle Minoan period (1900-1800 BCE), however, that the trade network of the Minoans starts expanding above the Cyclades: Minoan products and cultural influences starts to be found in mainland Greece, Asia Minor, the entire Mediterranean coast of the Middle East, and even as far as Egypt. At the same time, the Minoans are becoming the most powerful European civilization. Social development and economic growth are testified

[50] An interesting tablet, which dates back from the eighteenth century BCE is set up as a balanced account, listing the tin received and shipped in Mary. It describes tin received from the kings of Babylon (Hammuraby) and Susa (Shephard), stocked in Mari, and then shipped to individuals residing in Ugarit and Caphtorite, a town presumably located in Crete.

[51] See Powell (1977) for the Ur III period, Oppenheim 1954 for the Isin-Larsa period, and Leemans (1950, 1960, 1968) for the Old Babylonian period.

by several hallmarks. A state emerged together with writing, monumental burials, roads and other public infrastructures. Towns such as Knossos, Malia, Gournia, and Plaikastro are often described as the first urban settlements of Bronze Age Europe. These towns were centres of craft production (textile, pottery, and metalworking) and long-distance trade. They developed around royal "palaces", monumental buildings, some with true Cyclopean masonry. These buildings were at the centre of an economic system, which has often been referred to as "palace economy", in which a substantial share of wealth was flowing under the control of a centralised administration, centred in the palace, which gathered up, manufactured, traded and redistributed product and services needed in Crete. The palaces were at the heart of an extensive network of intra-regional and interregional maritime trade of agricultural products in exchange for obsidian and metals (copper and tin). A long-standing fascinating hypothesis in the historical and archaeological literature is that the centrality of Crete in the metal trade network in the Mediterranean might go a long way in explaining the rise of the palaces and the Minoan civilization. The Minoan civilization has often been referred to as the first example in history of a thalassocracy[52], a polity which derives its power from its naval/commercial supremacy on the seas. Already in the fifth century BCE a Greek historian, Thucydides, wrote:

"Minos is the first to whom tradition ascribes the possession of a navy. He made himself master of a great part of what is now termed the Hellenic sea; he conquered the Cyclades, and was the first colonisers of most of them, expelling the Carians and appointing his own sons to govern in them. Lastly, it was he who, from a natural desire to protect his growing revenues, sought, as far as he was able, to clear the sea of pirates."

More recently, Gordon Childe has emphasised the absolute centrality of the Minoans in the Mediterranean trade:

"In the Early Bronze Age peninsula Italy, central Europe, and the west Baltic coastlands, and the British Isles were united by a single system for the distribution of metalware, rooted in the Aegean market."

Minoan vessels were the main means of transportation of copper ingots in the Mediterranean (Kropp (1990), Muhly (1988)). In a shipwreck near present-day Israel, numerous tin ingots, with Minoan seals have been found: trace-element analysis points towards Cornwall, present-day England, as the most likely provenance of the tin (Berger et al, 2019). This finding puts the Minoans at the centre of a tin trade route connecting western and northern Europe with the Syrians civilizations.

The Mycenaean civilization appeared later in history, in the middle Bronze Age, spanning the period approximately 1750 to 1050 BCE. As for the Minoans, the centre of the Mycenaean economy were the palaces. The production of manufactures, the internal circulation, and the

[52]Thalassokrateo means "to be master of the sea"

long distance trade were conducted mainly under their control. In particular, several tables found in the palace in Pylos demonstrate a very tight palatial control of the metal industry. Bronze-smiths were distributed throughout the kingdom. Each smith was allocated raw ore and other materials from the palace and assigned a task, and then were expected to deliver the final product to the palace. Chadwick (1994: 141) argues that the total number of smiths in the Pylian kingdom was nearly 400 and he estimates that the production was likely to exceed the local demand. This fact together with the absence of local copper and, especially, tin deposits made of Pylos a major centre of exchange. It has been argued that long-distance trade became increasingly important in the region as the quality of the soil for growing cereals (which was already poor) progressively declined as a result of continuous intensive cultivation (Ascherson (2011)). Starting from 1550 BCE, the Mycenaean established a wide network of colonies in coastal Anatolia, in southern Italy and western Sicily as well as in the Black Sea, Spain and Southern France. These colonies helped to facilitate international trade with the Mycenaean states, by providing military protection and a uniform set of institutions and customs along the main Mediterranean trade routes. Long-distance trade promoted the rise of a political and administrative palatial elite that directly participated in the trade voyages and would often engage in wars to crush their trade rivals. In the Odyssey Book, Menelaus, the legendary Spartan wanax (king), describes the source of it wealth and power in the following way:

"But when it comes to men, I feel that few or none can rival me in wealth, for it took me seven years and great hardship to amass this fortune and bring it home in my ships. My travels took me to Cyprus, to Phoenicia, and to Egypt. Ethiopians, Sidonians, Erembians, I visited them all; and I saw Libya too..." (The Odyssey, Book 4, 75-85).

While there is little doubt that interregional trade in the Mediterranean was driven by bronze-making metals, it is also clear that it enabled the exchange of luxury, or less utilitarian, goods, items that were enabling powerful statements. This is particularly evident for Mycenaeans, where eastern regions made the strongest contribution, as the sophisticated states of Egypt, the Levant, Mesopotamia, and Anatolia provided a wealth of precious items that functioned as technological and artistic models for the development of local arts and society (Burns (2010)).

Another important Aegean civilization rose in Cyprus. Starting from the 1650 BCE, the island experienced a rapid change from a somewhat isolated, village-oriented culture to an international urban-centred and highly complex society. It is generally agreed that the first urban developments and the gradual movement of population from rural hinterland to coastal towns was not merely an internal socioeconomic process, but rather the outcome of overseas demand for Cypriot copper (Knapp, 2013; Negbi, 2005). The development of metallurgy on Cyprus was driven by the local copper mines and the need to meet the increasing demand for copper in the Mediterranean basin. Eventually the intensified production and trade of

copper catapulted Cyprus into the role of the most important purveyor of this metal in the Mediterranean region, which lasted until the Roman Empire (the name Cyprus is directly related to the Latin word for copper, cuprum). A large number of documents of the second millennium Egyptian, Syrian, Babylonian, Anatolian and Mycenaean mention exchanges with Cyprus (Alashiya) and gifts of coppers.

7.6 The Bronze Age in China and the Erlitou period (1900 BCE-1500 BCE)

Bronze metallurgy in China originated in what is referred to as the Erlitou period and it probably developed inside China separately from outside influence (Liu, 2004). The site of Erlitou is the largest among all its contemporary sites in China. In recent years, most Chinese archaeologists have reached a consensus that this site was most likely the capital of the Xia dynasty (Gao Wei et al. 1998). Significantly, Erlitou was located at an important transportation node, at the point in which two large rivers, the Yi and the Luo, join to discharge into the Yellow River.

In the last four decades, more than 200 sites containing Erlitou material assemblages have been found over a very broad region from the middle Yellow River to the middle Yangtze River regions. The sites are distributed along several river systems and the pattern of settlement distribution is indicative of the emergence of a highly integrated and centralised socio-political system (Liu, 2004, p.226). The line expansion of this first state suggests a series of attempts to achieve political domination of metal-rich peripheries. One notable example is Panlongcheng, a site located at the intersection between the Han and the Yangtze River, and in close proximity to both copper and tin deposits. There is evidence that copper was melted at the mining sites, while the elite in Panlongcheng was likely playing a major role in forwarding copper ingots to the primary centre at Erlitou (Liu and Chen, 2003). There is also evidence of limited bronze making dating from the Erlitou period. Another example of an outpost to control metal resources, set up by the Erlitou state, is the site of Donglongshan. Donglongshan is located on the north bank of the Dan river with close proximity to copper resources in Mt. Hongyan. Few pieces of metal slag were found at the site, suggesting that bronze metallurgy was carried out there (Yang Yachang 2000).

The formation of the Erlitou state involved rapid territorial expansion by colonising the surrounding regions, with the quest for bronze alloys as the main territorial driver. In the words of Liu (2004): “The Erlitou state formed an inter-regional network focused on the production and distribution of prestige goods, especially bronze vessels. This network incorporated two interdependent sectors, core and periphery. The dominant core controlled the production of prestige items (bronze products, etc.), and the subordinate periphery provided raw material resources (e.g, metal ingots) [..] The Erlitou elite in the core achieved domination through military force by establishing outpost in the periphery to ensure the flow of material and

information."

8 Conclusion

The prevailing literature attributes the emergence of the Urban Revolution to farming and sedentism. Although we do not deny that both might represent necessary conditions, we contend that they are sufficient ones. The regions in which the Urban Revolution started were not necessarily the most productive. Moreover, the invention of farming preceded by more than five thousand years the explosion of cities, states and inequality that can be observed from 3300 BCE.

We provide first empirical evidence that the discovery of bronze and the ensuing long-distance trade played an important role in explaining this phenomenon. Consistent with the qualitative archaeological literature we document that regions located along trade corridors connecting copper and tin mines to fertile lands were more likely to experience the Urban Revolution. We conjecture that transit bottlenecks allowed a tax-levying elite to emerge and to be sustained. We formally test this appropriability theory and provide several case studies in support.

References

Acemoglu, Daron, Simon Johnson, and James A. Robinson. 2002. "Reversal of Fortune: Geography and Institutions in the Making of the Modern World Income Distribution." *The Quarterly Journal of Economics* 117 (4): 1231–1294.

Adamson, Jeremy. 2021. "Trade and the rise of ancient Greek city-states."

Algaze, Guillermo. 1993. *The Uruk World System: The Dynamics of Expansion of Early Mesopotamian Civilization.* Chicago: University of Chicago Press.

Algaze, Guillermo. 2001. *The prehistory of imperialism: the case of Uruk period Mesopotamia.* na.

Algaze, Guillermo. 2009. "Ancient Mesopotamia at the Dawn of Civilization." In *Ancient Mesopotamia at the Dawn of Civilization*, edited by Guillermo Algaze. University of Chicago Press.

Allen, Robert C., Mattia C. Bertazzini, and Leander Heldring. 2022. "The Economic Origins of Government."

Ashraf, Quamrul, and Oded Galor. 2011. "Dynamics and Stagnation in the Malthusian Epoch." *American Economic Review* 101 (5): 2003–41.

Bagnall, Roger. 2022. "Pleiades: A Gazetteer of Past Places." pleiades.stoa.org.

Bakker, Jan David, Stephan Maurer, Jörn-Steffen Pischke, and Ferdinand Rauch. 2021. "Of Mice and Merchants: Trade and Growth in the Iron Age." *Review of Economics and Statistics* 103 (4): 652–665.

Barjamovic, Gojko, Thomas Chaney, Kerem Coşar, and Ali Hortaçsu. 2019. "Trade, Merchants, and the Lost Cities of the Bronze Age." *The Quarterly Journal of Economics* 134 (3): 1455–1503.

Bates, Robert H. 1983. *Essays on the Political Economy of Rural Africa.* University of California Press.

Bentzen, Jeanet Sinding, Nicolai Kaarsen, and Asger Moll Wingender. 2017. "IRRIGATION AND AUTOCRACY." *Journal of the European Economic Association* 15 (1): 1–53.

Bleaney, Michael, and Arcangelo Dimico. 2011. "How different are the correlates of onset and continuation of civil wars?" *Journal of Peace Research* 48 (2): 145–155.

Borcan, Oana, Ola Olsson, and Louis Putterman. 2018. "State history and economic development: evidence from six millennia." *Journal of Economic Growth* 23 (1): 1–40.

Brannan, James A. 1992. "On Modeling Resource Transport Costs: Suggested Refinements." *Current Anthropology* 33 (1): 56–60.

Carneiro, R L. 1970. "A Theory of the Origin of the State: Traditional theories of state origins are considered and rejected in favor of a new ecological hypothesis." *Science*

169 (3947): 733–738.

Chanda, Areendam, C. Justin Cook, and Louis Putterman. 2014. "Persistence of Fortune: Accounting for Population Movements, There Was No Post-Columbian Reversal." *American Economic Journal: Macroeconomics* 6 (3): 1–28.

Chandler, Tertius. 1987. *Four Thousand Years of Urban Growth: An Historical Census.* New York: Edwin Mellen.

Childe, Gordon. 1930. *The Bronze Age.* Cambridge University Press.

Childe, V. Gordon. 1950. "The Urban Revolution." *The Town Planning Review* 21 (1): 3–17.

Comin, Diego, William Easterly, and Erick Gong. 2010. "Was the Wealth of Nations Determined in 1000 BC?" *American Economic Journal: Macroeconomics* 2 (3): 65–97.

Conley, T. G. 1999. "GMM estimation with cross sectional dependence." *Journal of Econometrics* 92 (1): 1–45.

Cunliffe, Barry. 2011. *Europe Between the Oceans, 9000 BC-AD 1000.* Yale University Press.

Dal Bó, Ernesto, Pablo Hernández-Lagos, and Sebastián Mazzuca. 2022. "The paradox of civilization: Preinstitutional sources of security and prosperity." *American Political Science Review* 116 (1): 213–230.

Davis, Donald R., and David E. Weinstein. 2002. "Bones, Bombs, and Break Points: The Geography of Economic Activity." *American Economic Review* 92 (5): 1269–1289.

Diamond, Jared M. 1998. *Guns, Germs, and Steel: the Fates of Human Societies.* New York: W. W. Norton & Co.

Dijkstra, Edsger W. 1959. "A Note on Two Problems in Connexion with Graphs." *Numerische Mathematik* 1 (1): 269–271.

Donaldson, Dave. 2018. "Railroads of the Raj: Estimating the Impact of Transportation Infrastructure." *American Economic Review* 108 (4–5): 899–934.

Earle, Timothy. 2013. "The 3M: materiality, materialism and materialization." In *Counterpoint: essays in archaeology and heritage studies in honour of Professor Kristian Kristiansen*, *BAR International Series*, edited by Sophie Bergerbrant and Serena Sabatini, 353–360. Oxford: Oxbow.

Earle, Timothy, and Matthew Spriggs. 2015. "Political economy in prehistory: a Marxist approach to Pacific sequences." *Current Anthropology* 56 (4): 515–544.

Earle, Timothy, Johan Ling, Claes Uhnér, Zofia Stos-Gale, and Lene Melheim. 2015. "The Political Economy and Metal Trade in Bronze Age Europe: Understanding Regional Variability in Terms of Comparative Advantages and Articulations." *European Journal of Archaeology* 18 (4): 633–657.

Engels, Friedrich. 1942. *The origin of the Family.* Current Book Distributors.

Ertan, Arhan, Martin Fiszbein, and Louis Putterman. 2016. "Who was colonized and when? A cross-country analysis of determinants." *European Economic Review* 83: 165–184.

Fenske, James. 2014. "ECOLOGY, TRADE, AND STATES IN PRE-COLONIAL AFRICA." *Journal of the European Economic Association* 12 (3): 612–640.

Flückiger, Matthias, Erik Hornung, Mario Larch, Markus Ludwig, and Allard Mees. 2022. "Roman Transport Network Connectivity and Economic Integration." *The Review of Economic Studies* 8989 (2): 774–810.

Galor, Oded, and Ömer Özak. 2015. "Land Productivity and Economic Development: Caloric Suitability vs. Agricultural Suitability,." Brown University Working Paper.

Galor, Oded, and Ömer Özak. 2016. "The Agricultural Origins of Time Preference." *American Economic Review* 106 (10): 3064–3103.

Hahnekamp, Christine. 2011. "Vergleichende Untersuchung zum Fundkontext bronze- und urnenfelderzeitlicher Schwerter in Ostfrankreich und Süddeutschland." *Diplomarbeit, Universität Wien.*

Hänsel, Bernhard. 2014. "Atlas der Vorgeschichte: Europa von den ersten Menschen bis Christi Geburt: Europa von den ersten Menschen bis Christi Geburt." edited by Siegmar Frhr. v. Schnurbein 3., überarbeitete und erweiterte Edition edition, Chapter Bronzezeit. wbg Theiss in Wissenschaftliche Buchgesellschaft.

Harding, Anthony. 2000. *European societies in the Bronze Age.* Cambridge University Press.

Harding, Anthony. 2015. "The emergence of elite identities in Bronze Age Europe." *Origini* 37 (1): 111–121.

Harris, Chauncy D. 1954. "The Market as a Factor in the Localization of Industry in the United States." *Annals of the Association of American Geographers* 44 (4): 315–348.

Henderson, J Vernon, Tim Squires, Adam Storeygard, and David Weil. 2018. "The Global Distribution of Economic Activity: Nature, History, and the Role of Trade1." *The Quarterly Journal of Economics* 133 (1): 357–406.

Hibbs, Douglas A., and Ola Olsson. 2004. "Geography, biogeography, and why some countries are rich and others are poor." *Proceedings of the National Academy of Sciences* 101 (10): 3715–3720.

Jones, Kevin T., and David B. Madsen. 1989. "Calculating the Cost of Resource Transportation: A Great Basin Example." *Current Anthropology* 30 (4): 529–534.

Karger, Dirk Niklaus, Michael P. Nobis, Signe Normand, Catherine H. Graham, and Niklaus E. Zimmermann. 2021. "CHELSA-TraCE21k v1.0. Downscaled transient temperature and precipitation data since the last glacial maximum." *Climate of the Past Discussions* 2021: 1–27.

Kiszewski, A., A. Mellinger, A. Spielman, P. Malaney, S. E. Sachs, and J. Sachs. 2004. "A global index representing the stability of malaria transmission." *American Journal of Tropical Medicine and Hygiene* 70 (5): 486–498.

Klein Goldewijk, Kees, Arthur Beusen, and Peter Janssen. 2010. "Long-term dynamic modeling of global population and built-up area in a spatially explicit way: HYDE 3.1." *The Holocene* 20 (4): 565–573.

Kristiansen, K., and T. Earle. 2015. "Neolithic versus Bronze Age social formations: a political economy approach." In *Paradigm Found: Archaeological Theory: Present, Past and Future. Essays in Honour of Evzen Neustupny*, Oxbow Books.

Kristiansen, Kristian, and Paulina Suchowska-Ducke. 2015. "Connected Histories: The Dynamics of Bronze Age Interaction and Trade 1500–1100 BC." *Proceedings of the Prehistoric Society* 81: 361–392.

Kristiansen, Kristian, and Thomas Larson. 2005. *The Rise of Bronze Age Society: Travels, Transmissions and Transformations.* Cambridge University Press.

Kuhrt, A. 1995. *The ancient near east, c. 3000-330 BC.* Vol. 2. Taylor & Francis US.

Lieth, Helmut. 1975. "Modeling the Primary Productivity of the World." *Primary Productivity of the Biosphere*, edited by Helmut Lieth and Robert H. Whittaker, 237–263. Berlin, Heidelberg: Springer Berlin Heidelberg.

Maloney, William F., and Felipe Valencia Caicedo. 2016. "The Persistence of (Subnational) Fortune." *The Economic Journal* 126 (598): 2363–2401.

Matranga, Andrea, and Luigi Pascali. 2021. "Chapter 5 - The use of archaeological data in economics." In *The Handbook of Historical Economics*, edited by Alberto Bisin and Giovanni Federico, 125–145. Academic Press.

Mayoral, Laura, and Ola Olsson. 2020. "Pharaoh's Cage: Environmental Circumscription and Appropriability in Early State Development."

Mayshar, Joram, Omer Moav, and Luigi Pascali. 2022. "The Origin of the State: Land Productivity or Appropriability?" *Journal of Political Economy* 130 (4): 1091–1144.

Modelski, George. 2003. *World Cities: -3000 to 2000.* Washington, DC:: FAROS.

Murr, Lawrence E. 2015. "A Brief History of Metals." *Handbook of Materials Structures, Properties, Processing and Performance*, 3–9. Cham: Springer International Publishing.

Nessel, Bianka, Daniel Neumann, and Martin Bartelheim, ed. 2018. *Bronzezeitlicher Transport - Akteure, Mittel und Wege.* Vol. 8 of *RessourcenKulturenBand - Editor of Series: Martin Bartelheim and Thomas Scholten.* Tübingem University Press.

Nunn, Nathan, and Diego Puga. 2012. "Ruggedness: The Blessing of Bad Geography in Africa." *The Review of Economics and Statistics* 94 (1): 20–36.

OBrien, William. 2013. "The Oxford Handbook of the European Bronze Age." edited by Harry Fokkens and Anthony Harding, Chapter Bronze Age Copper mining in Europe.

Oxford University Press.

O'Brien, William. 2015. *Prehistoric Copper Mining in Europe: 5500-500 BC.* Oxford University Press.

Olsson, Ola, and Christopher Paik. 2020. "A Western Reversal Since the Neolithic? The Long-Run Impact of Early Agriculture." *The Journal of Economic History* 80 (1): 100–135.

Özak, Ömer. 2010. "The Voyage of Homo-economicus: Some Economic Measures of Distance." Department of Economics, Brown University mimeo.

Palmer, Leonard R. 1962. *Mycenaeans and Minoans: Aegean Prehistory in the Light of the Linear B Tablets.* New York: Alfred A. Knopf.

Petersen, Michael Bang, and Svend-Erik Skaaning. 2010. "Ultimate Causes of State Formation: The Significance of Biogeography, Diffusion, and Neolithic Revolutions / Ultimative Ursachen für die Staatsbildung: Die Signifikanz von Biogeographie, Diffusion und Neolithische Revolutionen." *Historical Social Research / Historische Sozialforschung* 35 (3 (133)): 200–226.

Pétrequin, Pierre, Serge Cassen, Michel Errera, L. Klassen, Alison Sheridan, and Anne Marie Pétrequin. 2012. *Jade: Grandes haches alpines du Néolithique européen, Ve et IVe millénaires av. J.-C.* Centre de Recherche Archéologique de la Vallée de l'Ain.

Polanyi, Karl, Harry Pearson, and C. M. Ahrensburg. 1957. *Trade and Market in the Early Empires.* Glencoe: Free Press.

Putterman, Louis, and David N. Weil. 2010. "Post-1500 Population Flows and The Long-Run Determinants of Economic Growth and Inequality*." *The Quarterly Journal of Economics* 125 (4): 1627–1682.

Radivojević, Miljana, Benjamin W. Roberts, Ernst Pernicka, Zofia Stos-Gale, Marcos Martinón-Torres, Thilo Rehren, Peter Bray, Dirk Brandherm, Johan Ling, Jianjun Mei, et al. 2019. "The Provenance, Use, and Circulation of Metals in the European Bronze Age: The State of Debate." *Journal of Archaeological Research* 27 (2): 131–185.

Rahmstorf, Lorenz. 2010. "Die Nutzung von Booten und Schiffen in der bronzezeitlichen Ägäis und die Fernkontakte der Frühbronzezeit." *Der Griff nach den Sternen Internationales Symposium in Halle (Saale) 16.-21. Februar 2005.* Landesamt für Denkmalpflege u. Archäologie Sachsen-Anhalt.

Ramsay, William Mitchell. 1890. *The historical geography of Asia Minor.* Vol. 4. John Murray.

Reba, Meredith, Femke Reitsma, and Karen C. Seto. 2016. "Spatializing 6,000 years of global urbanization from 3700 BC to AD 2000." *Scientific Data* 3 (1): 160034.

Renfrew, Colin, and Paul Bahn. 2016. *Archaeology: Theories, Methods and Practice, 11ed.* Thames & Hudson.

Riley, Shawn, Stephen Degloria, and S.D. Elliot. 1999. "A Terrain Ruggedness Index that Quantifies Topographic Heterogeneity." *Internation Journal of Science* 5: 23–27.

Sanders, William T. 1968. "Hydraulic Agriculture, Economic Symbiosis, and the Evolution of States in Central Mexico." In *Anthropological Archeology in the Americas*, edited by Betty J Meggers. Washington, DC: Anthropological Society of Washington.

Schauer, Peter, Andrew Bevan, Stephen Shennan, Kevan Edinborough, Tim Kerig, and Mike Parker Pearson. 2020. "British Neolithic Axehead Distributions and Their Implications." *Journal of Archaeological Method and Theory* 27: 836–859.

Schönholzer, David. 2020. "The Origin of the Incentive Compatible State: Environmental Circumscription."

Smith, Adam. 1978. *Lectures on jurisprudence.* Vol. 5. VM eBooks.

Testart, Alain, Richard G Forbis, Brian Hayden, Tim Ingold, Stephen M Perlman, David L Pokotylo, Peter Rowley-Conwy, and David E Stuart. 1982. "The significance of food storage among hunter-gatherers: Residence patterns, population densities, and social inequalities [and comments and reply]." *Current anthropology* 23 (5): 523–537.

Uckelmann, Marion. 2013. "The Oxford Handbook of the European Bronze Age." edited by Harry Fokkens and Anthony Harding, Chapter Land Transport in the Bronze Age. Oxford University Press.

U.S. Geological Survey. 2011. "Mineral Resources Data System."

Vogt, Burkhard. 1996. "Indian Ocean In Antiquity." Chapter Bronze Age maritime trade in the Indian Ocean: Harappan traits on the Oman peninsula. Routledge.

Vörösmarty, C. J., B. M. Fekete, M. Meybeck, and R. B. Lammers. 2000. "Global System of Rivers: Its Role in Organizing Continental Land Mass and Defining Land-to-ocean Linkages." *Global Biogeochemical Cycles* 14 (2): 599–621.

Wang, Yunchuan, Shasha Wang, and Yong Deng. 2019. "A modified efficiency centrality to identify influential nodes in weighted networks." *Pramana* 92.

Whitehouse, David, and Ruth Whitehouse. 1975. *Archaeological Atlas of the World. Documents of Revolution.* Thames and Hudson.

Wittfogel, K.A. 1957. *Oriental Despotism: A Comparative Study of Total Power. Oriental Despotism: A Comparative Study of Total Power.* Yale University Press.

Appendices

A Data and Summary statistics

A.1 Spatial distribution archaeological sites

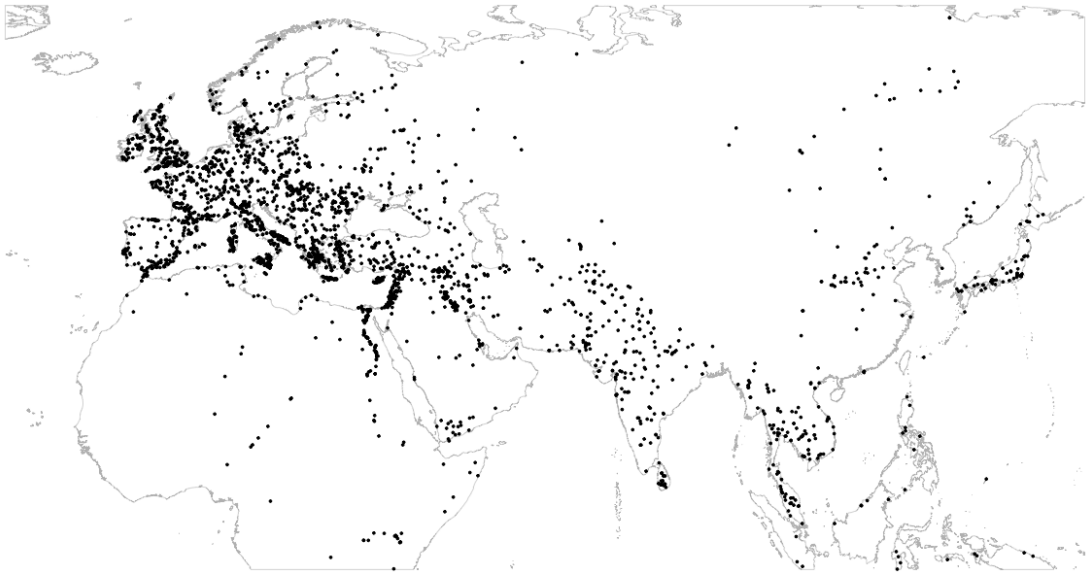


Figure A.1: Sites Whitehouse and Whitehouse (1975)
Figure depicts the location of archaeological sites from Whitehouse and Whitehouse (1975)'s Archaeological Atlas of the World used in our analysis.

A.2 Copper and Tin mines

To compile our database on location of copper and tin mines, we systematically scoured the archaeological literature. A prerequisite for the data to be included in our analysis is that (i) the precise location of the mines could be inferred, and (ii) we could ascertain that the mining sites were active during the Bronze Age. In total, we were able to identify 121 copper mines and 44 tin mines that fulfil these criteria.

Figure A.3 depicts the location of these mines, while Table A.1–A.2 list the names of the mines along with sources from which they were retrieved and the precise geographical coordinates.

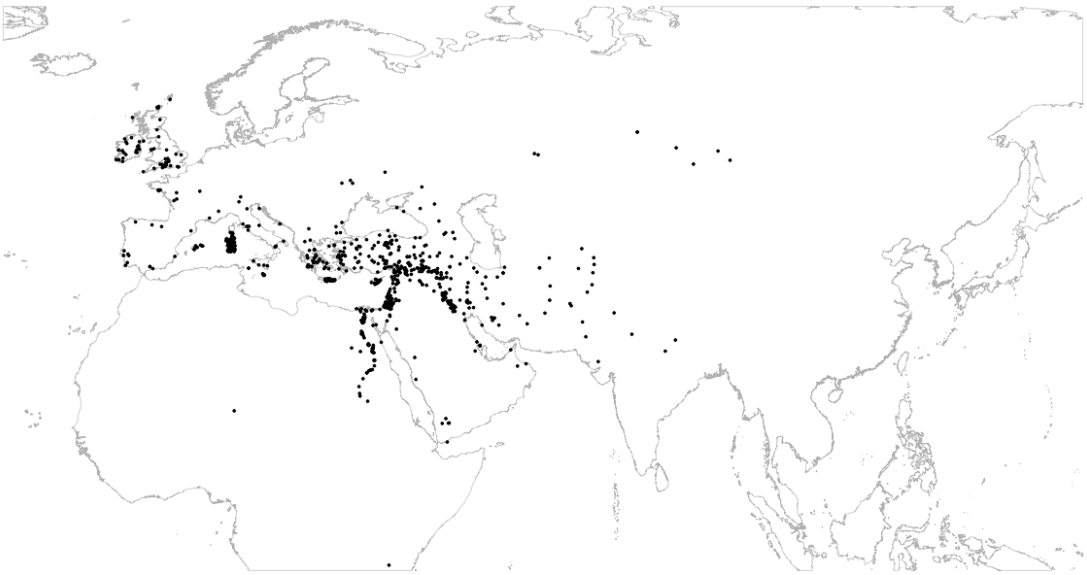


Figure A.2: Sites Pleiades Gazetteer
Figure depicts the location of archaeological sites from the Pleiades Gazetteer Bagnall (2022) used in our analysis.

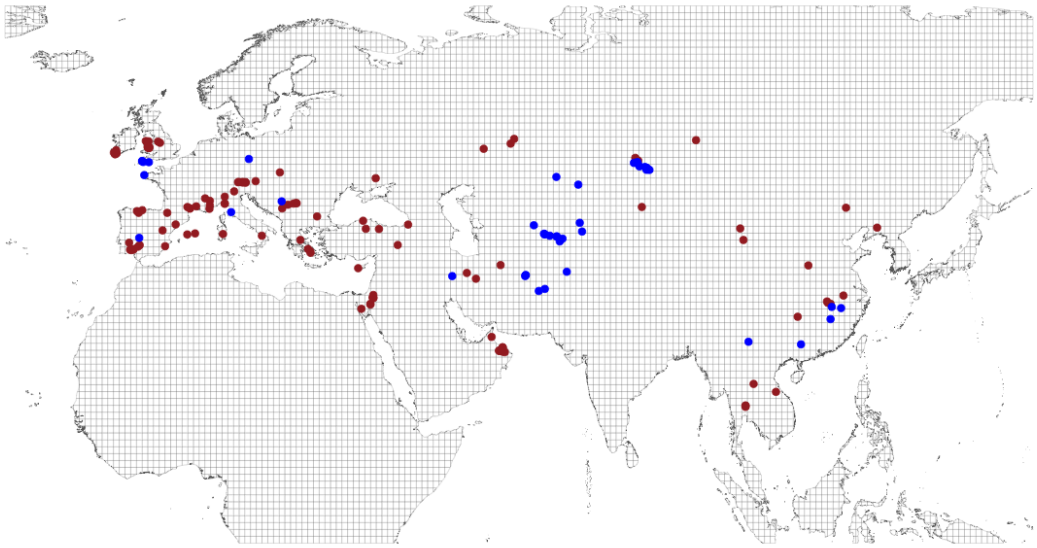


Figure A.3: Location of metal mines
Figure depicts the location copper (brown dots) and tin (blue dots) mines.

Table A.1: References for database of copper mine locations

Name	Country	Latitude	Longitude	Source
Kelchalpe (Kelchalm)	Austria	47.3869	12.4661	O'Brien (2015)
Leogang-Shwartzleo/Gunzereit	Austria	47.4253	12.6808	O'Brien (2015)
Mauken Mining Area	Austria	47.4306	11.9375	Schibler et al. (2011)
Mitterberg Mining Area	Austria	47.4094	13.1281	O'Brien (2015)
Obersteiermark	Austria	47.5500	14.8833	O'Brien (2015)
Schwaz-Brixlegg	Austria	47.4053	11.7978	O'Brien (2015)
St. Veit Mining Area	Austria	47.3372	13.1369	O'Brien (2015)
Viehofen-Wirtsalm	Austria	47.3667	12.7167	O'Brien (2015)
Ai Bunar	Bulgaria	42.4328	25.6419	O'Brien (2015)
Baishantang Copper Mine	China	40.6833	99.7333	Jaang (2015)
Gangxia	China	29.8992	115.0725	Liu et al. (2019)
Jinniudong	China	30.9450	117.8111	Reinhardt (1997)
Linxi	China	43.6917	118.2656	Pollard et al. (2017)
Mayang	China	27.8639	109.8011	Reinhardt (1997)
Nulasai Mine	China	43.8003	82.5117	Wang et al. (2019)
Tongling	China	29.7533	115.5475	Liu et al. (2019)
Tonglushan	China	30.0839	114.9347	Larreina-García (2017)
Xichengyi (Originally Heishuiguo)	China	39.0100	100.3000	Jaang (2015)
Xiquegou	China	40.7997	123.7081	Pollard et al. (2017)
Zhongtiaoshan ore field	China	35.3167	111.6667	Liu et al. (2019)
Investigate all the mines here	Cyprus	34.9167	32.8333	Constantinou (2012)
Wadi Maghara	Egypt	29.0203	33.4019	Hauptmann (1997)
Alderly Edge Mines	England (UK)	53.2975	-2.2100	National Trust
Ecton	England (UK)	53.1217	-1.8561	Timberlake and Marshall (2018)
Bouco-Payrol Mines	France	43.7950	2.9325	O'Brien (2015)
Causiat	France	42.9500	-0.6000	O'Brien (2015)
Clue de Roua	France	44.0350	6.8578	O'Brien (2015)
La Roussignole	France	43.8964	4.4817	O'Brien (2015)
Les Rousses Mining Centre	France	45.0500	6.0333	O'Brien (2015)
Maraval	France	43.5406	6.7942	O'Brien (2015)
Pioch Farrus	France	43.5794	3.3714	O'Brien (2015)
Saint Veran	France	44.7000	6.8644	O'Brien (2015)
Vallarade	France	43.5931	3.3803	O'Brien (2015)
Kythnos	Greece	37.3833	24.4167	Catapotis (2007)
Lavrion Mine Area	Greece	37.7000	24.0497	Gale and Stos-Gale (2002)
Othrys Mountains	Greece	39.0169	22.7097	Gale and Stos-Gale (2002)
Seriphos	Greece	37.1500	24.5000	O'Brien (2015)
Anarak Talmessi	Iran	33.3858	53.4631	Nezafati and Stöllner (2018)
Taknar	Iran	35.3719	57.7719	Nezafati and Stöllner (2018)
Veshnāveh (Ghar Chale)	Iran	34.2250	51.8681	Nezafati and Stöllner (2018)
Ballyrisode Hill	Ireland	51.5158	-9.6719	O'Brien (2015)
Canshanavoe	Ireland	51.7194	-9.7019	O'Brien (2015)
Derrycarhoon	Ireland	51.6092	-9.4572	O'Brien (2015)
Mount Gabriel	Ireland	51.5500	-9.5364	O'Brien (1999)
Ross Island	Ireland	52.0381	-9.5369	Northover, O'Brien and Stos (2001)
Tooreen	Ireland	51.7983	-9.5653	O'Brien (2015)
Boulysallagh	Ireland	51.4753	-9.7361	O'Brien (2015)
Callaros Oughter	Ireland	51.4922	-9.7325	O'Brien (2015)
Carrigacat	Ireland	51.5161	-9.7575	O'Brien (2015)
Crumpane	Ireland	51.6933	-9.9397	O'Brien (2015)

Nahal 'Amram	Israel	29.6281	34.9833	Avner et al. (2018)
Timna	Israel	29.7469	34.9794	Avner (2014)
Campolungo	Italy	45.2942	9.4719	O'Brien (2015)
Grotta della Monaca	Italy	39.6278	15.9756	Quarta et al. (2013)
Libiola	Italy	44.3047	9.4483	O'Brien (2015)
Monte Loreto	Italy	44.2703	9.4933	O'Brien (2015)
Trentino	Italy	46.0678	11.1211	O'Brien (2015)
Madsus	Jordan	30.6717	35.4106	Hauptmann (2007)
Qalb Ratiye Mining District	Jordan	30.6450	35.4781	Hauptmann (2007)
Umm el-Amad	Jordan	30.5719	35.4956	Hauptmann (2007)
Umm ez-Zuhur	Jordan	30.6667	35.4067	Hauptmann (2007)
Wadi Abiad Mining District	Jordan	31.0283	35.4889	Hauptmann (2007)
Wadi Khalid	Jordan	30.6331	35.4700	Hauptmann (2007)
Nikolaevskoe	Kazakhstan	50.5331	81.8756	Stöllner et al. (2011)
Orlovskoe	Kazakhstan	50.9333	81.3650	Stöllner et al. (2011)
Vilabouly Complex	Laos	16.9603	105.9989	Cadet et al. (2019)
Al-Moyassar i.e. Maysar	Oman	22.7964	58.1292	Giardino (2019)
Batin	Oman	22.7289	58.5189	Giardino (2019)
Bilad Al-Maidin	Oman	23.4131	58.1242	Giardino (2019)
Gebel Saleli	Oman	22.9333	57.5333	Giardino (2019)
Huqain	Oman	22.9333	57.5333	Giardino (2019)
Nujum	Oman	23.4131	58.1242	Giardino (2019)
Tawi Ubaylah	Oman	22.9333	57.5333	Giardino (2019)
Wadi Miadin	Oman	23.4131	58.1242	Giardino (2019)
Mociços	Portugal	38.6222	-7.2633	O'Brien (2015)
Kargaly Mines	Russia	52.2500	54.8167	O'Brien (2015)
Minussinsk basin	Russia	53.5000	92.0000	Stöllner et al. (2011)
Novonikolayevskiy	Russia	47.9767	35.9094	XY
Novotemirskiy	Russia	53.6842	60.1492	XY
Vorovskaya Yama	Russia	52.9992	59.5375	XY
Funtana Raminosa	Sardinia	39.8775	9.1719	O'Brien (2015)
Jarmovac	Serbia	43.6000	19.5333	Derikonjic, Pernicka and Rehren (n.d.)
Majdanpek	Serbia	44.3831	21.9500	Radivojević et al. (2010)
Mali Sturak	Serbia	44.1314	20.5403	O'Brien (2015)
Rudna Glava	Serbia	44.3389	22.0722	O'Brien (2015)
Zdrelo	Serbia	44.2981	21.5069	Radivojević et al. (2010)
Spania Dolina	Slovakia	48.8175	19.1308	O'Brien (2015)
Cabezo Jure	Spain	37.5964	-7.1106	O'Brien (2015)
Chinflon	Spain	37.5500	-6.9167	O'Brien (2015)
Cuchillares	Spain	37.6992	-6.5708	O'Brien (2015)
El Aramo	Spain	43.2000	-5.9000	O'Brien (2015)
La Loba	Spain	38.2667	-5.4167	O'Brien (2015)
Las Navas, Berrocal	Spain	37.6000	-6.5333	O'Brien (2015)
Loma de la Tejeria	Spain	40.4011	-1.4169	O'Brien (2015)
Mallorca	Spain	39.8153	2.9133	O'Brien (2015)
Redondilla	Spain	38.0381	-5.7136	O'Brien (2015)
Sierra de Orihuela	Spain	38.1078	-0.9689	O'Brien (2015)
El Milagro	Spain	43.3353	-4.9675	O'Brien (2015)
La Profunda	Spain	42.9500	-5.6000	O'Brien (2015)
Solana del Bepo	Spain	41.2664	0.8761	Rafel et al. (2019)
Khao Sai On	Thailand	14.7833	100.6667	Pryce et al. (2011*a*)
Nil Kham Haeng	Thailand	14.9569	100.6561	Higham et al. (2020)
Non Pa Wai	Thailand	14.9711	100.6781	Pryce et al. (2011*b*)
Phu Lon	Thailand	18.1167	102.0831	Higham et al. (2020)

Derekutugun	Turkey	40.6364	34.1772	XY
Ergani Maden	Turkey	38.2831	39.7664	Özbal, Adriaens and Earl (1999)
Kure	Turkey	41.8000	33.7000	XY
Murgul	Turkey	41.2475	41.5817	Kaptan (1990)
Tokat-Erbaa, Kozlu	Turkey	40.6089	36.4817	Lehner and Yener (2013)
Wadi al-Hilo	UAE	24.9425	56.2056	Kutterer, Neureiter and Jasim (2013)
Copa Hill	Wales (UK)	52.3603	-3.7542	Hughes (1981)
Erglodd	Wales (UK)	52.4944	-3.9783	O'Brien (2015)
Great Orme	Wales (UK)	53.3333	-3.8533	Lewis (1997)
Llancynfelin	Wales (UK)	52.5164	-4.0333	O'Brien (2015)
Nantyrarian	Wales (UK)	52.4147	-3.9042	O'Brien (2015)
Nantyreira	Wales (UK)	52.4714	-3.7283	O'Brien (2015)
Ogof Wyddon	Wales (UK)	52.5847	-3.8325	O'Brien (2015)
Parys Mountain	Wales (UK)	53.3761	-4.3514	O'Brien (2015)
Twll-y-mwyn	Wales (UK)	52.4311	-3.9417	O'Brien (2015)
Tyn y fron	Wales (UK)	52.3886	-3.8783	O'Brien (2015)

Notes: This table lists the location of copper mines by reference.

A.3 Spatial distribution croplands, NPP, deposits, and IV

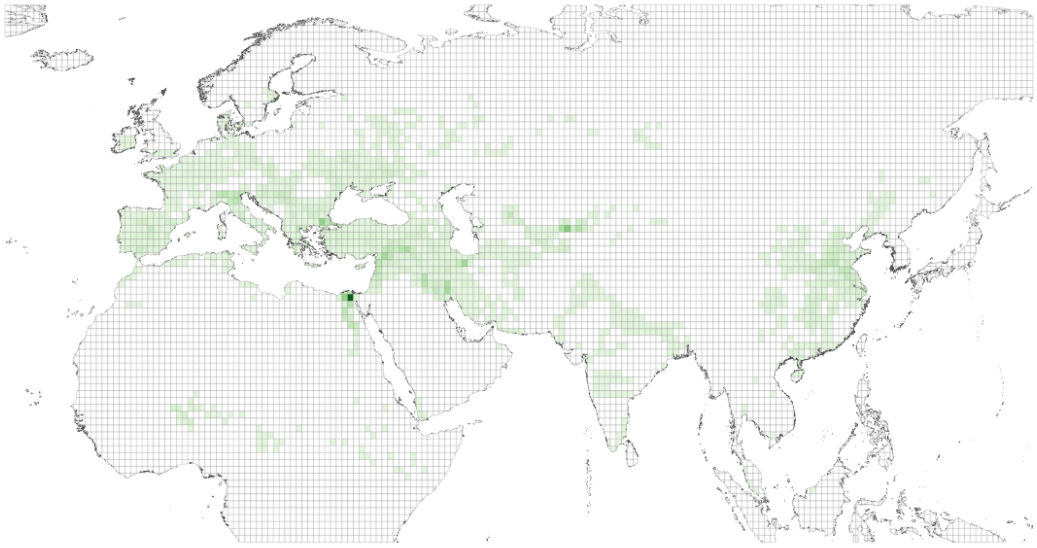
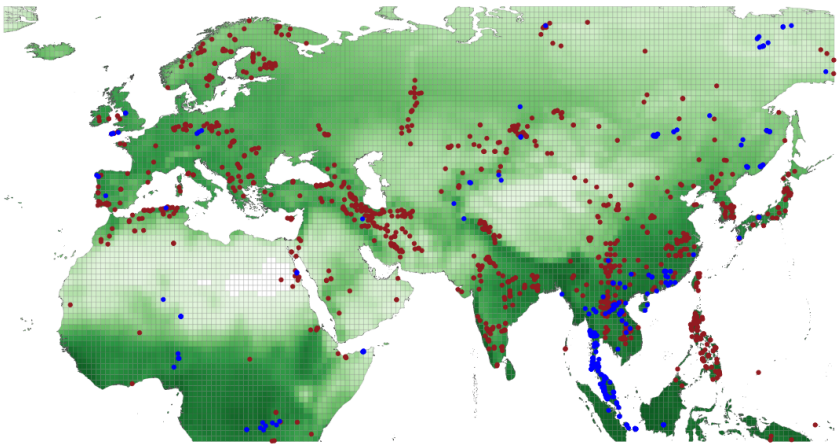


Figure A.4: Distribution Croplands
Figure depicts spatial distribution of croplands for the year 3000 BCE (source: Klein Goldewijk, Beusen and Janssen (2010). Darker shadings imply larger areas of croplands.

(a)



(b)

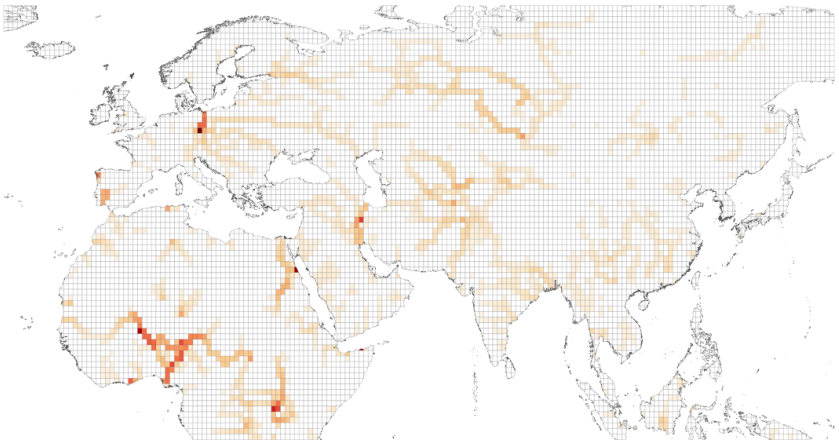


Figure A.5: Deposits, NPP and IV

Panel (a) depicts the spatial distribution copper deposits (brown dots), tin deposits (blue dots), and NPP (green shadings, where darker shadings imply higher values of NPP). Panel (b) visualises the instrumental variable (where continent fixed effects are partialled out). Klein Goldewijk, Beusen and Janssen (2010).

Table A.2: References for database of tin mine locations

Name	Country	Latitude	Longitude	Source
Ebrahimi	Afghanistan	33.7740	62.0831	Cleuziou (1982)
Mes Aynak	Afghanistan	34.4002	69.3667	Massoudi (2011)
Misgaran	Afghanistan	33.8827	62.1662	Cleuziou (1982)
Mundigak	Afghanistan	31.9039	65.5246	Liverani and Tabatabai (2014)
Sarkar	Afghanistan	31.6108	64.4685	Cleuziou (1982); Garner (2014)
Shaida	Afghanistan	33.9223	62.1789	Cleuziou (1982)
De'an	China	29.2986	115.7675	Liu et al. (2015, 2018, 2019)
Guangxi	China	23.8563	110.3799	Liu et al. (2015, 2018)
Jiangxi	China	27.5246	115.5575	Liu et al. (2015, 2018)
Qiaomailing	China	29.1231	117.4019	Liu et al. (2015, 2018)
Yunnan	China	24.2362	101.1912	Liu et al. (2015, 2018)
Brittany	France	48.4317	-4.6206	Benvenuti et al. (2003); Tolksdorf et al. (2020); Valera and Valera (2003)
Schellerhau	Germany	50.7711	13.6944	Tolksdorf et al. (2020)
Deh Hosein	Iran	33.7667	49.3083	Valamoti and Jones (2010)
Askaraly	Kazakhstan	50.2035	81.1148	Garner (2014)
Bajmurza	Kazakhstan	49.4587	83.3580	Garner (2014)
Čerdojak	Kazakhstan	49.1888	83.8428	Garner (2014); Stöllner et al. (2011)
Čudskoje	Kazakhstan	49.2021	83.3180	Stöllner et al. (2011)
Delbegetej	Kazakhstan	50.0730	81.8324	Stöllner et al. (2011)
Južnyj Bulattau	Kazakhstan	47.0436	71.3797	Garner (2014)
Kalai Topkan	Kazakhstan	49.4587	83.3580	Garner (2014)
Karagoin	Kazakhstan	49.4587	83.3580	Garner (2014)
Mynčunkur	Kazakhstan	49.6916	82.0868	Stöllner et al. (2011)
Ubinskoe	Kazakhstan	50.3302	81.7358	Garner (2014); Stöllner et al. (2011)
Ulytauskie ross-	Kazakhstan	48.1638	67.5453	Garner (2014)
Urunčaj	Kazakhstan	49.6185	83.0543	Stöllner et al. (2011)
Mount Cer	Serbia	44.6217	19.4392	Huska et al. (2014)
Cerro de San Cristobal	Spain	39.3214	-5.5053	Benvenuti et al. (2003); Tolksdorf et al. (2020); Valera and Valera (2003)
Džaupai	Tajikistan	38.8027	68.1332	Garner (2014)
Mushiston	Tajikistan	39.5000	67.6167	Garner (2014, 2015); Valamoti and Jones (2010)
Mušiston	Tajikistan	39.5359	67.5984	Garner (2014)
Takfon	Tajikistan	39.2061	68.6223	Garner (2014)
Monte Valerio	Tuscany	43.0505	10.5932	Valamoti and Jones (2010); Muhly (1985)
Cornwall	UK	50.4483	-4.9990	Benvenuti et al. (2003); Tolksdorf et al. (2020); Valera and Valera (2003)
Devon	UK	50.3078	-3.8111	Benvenuti et al. (2003); Tolksdorf et al. (2020); Valera and Valera (2003)
St Austell	UK	50.3378	-4.7950	Muhly (1985)
St Eval	UK	50.4780	-4.9840	Muhly (1985)
Auminza-tau	Uzbekistan	41.1464	63.6024	Garner (2014)
Čhangali	Uzbekistan	39.6275	66.3947	Garner (2015); Stöllner et al. (2011)
Isfajramsaj	Uzbekistan	40.2358	72.0442	Garner (2014)
Karatube	Uzbekistan	41.5059	71.6400	Garner (2014)
Karnab	Uzbekistan	39.8297	65.4917	Garner (2014, 2015); Valamoti and Jones (2010)
Karnab	Uzbekistan	39.8297	65.4917	Stöllner et al. (2011); Valamoti and Jones (2010)
Lapas	Uzbekistan	39.9151	65.3768	Garner (2014); Stöllner et al. (2011)

Notes: This table lists the location of tin mines by reference.

A.4 Summary statistics

Table A.3: Summary statistics of key variables

Variable	Mean	Std. Dev.	Min.	Max.	Obs.
	Cross-sectional dataset (Section 5.1)				
Any City by 1300 BCE (×100)	0.477	6.893	0	100	9,426
# Cities (×100)	0.668	12.126	0	700	9,426
Transit Index	118.701	526.694	0	12,715.225	9,426
IV Transit trade	667.199	1,534.857	0	35,774.016	9,426
Blockage cost	335.142	1,593.934	0	82,151.688	9,426
Proximity mines	41.487	59.391	0.009	1,871.977	9,426
Proximity croplands	248.456	128.630	0.225	976.780	9,426
Land productivity	88,392.568	107,047.227	0	429,868.531	9,426
	Panel dataset archaeological sites (Section 5.2)				
Any Site (×100)[a]	8.498	27.886	0	100	18,852
# Sites[a] (×100)	23.122	131.761	0	5700	18,852
Any Settlement (×100)[a]	5.617	23.026	0	100	18,852
# Settlements[a] (×100)	10.179	58.836	0	1900	18,852
Any Site (×100)[b]	2.376	15.232	0	100	18,852
# Sites[b] (×100)	6.265	79.369	0	5100	18,852
Any Settlement (×100)[b]	1.851	13.480	0	100	18,852
# Settlements[b] (×100)	3.962	42.950	0	1900	18,852
Transit Index	59.350	377.119	0	12,715.225	18,852
IV Transit trade	333.600	1,135.396	0	35,774.016	18,852
Blockage cost	167.571	1,139.442	0	82,151.688	18,852
	China (Section 5.3)				
Any Criterion (×100)	15.108	35.821	0	100	2,138
#Criteria	1.206	7.311	0	220	2,138
Transit Index	90.627	511.601	0	7,133.541	2,138
IV Transit trade	183.127	349.505	0	3,624.518	2,138
	Europe (Section 5.4)				
Any Weapon in Grave (×100)	38.154	48.610	0	100	726
Number of Weapons in Grave	2.686	6.952	0	61	726
Share of Weapons in Grave (×100)	14.439	27.111	0	100	726
Transit Index	891.122	1,957.730	0	14,686.713	726

Notes: [a]data from Whitehouse and Whitehouse (1975); [b]data from Pleiades.

B Period-specific per-unit transport costs

To estimate period-specific transport cost we require two main inputs: bilateral trade data and a suitable estimation framework. We describe these two components below.

B.1 Bilateral trade data

Following Flückiger et al. (2022), we reconstruct trade flows by defining the archaeological excavation site of an artefact as the destination and the production site as the origin. A first prerequisite for artefacts to be included in our analysis therefore is that their find site as well as provenance can be identified. A second prerequisite is that the time period can be assigned to the artefacts (i.e., Stone or Bronze Age). To identify suitable data, we systematically scoured the archaeological literature. We identified two existing large-scale databases on trade during the Stone Age that report precise origin and destination of artefacts. Trade data for the Bronze Age are drawn from the database created by Flückiger et al. (2022). Below, we describe the characteristics of the databases as well as the aggregation process from artefact-level to regional-level trade flows. The origins and destinations of artefacts are depicted in Figure B.1. In the context of our analysis, it is important to note that the overwhelming majority of artefacts contained in our datasets were traded within Europe.

B.1.1 Stone Age trade data[53]

Alpine jade–Neolithic period The Alpine jade database was compiled by more than 50 researchers from several European countries as part of the project "JADE: Social inequalities in Neolithic Europe: the circulation of long axeheads of Alpine jades" (Pétrequin et al., 2012). The data was compiled between 2008 and 2018 and focuses on long axeheads made from jade (mainly extracted in the Alps). In total, the database contains precise information on the find site of 2,173 jade axeheads which can be downloaded at http://jade.univ-fcomte.fr. These axes mainly circulated within Europe during the 5th and 4th millennia BCE, but some of the objects moved over long distances from the Alpes to the Atlantic coast and the Black Sea via extensive exchange networks. To identify the provenance of the axeheads, the researchers used visual analysis and spectroradiometry. For 1,355 axeheads, the database includes information on the origin of the artefacts with sufficient precision for the purpose of our analysis. The jade included in our analysis primarily originates from high-altitude quarries at Monte Viso near Turin (973 pieces) and Monte Beigua near Genoa (151 pieces) in the Italian Alps. Some of the finds can also be reliably traced back to the Vosges in France or the Pennine Alps in Switzerland.

British axeheads–Early Neolithic period Schauer et al. (2020) provide an extensive database on British axeheads that combines information collected in projects overseen by the Imple-

[53] Description of the Stone Age trade data is taken from Flückiger et al. (2022) in large parts.

ment Petrology Group (IPG), the Neolithic Axehead Archive, and the Irish Stone Axe Project. The database contains precise information on the find site of 5,809 axeheads from the Early Neolithic (4100–3400 BCE) discovered across England, Wales and southern Scotland. Provenance of the axeheads is identified via petrological analysis. For our analysis, we exclude axeheads made from flint (1,512 pieces) due to fact that origins could not be unambiguously determined. We further exclude axeheads for which the source was specified as 'other' (1,766 pieces) which includes jade pieces originating from continental Europe. These restrictions leave us 2,345 artefacts for which the provenance is pinpointed within a radius of less than 50 km in Schauer et al. (2020).

B.1.2 Bronze Age trade data

We draw information on goods traded during the Bronze Age from the database compiled by Flückiger et al. (2022). A large share of the objects contained in their database are weapons, tools, and jewellery. In total, this database encompasses 3,744 artefacts for which find site and provenance can be determined with sufficient precision. In most cases, the artefacts' provenance was idetified based on metal parts, such as copper, silver, tin, or lead, using lead isotope analysis and trace element pattern analysis. In few cases it was determined by typology of similar instruments. For more details on the data construction process and a list of sources, see Online Appendix E in Flückiger et al. (2022).

B.1.3 Aggregation

For the inference of trade costs, we aggregate the information of the individual artefacts to the grid-cell-pair level. In keeping with the spatial unit of analysis of our main analysis, we first identify into which of the 1×1 degree grid cell its origin and destination fall. We then aggregate this information to the grid-cell-pair level giving us the number of finds within cell j that originate from cell i. The resulting trade volume represents the dependent variable used in the regression framework. This framework is described next.

B.2 Estimation framework

To infer period-and mode-specific per-unit distance transport costs we proceed in three steps. First, we divide the world into grid cells of 0.25×0.25 degrees and classify each grid as being either a sea, river, or land grid.[54] The classification of grids—and equivalently transport modes—is based on spatial data from Natural Earth.

Second, we assign (relative) per-unit-distance transport cost to each shipping mode: $\alpha^{sea}, \alpha^{river}$, and α^{land}. For the transport cost vector $\boldsymbol{\alpha} \equiv \left(1, \alpha^{river}, \alpha^{land}\right)$ we then use Dijkstra (1959)'s algorithm to identify the least-cost path and associated transport cost between any two 1×1

[54] The relative coarse size of cells is chosen to account for the fact that coastlines as well as river courses can shift over time.

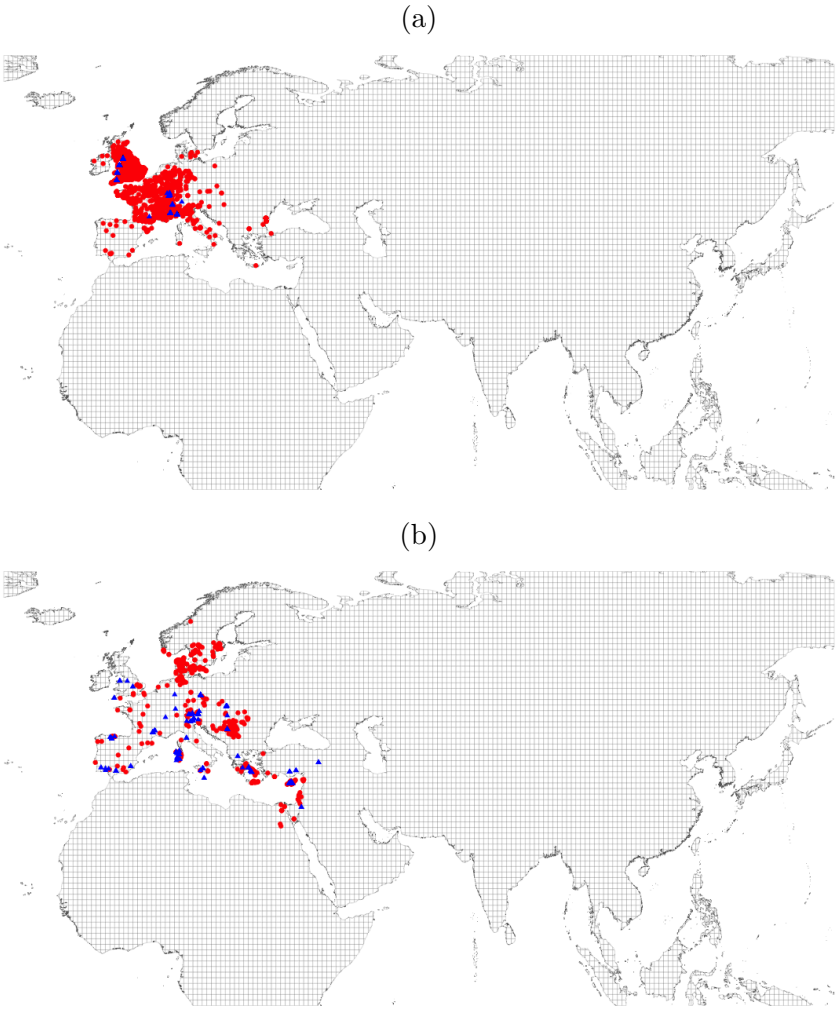


Figure B.1: Origins and Destinations of Artefacts
Panel (a) depicts origins (blue triangles) and destinations (red dots) of artefacts traded during the Stone Age. Panel (b) depicts origins (blue triangles) and destinations (red dots) of artefacts traded during the Bronze Age.

degree grid cells.[55] Throughout, we assume that transshipment between different transport modes is costless.

In the third step, we use the (logarithmized) costs associated with transporting goods along the least-cost path as the explanatory variable in a standard gravity equation:

$$\mathcal{X}_{ij}^{p} = \exp\left(\delta \ln LC(\boldsymbol{\alpha})_{ij} + \beta_i + \beta_j\right) + \varepsilon_{ij}, \tag{B.1}$$

where $\mathcal{X}_{ij}^{p}$ denotes the number of period-specific artefacts excavated in grid cell j that originate from grid cell i, as described above. The main explanatory variable—$LC(\boldsymbol{\alpha})_{ij}$—is the cost associated with transport along the least-cost path given the transport cost vector $\boldsymbol{\alpha}$. We

[55] The geographical centres (centroids) of grid cells are set as origins and destinations.

account for the full set of origin and destination fixed effects (represented by β_i and β_j, respectively).

Separately for each period (i.e. Stone and Bronze Age), we repeat the three-step procedure described above iterating over all cost combinations $\alpha^{sea} = [1, 50]$, $\alpha^{river} = [1, 50]$, and $\alpha^{land} = [1, 100]$. This implies that we run regression model (B.1) 250,000 times for a given period. Each time we measure model fit using the log-likelihood. Akin to Donaldson (2018) we then define the cost vector that minimises the log-likelihood as our period-specific transport costs ($\boldsymbol{\alpha_P}$)). For the Bronze Age, this fit-maximising transport cost vector is given by $\boldsymbol{\alpha_{BA}} = (1, 2, 6)$, where we normalise $\alpha^{sea} = 1$ for ease of interpretation. For the Stone Age, the transport costs are $\boldsymbol{\alpha_{SA}} = (1, 1/14, 2/7)$.

C Support for validity of estimation strategy

C.1 Robustness cross-sectional regressions

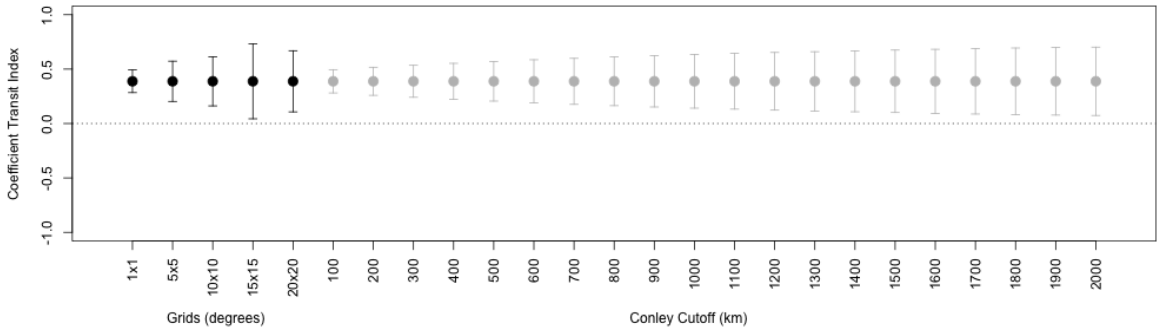
This appendix reports the robustness exercises discussed in Section 5.1. For compactness and ease of exposition, we focus on the primary outcome variables and report results only for our preferred regression specification (i.e., including the full set of control variables). Table C.1 shows results of the validity checks for our cross-sectional regressions (c.f. Section 5.1) and Tables C.3–C.4 list the results for the panel data analysis of archaeological sites (c.f. 5.2). All Tables have the same structure: Panel A reports the OLS estimates, Panel B the second-stage estimates of our 2SLS-IV approach, and Panel C the corresponding first-stage estimates. Each column represents the result of a different validity test.

Table C.1: Threats to identification: Reba, Reitsma and Seto (2016) city data

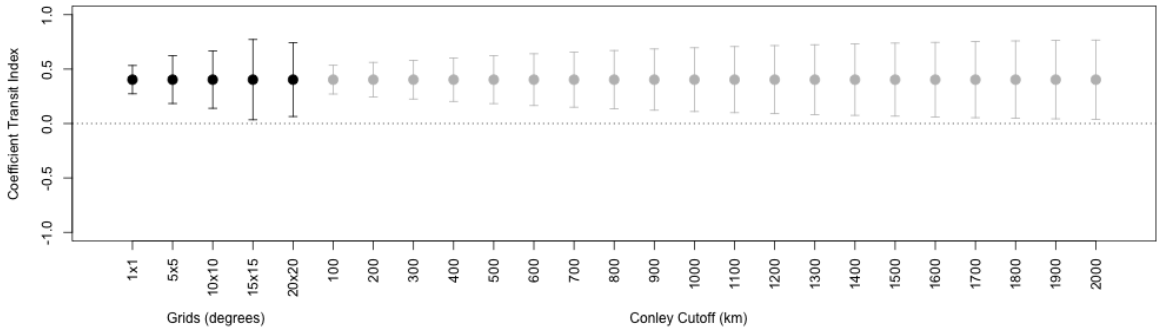
	Any City by 1000 BCE (×100)				
	(1)	(2)	(3)	(4)	(5)
	Panel A: OLS				
Transit Index	0.280	0.377	0.357	0.394	0.272
	(0.095)***	(0.109)***	(0.100)***	(0.116)***	(0.088)***
	[0.113]**	[0.142]***	[0.135]***	[0.151] ***	[0.111]**
	Panel B: Second stage 2SLS-IV				
Transit Index	0.335	0.394	0.361	1.284	0.325
	(0.120)***	(0.157)**	(0.198)*	(0.482)***	(0.176)*
	[0.147]**	[0.174]**	[0.224]	[0.650]**	[0.185]*
	Panel C: First stage 2SLS-IV				
IV Transit Index	0.362	0.352	0.347	0.183	0.325
	(0.035)***	(0.032)***	(0.030)***	(0.044)***	(0.028)***
	[0.051]***	[0.045]***	[0.043]***	[0.057]***	[0.041]***
Proximity to metal mines	Yes	Yes	Yes	Yes	Yes
Market potential	Yes	Yes	Yes	Yes	Yes
Land productivity	Yes	Yes	Yes	Yes	Yes
Geography controls	Yes	Yes	Yes	Yes	Yes
Continent fixed effects	Yes	Yes	Yes	Yes	Yes
Observations	8,496	9,426	9,426	9,426	9,426
Mean dependent variable	0.330	0.477	0.477	0.477	0.477
First-stage F-statistic (5×5 grids)	107.2	121.8	132.4	17.58	136.7
First-stage F-statistic (Conley 1000km)	50.75	61.18	64.96	10.04	62.17
Check	Drop extent $\boldsymbol{\alpha_{BA}}$	IV using $\boldsymbol{\alpha_{SA}}$	Controls Henderson et al. (2018)	Metal transit	Alternative transport cost

Notes: Panel A reports estimates of the cross-sectional OLS model (3). Panel B reports second-stage estimates of the cross-sectional 2SLS-IV model (4), while panel C reports the corresponding first-stage estimates. Standard errors clustered at the level of 5×5 degree grid cells reported in parentheses. Standard errors computed using the approach of Conley (1999) (cut-off 1000km) are reported in square brackets. 'Any city by 1000 BCE' is a dummy equal to one if a city was present in a given 1×1 degree grid cell by 1000 BCE. Variable is multiplied by hundred to facilitate interpretation. All regressions account for the full set of controls (see Section 3 and notes in Table 1). Column (1) restricts the spatial extent of the analysis to grid cells not used in the estimation of $\boldsymbol{\alpha_{BA}}$. In column (2) we construct the instrument using the transport cost estimates of the Stone Age ($\boldsymbol{\alpha_{SA}}$). Column (3) extends the set of controls by the characteristics used in Henderson et al. (2018). Column (4) controls for the transit trade index in gold, iron, lead, mercury, and silver. Column (5) controls for the transit trade index computed using the HMIsea and $\boldsymbol{\alpha_{SA}}$ as cost surfaces. * $p < 0.10$, ** $p < 0.05$, *** $p < 0.01$.

Robustness standard error clustering



(a) Figure shows the point estimate of Table 1 (column (1)) along with alternative standard error clustering approaches. Standard errors depicted in black are clustered at grid cells of various sizes, while Conley (1999) standard errors are shown in grey using different cutoff levels.



(b) Figure shows the point estimate of Table 2 (column (1)) along with alternative standard error clustering approaches. Standard errors depicted in black are clustered at grid cells of various sizes, while Conley (1999) standard errors are shown in grey using different cutoff levels.

Alternative outcome variable: HYDE 3.1 urbanisation data

Table C.2: Cross-sectional evidence: Klein Goldewijk, Beusen and Janssen (2010) urban areas

	Any urban area by 2000 BCE (×100)				
	(1)	(2)	(3)	(4)	(5)
	Panel A: OLS				
Transit Index	4.392	3.879	4.143	3.545	3.259
	(0.306)***	(0.311)***	(0.302)***	(0.340)***	(0.336)***
	[0.488]***	[0.471]***	[0.470]***	[0.518]***	[0.499]***
	Panel B: Second stage 2SLS-IV				
Transit Index	4.047	2.733	3.156	2.814	9.179
	(0.492)***	(0.700)***	(0.671)***	(0.598)***	(1.055)***
	[0.657]***	[0.925]***	[0.879]***	[0.783]***	[1.346]***
	Panel C: First stage 2SLS-IV				
IV Transit Index	0.600	0.453	0.478	0.488	0.396
	(0.036)***	(0.036)***	(0.035)***	(0.032)***	(0.033)***
	[0.055]***	[0.053]***	[0.051]***	[0.048]***	[0.048]***
Proximity to metal mines	No	Yes	No	No	Yes
Market potential	No	No	Yes	No	Yes
Land productivity	No	No	No	Yes	Yes
Geography controls	No	No	No	No	Yes
Continent fixed effects	Yes	Yes	Yes	Yes	Yes
Observations	9,426	9,426	9,426	9,426	9,426
Mean dependent variable	16.09	16.09	16.09	16.09	16.09
First-stage F-statistic (5×5 grids)	275.6	161.8	187.1	237.3	141.1
First-stage F-statistic (Conley 1000km)	118.7	71.09	85.95	102.8	66.82

Notes: Panel A reports estimates of the cross-sectional OLS model (3). Panel B reports second-stage estimates of the cross-sectional 2SLS-IV model (4), while panel C reports the corresponding first-stage estimates. Standard errors clustered at the level of 5×5 degree grid cells reported in parentheses. Standard errors computed using the approach of Conley (1999) (cut-off 1000km) are reported in square brackets. 'Any city by 1300 BCE' is a dummy equal to one if a city was present in a given 1×1 degree grid cell by 1300 BCE. Variable is multiplied by hundred to facilitate interpretation. '# Cities' is the total number of cities that had emerged in a grid grid cell by 1300 BCE. 'Transit trade index' is the cropland and metal input weighted number of least-cost paths that intersect a grid cell, as defined in Equation (1). 'IV Transit trade' is the NPP and metal input weighted number of least-cost paths that intersect a grid cell, as defined in Equation (2). 'Proximity mines' is the inverse input weighted average transport costs to metal mines. 'Proximity croplands' represents the grid's proximity to croplands, defined as the inverse transport cost weighted distance to croplands. 'Land productivity' is the cell's agricultural potential, measured by the caloric suitability index of Galor and Özak (2016). 'Geography controls' include latitude, elevation, precipitation, temperature, Strahler index, log distance to the coastline, and a dummy variable indicating whether a grid cell lies at the coast. * $p < 0.10$, ** $p < 0.05$, *** $p < 0.01$.

C.2 Robustness difference-in-difference regressions

This appendix reports the robustness exercises discussed in Section 5.2. For compactness and ease of exposition, we focus on the primary outcome variables and report results only for our preferred regression specification (i.e., including the full set of control variables). Table C.1 shows results of the validity checks for our cross-sectional regressions (c.f. Section 5.1) and Tables C.3–C.4 list the results for the panel data analysis of archaeological sites (c.f. 5.2). All Tables have the same structure: Panel A reports the OLS estimates, Panel B the second-stage estimates of our 2SLS-IV approach, and Panel C the corresponding first-stage estimates. Each column represents the result of a different validity test.

Table C.3: Threats to identification: Whitehouse and Whitehouse (1975) archaeological sites

	Any Site (×100)				
	(1)	(2)	(3)	(4)	
	Panel A: OLS				
Transit Index×Bronze Age	0.659	1.211	0.984	1.260	0.991
	(0.175)***	(0.205)***	(0.176)***	(0.213)***	(0.199)***
	[0.142]***	[0.199]***	[0.165]***	[0.215]***	[0.174]***
	Panel B: Second stage 2SLS-IV				
Transit Index×Bronze Age	1.221	1.300	1.240	4.531	1.304
	(0.424)***	(0.473)***	(0.517)**	(1.489)***	(0.536)**
	[0.365]***	[0.359]***	[0.388]***	[1.324]***	[0.436]***
	Panel C: First stage 2SLS-IV				
IV Transit Index×Bronze Age	0.362	0.352	0.347	0.183	0.325
	(0.035)***	(0.032)***	(0.030)***	(0.044)***	(0.028)***
	[0.036]***	[0.032]***	[0.030]***	[0.041]***	[0.029]***
Proximity to metal mines	Yes	Yes	Yes	Yes	Yes
Market potential	Yes	Yes	Yes	Yes	Yes
Land productivity	Yes	Yes	Yes	Yes	Yes
Geography controls	Yes	Yes	Yes	Yes	Yes
Grid cell fixed effects	Yes	Yes	Yes	Yes	Yes
Continent×period fixed effects	Yes	Yes	Yes	Yes	Yes
Observations	16,992	18,852	18,852	18,852	18,852
Mean dependent variable	4.620	8.498	8.498	8.498	8.498
First-stage F-statistic (5×5 grids)	107.3	121.9	132.8	17.59	136.8
First-stage F-statistic (Conley 1000km)	100.4	119.6	129.4	19.93	123
Check	Drop extent $\boldsymbol{\alpha_{BA}}$	IV using $\boldsymbol{\alpha_{SA}}$	Controls Henderson et al. (2018)	Metal transit	Alternative transport cost

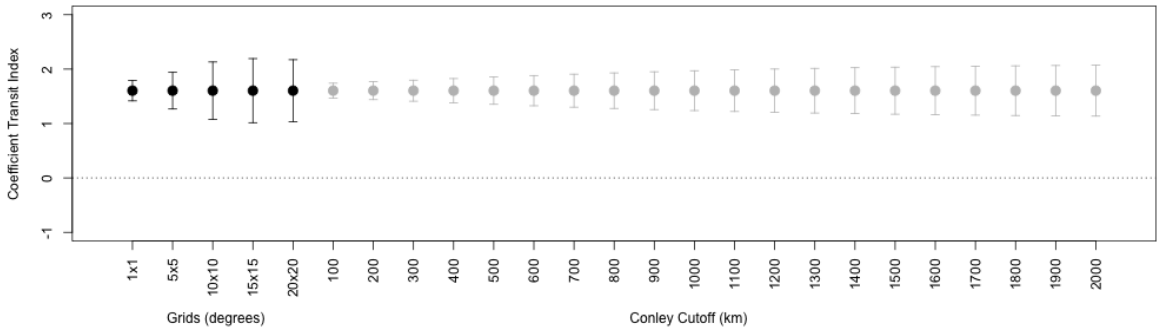
Notes: Panel A reports estimates of the OLS panel model (5). Panel B reports second-stage estimates of the panel 2SLS-IV model (6), while panel C reports the corresponding first-stage estimates. Standard errors clustered at the level of 5×5 degree grid cells reported in parentheses. Standard errors computed using the approach of Conley (1999) (cut-off 1000km) are reported in square brackets. Any Site' is a dummy equal to one if an archaeological site was present in a given 1×1 degree grid and period. Variable is multiplied by hundred to facilitate interpretation. All regressions account for the full set of controls (see Section 3 and notes in Table 3). Column (1) restricts the spatial extent of the analysis to grid cells not used in the estimation of $\boldsymbol{\alpha_{BA}}$. In column (2) we construct the instrument using the transport cost estimates of the Stone Age ($\boldsymbol{\alpha_{SA}}$). Column (3) extends the set of controls by the characteristics used in Henderson et al. (2018). Column (4) controls for the transit trade index in gold, iron, lead, mercury, and silver. Column (5) controls for the transit trade index computed using the HMIsea and $\boldsymbol{\alpha_{SA}}$ as cost surfaces. * $p < 0.10$, ** $p < 0.05$, *** $p < 0.01$.

Table C.4: Threats to identification: Pleiades Gazetteer (Bagnall, 2022)

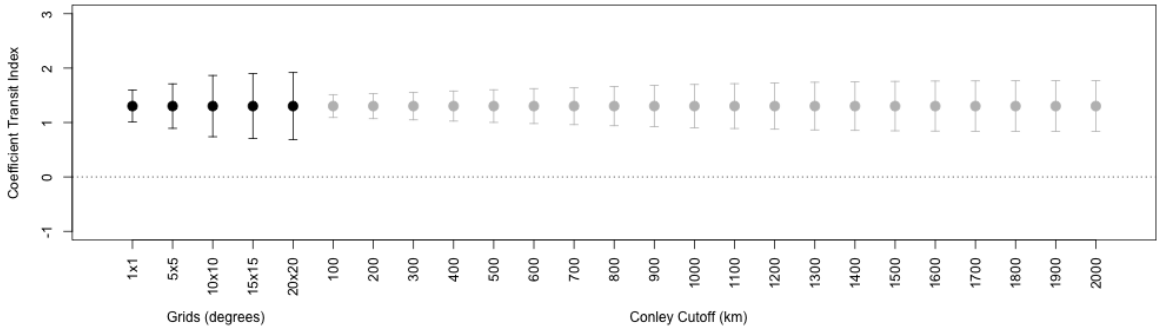
	Any Site (×100)				
	(1)	(2)	(3)	(4)	
	Panel A: OLS				
Transit Index×Bronze Age	0.356	0.712	0.699	0.759	0.545
	(0.097)***	(0.144)***	(0.141)***	(0.152)***	(0.121)***
	[0.093]***	[0.141]***	[0.129]***	[0.147]***	[0.109]***
	Panel B: Second stage 2SLS-IV				
Transit Index×Bronze Age	0.464	0.762	0.828	2.588	0.565
	(0.298)	(0.329)**	(0.382)**	(1.055)**	(0.388)
	[0.256]*	[0.281]***	[0.308]***	[0.930]***	[0.306]*
	Panel C: First stage 2SLS-IV				
IV Transit Index×Bronze Age	0.362	0.352	0.347	0.183	0.325
	(0.035)***	(0.032)***	(0.030)***	(0.044)***	(0.028)***
	[0.036]***	[0.032]***	[0.030]***	[0.041]***	[0.029]***
Proximity to metal mines	Yes	Yes	Yes	Yes	Yes
Market potential	Yes	Yes	Yes	Yes	Yes
Land productivity	Yes	Yes	Yes	Yes	Yes
Geography controls	Yes	Yes	Yes	Yes	Yes
Grid cell fixed effects	Yes	Yes	Yes	Yes	Yes
Continent×period fixed effects	Yes	Yes	Yes	Yes	Yes
Observations	16,992	18,852	18,852	18,852	18,852
Mean dependent variable	1.236	2.376	2.376	2.376	2.376
First-stage F-statistic (5×5 grids)	107.3	121.9	132.8	17.59	136.8
First-stage F-statistic (Conley 1000km)	100.4	119.6	129.4	19.93	123
Check	Drop extent $\boldsymbol{\alpha_{BA}}$	IV using $\boldsymbol{\alpha_{SA}}$	Controls Henderson et al. (2018)	Metal transit	Alternative transport cost

Notes: Panel A reports estimates of the OLS panel model (5). Panel B reports second-stage estimates of the panel 2SLS-IV model (6), while panel C reports the corresponding first-stage estimates. Standard errors clustered at the level of 5×5 degree grid cells reported in parentheses. Standard errors computed using the approach of Conley (1999) (cut-off 1000km) are reported in square brackets. Any Site' is a dummy equal to one if an archaeological site was present in a given 1×1 degree grid and period. Variable is multiplied by hundred to facilitate interpretation. All regressions account for the full set of controls (see Section 3 and notes in Table 3). Column (1) restricts the spatial extent of the analysis to grid cells not used in the estimation of $\boldsymbol{\alpha_{BA}}$. In column (2) we construct the instrument using the transport cost estimates of the Stone Age ($\boldsymbol{\alpha_{SA}}$). Column (3) extends the set of controls by the characteristics used in Henderson et al. (2018). Column (4) controls for the transit trade index in gold, iron, lead, mercury, and silver. Column (5) controls for the transit trade index computed using the HMIsea and $\boldsymbol{\alpha_{SA}}$ as cost surfaces. * $p < 0.10$, ** $p < 0.05$, *** $p < 0.01$.

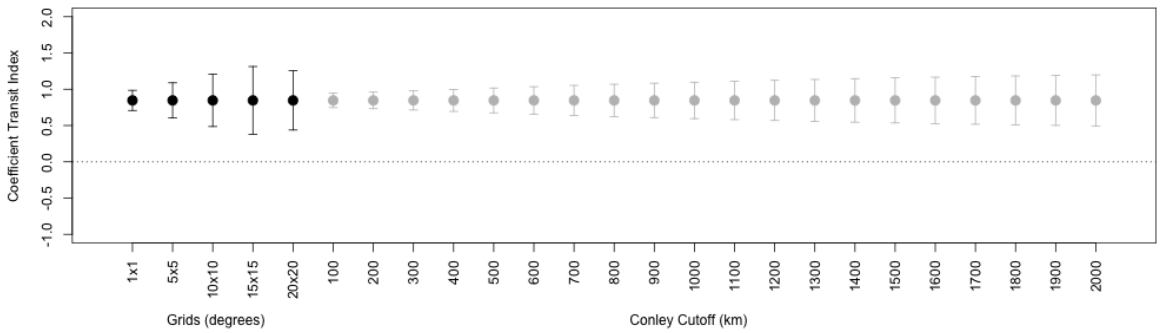
Robustness standard error clustering



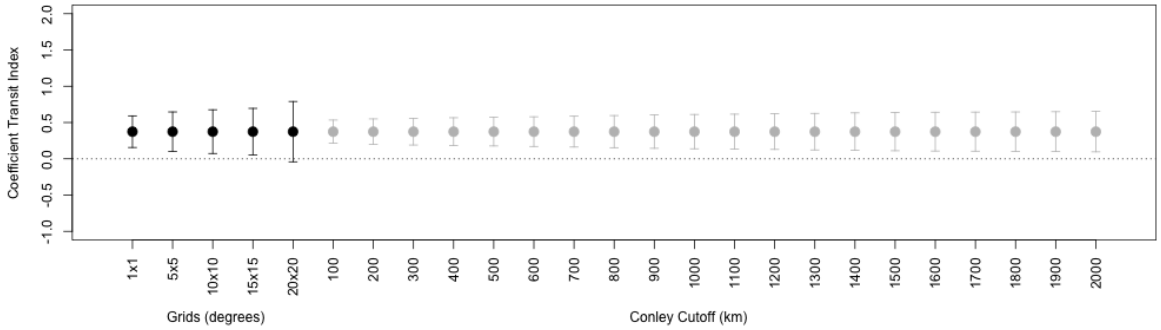
(a) Figure shows the point estimate of Table 3 (Panel A column (1)) along with alternative standard error clustering approaches. Standard errors depicted in black are clustered at grid cells of various sizes, while Conley (1999) standard errors are shown in grey using different cutoff levels.



(b) Figure shows the point estimate of Table 3 (Panel A column (6)) along with alternative standard error clustering approaches. Standard errors depicted in black are clustered at grid cells of various sizes, while Conley (1999) standard errors are shown in grey using different cutoff levels.



(c) Figure shows the point estimate of Table 3 (Panel B column (1)) along with alternative standard error clustering approaches. Standard errors depicted in black are clustered at grid cells of various sizes, while Conley (1999) standard errors are shown in grey using different cutoff levels.



(d) Figure shows the point estimate of Table 3 (Panel B column (6)) along with alternative standard error clustering approaches. Standard errors depicted in black are clustered at grid cells of various sizes, while Conley (1999) standard errors are shown in grey using different cutoff levels.

D Blockage

D.1 Theoretical model

IN PROGRESS

D.2 Measuring blockage costs

For each grid cell g, we compute the blockage cost in the following way:

1. Block cell g for transit trade.
2. For all other cells $j \neq g$: identify cost-minimising copper and tin mine; compute associated transport costs (TB_j)
3. Compute difference between unrestricted transport costs (TU_j) and 'blocked' cost: $\Delta_j = TB_j - TU_j$
4. Aggregate additional transport costs across all cells, weighting by cropland area. This represents the global additional cost in metal trade when grid cell g is blocked for transit trade. We refer to this cost as 'blockage cost' (B_g). Formally, i can be written as:

$$B_g = \sum_{j \neq g}^{J} \Delta_j \times w_j \tag{D.1}$$

E Data construction China



Figure E.1: Sites Atlas of Chinese relics
Figure depicts the location of archaeological sites of the Atlas of Chinese relics. Data is unavailable for provinces shaded in grey.

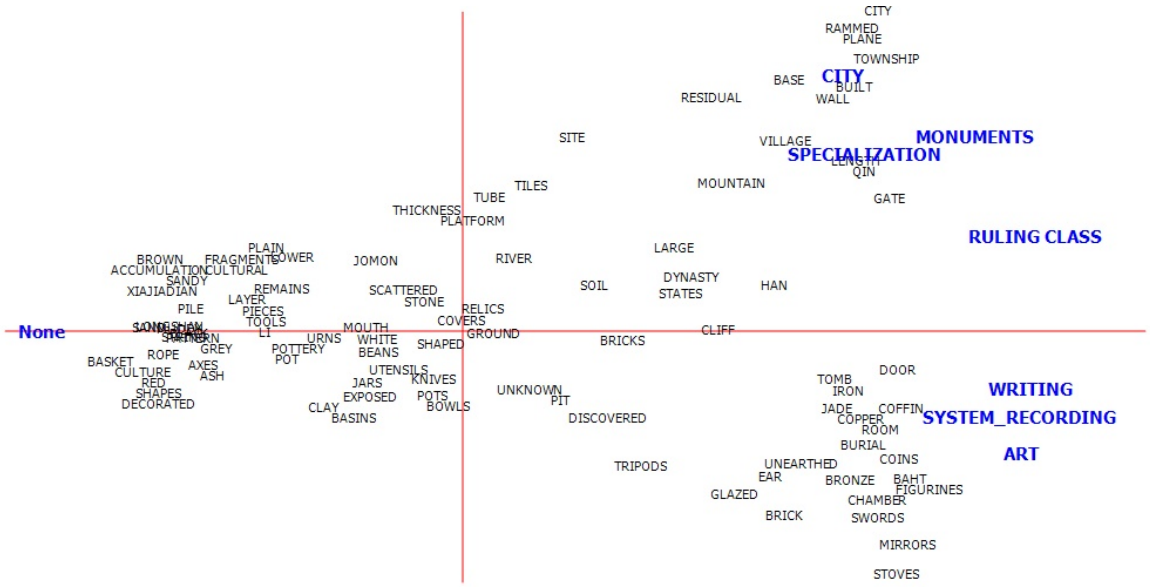


Figure E.2: Correspondence plot
Figure depicts the correspondence plot of the most frequent 100 words according the seven criteria indicative of the rise of the Urban Revolution in China.

F Data construction Europe

IN PROGRESS

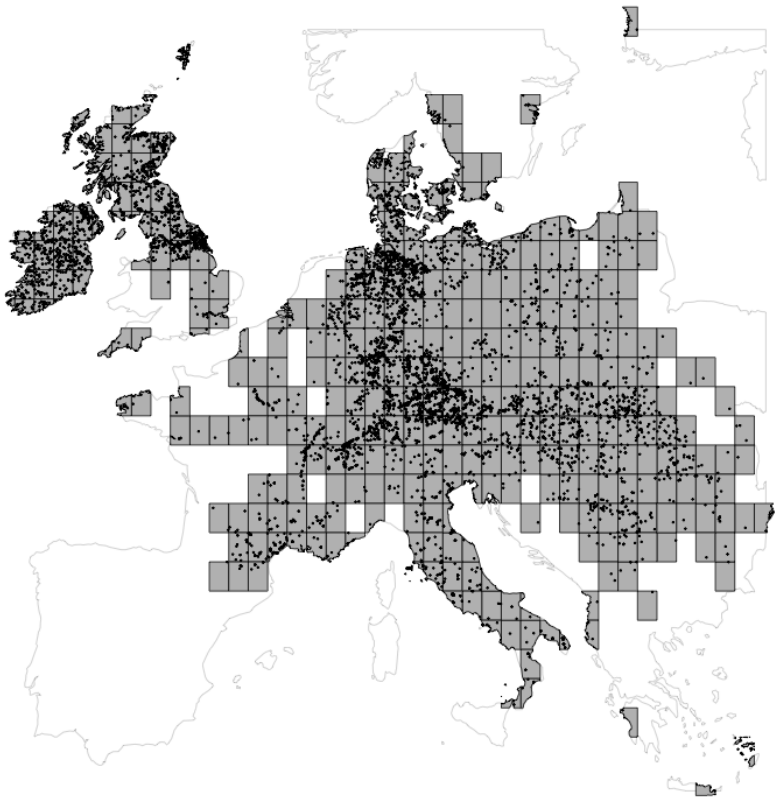


Figure F.1: Bronze weapons
Figure depicts the location of bronze weapon finds as recorded by Prähistorische Bronzefunde (*Abteilung IX* and *Abteilung IV*). Grid cells in which at least one bronze weapon was excavated are shaded in gray. Our regression analysis is restricted to these cells (see Section 5.4 for more details.

References

Avner, Uzi. 2014. "Egyptian Timna- Reconsidered." *Ancient Near Eastern Studies Supplement 45* 45.

Avner, Uzi, Hanan Ginat, Sariel Shalev, Sana Shilstine, Boaz Langford, Amos Frumkin, Rachamim Shem-Tov, Reuma Arav Sagi Filin and, Uri Basson, Omer Shamir, and Linda Scott-Cummings. 2018. "Ancient copper mines at Nahal 'Amram, southern Arabah." In *Mining for Ancient Copper: Essays in Memory of Beno Rothenberg*, The Institute of Archaeology of Tel Aviv University.

Bagnall, Roger. 2022. "Pleiades: A Gazetteer of Past Places." pleiades.stoa.org.

Benvenuti, M, L Charantini, L Norfini, A Casini, S Guideri, and G Tanelli. 2003. "The "Etruscan tin": A preliminary contribution from researches at Monte Valerio and Baratti-Populonia (southern Tuscany, Italy)." *BAR International Series* 1199: 55–66.

Cadet, Mélissa, Thongsa Sayavongkhamdy, Viengkeo Souksavatdy, Thonglith Luangkhoth, Philippe Dillmann, Christophe Cloquet, Justine Vernet, Paolo Piccardo, Nigel Chang, John Edgar, Eddy Foy, and T.O. Pryce. 2019. "Laos' central role in Southeast Asian copper exchange networks: A multi-method study of bronzes from the Vilabouly Complex." *Journal of Archaeological Science* 109: 104988.

Catapotis, Mihalis. 2007. "On the Spatial Organisation of Copper Smelting Activities in the Southern Aegean during the Early Bronze Age." In *Metallurgy in the Early Bronze Age Aegean*, edited by P.M. Day and R.C.P. Doonan. Oxbow Books, Oxford.

Cleuziou, Serge. 1982. "Early Tin in the Near East." *Expedition Magazine* 25 (1).

Conley, T. G. 1999. "GMM estimation with cross sectional dependence." *Journal of Econometrics* 92 (1): 1–45.

Constantinou, G. 2012. "Late Bronze Age copper production on Cyprus from a mining geologist's perspective." In *Eastern Mediterranean Metallurgy and Metalwork in the Second Millennium bc*, edited by V. Kassianidou and G. Papasavvas, 4–13. Oxbow Books, Oxford.

Derikonjic, S., E. Pernicka, and T. Rehren. n.d.. "The Vinca culture mining complex in Jarmovac, southwest Serbia." Vol. 4 of *Sonderheft*, 2001. Bochum.

Dijkstra, Edsger W. 1959. "A Note on Two Problems in Connexion with Graphs." *Numerische Mathematik* 1 (1): 269–271.

Donaldson, Dave. 2018. "Railroads of the Raj: Estimating the Impact of Transportation Infrastructure." *American Economic Review* 108 (4–5): 899–934.

Flückiger, Matthias, Erik Hornung, Mario Larch, Markus Ludwig, and Allard Mees. 2022. "Roman Transport Network Connectivity and Economic Integration." *The Review of Economic Studies* 8989 (2): 774–810.

Gale, N., and S. Stos-Gale. 2002. "Archaeometallurgical research in the Aegean." In *The*

Beginnings of Metallurgy in the Old World, edited by M. Bartelheim, E. Pernicka and R. Krause, 277–302. Rahden: Verlag Marie Leidorf GmbH.

Galor, Oded, and Ömer Özak. 2016. "The Agricultural Origins of Time Preference." *American Economic Review* 106 (10): 3064–3103.

Garner, Jennifer. 2014. *Das Zinn der Bronzezeit in Mittelasien II. Die montanarchäologischen Forschungen an den Zinnlagerstätten.* Philipp von Zabern.

Garner, Jennifer. 2015. "Bronze Age tin mines in central Asia." *Archaeometallurgy in Europe III. Bochum* 135–143.

Giardino, Claudio. 2019. *Magan - the Land of Copper: Prehistoric Metallurgy of Oman. Archaeopress Archaeology.* Archaeopress Archaeology.

Hauptmann, Andreas. 1997. "Feinan." In *The Oxford Encyclopedia of Archaeology in the Near East*, edited by Eric M. Meyers, 310–311. Oxford University Press.

Hauptmann, Andreas. 2007. *The Archaeometallurgy of Copper: Evidence from Faynan, Jordan. Natural Science in Archaeology.* Springer Berlin Heidelberg.

Henderson, J Vernon, Tim Squires, Adam Storeygard, and David Weil. 2018. "The Global Distribution of Economic Activity: Nature, History, and the Role of Trade1." *The Quarterly Journal of Economics* 133 (1): 357–406.

Higham, Thomas F. G., Andrew D. Weiss, Charles F. W. Higham, Christopher Bronk Ramsey, Jade d'Alpoim Guedes, Sydney Hanson, Steven A. Weber, Fiorella Rispoli, Roberto Ciarla, Thomas O. Pryce, and Vincent C. Pigott. 2020. "A prehistoric copper-production centre in central Thailand: its dating and wider implications." *Antiquity* 94 (376): 948–965.

Hughes, Simon J. S. 1981. "The Cwmystwyth Mines." *British Mining Monopgraph* 17.

Huska, A., W. Powell, S. Mitrović, H. A. Bankoff, A. Bulatović, V. Filipović, and R. Boger. 2014. "Placer Tin Ores from Mt. Cer, West Serbia, and Their Potential Exploitation during the Bronze Age." *Geoarchaeology* 29 (6): 477–493.

Jaang, Li. 2015. "The Landscape of China's Participation in the Bronze Age Eurasian Network." *Journal of World Prehistory* 28 (3): 179–213.

Kaptan, Ergun. 1990. "Findings Related to the History of Mining in Turkey." *Bulletin of the Mineral Research and Exploration* 111.

Klein Goldewijk, Kees, Arthur Beusen, and Peter Janssen. 2010. "Long-term dynamic modeling of global population and built-up area in a spatially explicit way: HYDE 3.1." *The Holocene* 20 (4): 565–573.

Kutterer, Johannes, Christina Neureiter, and Sabah Jasim. 2013. "Second report on the copper smelting site HLO1 in Wādī al-Ḥilo (Sharjah, UAE)." *Proceedings of the Seminar for Arabian Studies* 43: 185–196.

Larreina-García, David. 2017. "Copper and bloomery iron smelting in Central China:

Technological traditions in the Daye County (Hubei)." PhD diss. University College London Institute of Archaeology.

Lehner, Joseph, and K. Yener. 2013. "Organization and Specialization of Early Mining and Metal Technologies in Anatolia." *Archaeometallurgy in Global Perspective: Methods and Syntheses* 529–557.

Lewis, Christopher Andrew. 1997. "Prehistoric Mining at the Great Orme-Criteria for the Identification of Early Mining." PhD diss. MPhil. thesis, University of Wales, Bangor.

Liu, Ruiliang, A. Mark Pollard, Jessica Rawson, Xiaojia Tang, Peter Bray, and Changping Zhang. 2019. "Panlongcheng, Zhengzhou and the Movement of Metal in Early Bronze Age China." *Journal of World Prehistory* 32 (4): 393–428.

Liu, Ruiliang, Peter Bray, A.M. Pollard, and Peter Hommel. 2015. "Chemical analysis of ancient Chinese copper-based objects: Past, present and future." *Archaeological Research in Asia* 3: 1–8.

Liu, S., K. L. Chen, Th. Rehren, J. J. Mei, J. L. Chen, Y. Liu, and D. Killick. 2018. "Did China Import Metals from Africa in the Bronze Age?" *Archaeometry* 60 (1): 105–117.

Liverani, M., and S. Tabatabai. 2014. *The Ancient Near East: History, Society and Economy.* Routledge/Taylor & Francis Group.

Massoudi, Omara Khan. 2011. *Mes Aynak - Recent Discoveries Along the Silk Road.* Kabul: National Museum of Afghanistan.

Muhly, James D. 1985. "Sources of Tin and the Beginnings of Bronze Metallurgy." *American Journal of Archaeology* 89 (2): 275–291.

Nezafati, Nima, and Thomas Stöllner. 2018. "Economic Geology, Mining Archaeological and Archaeometric Investigations at the Veshnaveh Ancient Copper Mine, Central Iran." *Metalla* 23: 67–90.

Northover, J. P. N., W. O'Brien, and S. Stos. 2001. "Lead Isotopes and Metal Circulation In Beaker/Early Bronze Age Ireland." *The Journal of Irish Archaeology* 10: 25–47.

O'Brien, William. 1999. "Arsenical copper in early Irish metallurgy." In *Metals in Antiquity*, edited by Suzanne M. M. Young, A. Mark Pollard, Paul Budd and Robert A. Ixer, Chapter 4, 33–42. Cambridge, United Kingdom: Proceedings of the 1995 Harvard Conference British Archaeological Reports, Archaeopress.

O'Brien, William. 2015. *Prehistoric Copper Mining in Europe: 5500-500 BC.* Oxford University Press.

Özbal, Hadi, Annemie Mieke Adriaens, and Bryan Earl. 1999. "Hacinebi Metal Production and Exchange." *Paléorient* 25 (1): 57–65.

Pétrequin, Pierre, Serge Cassen, Michel Errera, L. Klassen, Alison Sheridan, and Anne Marie Pétrequin. 2012. *Jade: Grandes haches alpines du Néolithique européen, Ve et IVe millénaires av. J.-C.* Centre de Recherche Archéologique de la Vallée de l'Ain.

Pollard, A. M., P. Bray, P. Hommel, Y. K. Hsu, R. Liu, and J. Rawson. 2017. "Bronze Age metal circulation in China." *Antiquity* 91 (357): 674–687.

Pryce, T. O., A. H. Bevan, R. Ciarla, F. Rispoli, C. Castillo, B. Hassett, and J. L. Malakie. 2011*a*. "Intensive Archaeological Survey in Southeast Asia: Methodological and Metallurgical Insights from Khao Sai On, Central Thailand." *Asian Perspectives* 50 (1/2): 53–69.

Pryce, T. O., M. Pollard, M. Maritinon-Torres, V. C. Pigott, and E. Pernicka. 2011*b*. "Southeast Asia's first isotopically defined prehistoric copper proudction system: When did extractive metallurgy begin in the Khao Wong Prachan Valley of Central Thailand?" *Archaeometry* 53 (1): 146–163.

Quarta, Gianluca, Felice Larocca, Marisa D'Elia, Valentina Gaballo, Maria Macchia, Giuseppe Palestra, and Lucio Calcagnile. 2013. "Radiocarbon Dating the Exploitation Phases of the Grotta Della Monaca Cave in Calabria, Southern Italy: A Prehistoric Mine for the Extraction of Iron and Copper." *Radiocarbon* 55 (3): 1246–1251.

Radivojević, Miljana, Thilo Rehren, Ernst Pernicka, Dušan Šljivar, Michael Brauns, and Dušan Borić. 2010. "On the origins of extractive metallurgy: new evidence from Europe." *Journal of Archaeological Science* 37 (11): 2775–2787.

Rafel, Núria, Mark A. Hunt Ortiz, Ignacio Montero, Ignacio Soriano, Selina Delgado-Raack, and Dioscórides Marín. 2019. "New Bronze Age absolute datings for Solana del Bepo copper mine (Ulldemolins, Tarragona Province, Spain)." *Mediterranean Archaeology and Archaeometry* 19 (1): 9–24.

Reba, Meredith, Femke Reitsma, and Karen C. Seto. 2016. "Spatializing 6,000 years of global urbanization from 3700 BC to AD 2000." *Scientific Data* 3 (1): 160034.

Reinhardt, Katrinka. 1997. "Mining and smelting technology and the politics of bronze in Shang and Western Zhou China : an inquiry into the Bronze Age interaction sphere." PhD diss. Department of East Asian Studies McGill University.

Schauer, Peter, Andrew Bevan, Stephen Shennan, Kevan Edinborough, Tim Kerig, and Mike Parker Pearson. 2020. "British Neolithic Axehead Distributions and Their Implications." *Journal of Archaeological Method and Theory* 27: 836–859.

Schibler, Jörg, Elisabeth Breitenlechner, Sabine Deschler-Erb, Gert Goldenberg, Klaus Hanke, Gerald Hiebel, Heidemarie Plogmann, Kurt Nicolussi, Elisabeth Marti-Grädel, Sandra Pichler, Alexandra Schmidl, Anton Schwarz, Barbara Stopp, and Klaus Oeggl. 2011. "Miners and mining in the Late Bronze Age: A multidisciplinary study from Austria." *Antiquity* 85: 1259–1278.

Stöllner, Thomas, Zeinolla Samaschev, Sergej Berdenov, Jan Cierny, Monika Doll, Jennifer Garner, Anton Gontscharov, Alexander Gorelik, Andreas Hauptmann, H Rainer, et al. 2011. "Tin from Kazakhstan: Steppe tin for the West." *Anatolian*

Metal V Der Anschnitt Beiheft 24: 231–251.

Timberlake, Simon, and Peter Marshall. 2018. "Copper mining and smelting in the British Bronze Age: new evidence of mine sites including some reanlysis of dates and ore sources." In *Mining for Ancient Copper: Essays in Memory of Beno Rothenberg*, edited by Erez Ben-Yosef, Chapter 29, 418–434. Tel Aviv: Eisenbrauns: Winona Lake, Indiana and Emery and Claire Yass Publications in Archaeology.

Tolksdorf, Johann Friedrich, Frank Schröder, Libor Petr, Christoph Herbig, Knut Kaiser, Petr Kočár, Alexander Fülling, Susann Heinrich, Heide Hönig, and Christiane Hemker. 2020. "Evidence for Bronze Age and Medieval tin placer mining in the Erzgebirge mountains, Saxony (Germany)." *Geoarchaeology* 35 (2): 198–216.

Valamoti, Soultana-Maria, and Glynis Jones. 2010. "Bronze and Oil: A Possible Link between the Introduction of Tin and Lallemantia to Northern Greece." *The Annual of the British School at Athens* 105: 83–96.

Valera, R., and Paolo Valera. 2003. "Tin in the mediterranean: History and geology." *The Problem of Early Tin* 3–14.

Wang, Lu, Fan Chen, Yongqiang Wang, Wei Qian, Jianjun Mei, Marcos Martinón-Torres, and Kunlong Chen. 2019. "Copper metallurgy in prehistoric upper Ili Valley, Xinjiang, China." *Archaeological and Anthropological Sciences* 11 (6): 2407–2417.

Whitehouse, David, and Ruth Whitehouse. 1975. *Archaeological Atlas of the World. Documents of Revolution.* Thames and Hudson.